APPROVAL SHEET

Title of Dissertation: ENVIRONMENTAL FACTORS AFFECTING THE MEASUREMENT OF THE PHYSICAL AND CHEMICAL PROPERTIES OF AEROSOLIZED BIOLOGICAL PARTICLES

Name of Candidate: Shanna Ratnesar-Shumate

Doctor of Philosophy, 2015

Dissertation and Abstract Approved: _____

Upal Ghosh

Professor

Chem. Biochem. & Env. Engineering

Date Approved: _____

ABSTRACT

Title of Document: ENVIRONMENTAL FACTORS AFFECTING THE MEAUSUREMENT OF THE PHYSICAL AND CHEMICAL PROPERTIES OF AEROSOLIZED BIOLOGICAL PARTICLES

Shanna Ratnesar-Shumate, Doctor of Philosophy, 2015

Directed By: Upal Ghosh, Dept of Chem. Biochem. & Env. Engineering Sciences

Biological aerosols, also known as bioaerosols, are a subset of organic carbon aerosols that consist of airborne particles that may be alive, may contain other live organisms, or released from living organisms. Many methods can be used to study bioaerosols. These methods range from collection and characterization of samples via culture, polymerase chain reaction, and immunoassay, to spectroscopic methods such as Raman spectroscopy and fluorometry. When biological particles are released into the atmosphere, they have the potential to interact with atmospheric constituents such as water vapor, solar radiation, free radicals, volatile organic, semi-volatile organic and inorganic gas-phase compounds.

The objective of this work was to access the environmental factors that affect the physical and chemical properties and measurement of aerosolized biological aerosols.

A novel test system was demonstrated to re-create natural fluctuations in biological and non-biological aerosol concentrations in a controllable laboratory setting for evaluating sensor performance. The Dynamic Concentration Aerosol Generator (DyCAG) can be used for bioaerosol sensor evaluation by generation of challenges of biological aerosols of interest at specific concentrations in the presence of varying levels of environmentally relevant aerosols.

To understand the limitations of fluorescence-based measurements for detection and characterization of biological aerosols and to develop improved instrumentation and methods for making measurements, changes that occurred to biological particles due atmospheric exposure to ozone and water vapor were measured using a rotating drum chamber. The spectral properties of ultra-violet laser-induced fluorescence (UV-LIF) of two types of biological aerosols, *Bacillus thuringiensis* Al Hakam (Bt Al Hakam) spores and MS2 bacteriophage when excited at 263, 351, and 355 nm were shown to change when exposed to ozone and water vapor. In addition, changes in the biological activity of these bioaerosols as a function of the exposure conditions were observed.

The hygroscopic properties of several types of biological aerosols and the media used for culturing and aerosolized bioaerosols were measured. Media containing high concentrations of salt showed the highest affinity for the uptake of water and dominated the hygroscopic properties of the aerosols measured.

The studies presented in this dissertation describe some of the factors that contribute to how the physical and chemical properties of biological aerosols and their measurement are impacted by external factors when in their native state.

ENVIRONMENTAL FACTORS AFFECTING THE MEASUREMENT OF THE PHYSICAL AND CHEMICAL PROPERTIES OF AEROSOLIZED BIOLOGICAL PARTICLES

By

Shanna Ratnesar-Shumate

Dissertation submitted to the Faculty of the Graduate School of the
University of Maryland, Baltimore County, in partial fulfillment
of the requirements for the degree of

Doctor of Philosophy

2015

Dedication

This dissertation is dedicated to my father Vijaya Chandra Ratnesar.

Acknowledgements

The work presented in this dissertation was funded by the Department of Defense Joint Program Executive Office Joint Project Manager for Contamination Avoidance (JPEO JPMCA) and the Defense Threat Reduction Agency (DTRA).

Table of Contents

List of Tables

List of Figures

Chapter 1: INTRODUCTION

The atmosphere contains naturally occurring aerosols that fluctuate in concentration and make-up. Biological aerosols, also known as bioaerosols, are a subset of organic carbon aerosols that consist of airborne particles that may be alive, may contain other live organisms, or released from living organisms (Ariya and Amyot, 2004). Some examples of bioaerosols include bacteria, fungi, pollens, viruses, toxins, cell debris and plant matter (Ariya and Amyot, 2004; Deguillaume et al., 2008; Hinds, 1999, Santarpia et al., 2012). The negative health effects of bioaerosols may be due to infectious pathogens or toxins produced by organisms that cause disease, or negative bodily reactions to toxins such as asthma or rashes (Hinds, 1999). The potential use of pathogenic biological aerosols as weapons of mass destruction has long been a concern. Biological aerosols are also known to serve as ice nuclei (IC) and cloud condensation nuclei (CCN). Due to their roles as IC and CCN, bioaerosols may influence cloud coverage and therefore the global radiative balance (Ariya and Amyot, 2004, Deguillaume et al., 2008). Living bioaerosols have been shown to metabolize atmospheric organic compounds and oxidants, resulting in the production of new atmospheric chemical species (Sun and Ariya, 2006; Deguillaume et al., 2008). Understanding the composition, fate and transport of biological aerosols in the atmosphere is important for understanding health and climate effects, hazard assessments for disease control, forensic insights for attribution in the case of biological weaponry, and biological detection technologies.

Many methods can be used to study bioaerosols. These methods range from collection and characterization via culture, polymerase chain reaction, and immunoassay to spectroscopic methods such as Raman spectroscopy and fluorometry (Santarpia, et al., 2012).

Characterization of naturally or artificially occurring biological aerosols in the environment should include the size distribution, concentration, temporal variability and (if applicable) species identification. The need to identify pathogenic biological aerosols before symptoms manifest in host populations is critical to protecting public health. This concern has led to the development of a variety of sensors to detect the full spectrum of potentially disease causing biological aerosols including spores, bacteria, viruses, and toxins. Pathogenic organisms that cause disease in humans may be chemically and physically very similar to a wide range of other largely innocuous atmospheric particles of biological origin. Optical sensors, based on spectroscopic techniques, are obvious candidates for bioaerosol measurement. They can measure biological aerosol concentrations at very rapid rates (seconds to minutes), providing real-time information on bioaerosol populations (Ivnitski et al., 2005; Samuels et al., 2006; Vanderberg, 2000). However, these sensors have not been shown to discriminate between different types of microorganisms and may incorrectly classify certain non-biological aerosol particles as being those of a biological origin. Several different types of optical detection technologies, including fluorescence spectroscopy, vibrational spectroscopy, and transduction methods have been investigated (Vanderberg, 2000) for measurement of biological aerosols. The most common type of optical biological

aerosol sensor utilizes spectroscopic autofluorescence or light induced fluorescence (LIF) (Wilson and Defreeze, 2003; Schroder et al. 1999; Eversole et al. 2001; Hill et al. 1999; Tilley et al. 2001). Systems using LIF technology detect fluorescent compounds present in most biological materials including tryptophan, nicotinamide adenine dinucleotide plus hydrogen (NADH), and flavins. The spectroscopic signal detected by a sensor is dependent upon the wavelength used to excite the molecules in the particle, as well as the relative ratios of signature compounds within the biological species being interrogated. In many cases, light scattering from a particle is also used to infer size and shape information. These non-specific biological detection systems can be affected by the natural fluctuations in the ambient background of biological and non-biological aerosol as well as changes in ambient environmental conditions such as temperature and relative humidity.

The Aerodynamic Particle Sizer® spectrometer(APS®, TSI Inc. and the Ultra-Violet Aerodynamic Particle Sizer spectrometer (UV-APS, TSI Inc.) are two examples of commercially available optical particle counter and sizers that provides real-time measurement of the aerodynamic size, light scattering intensity, and fluorescence of aerosols (TSI Inc., 2004, 2012). The aerodynamic diameter of an aerosol is generally defined as the diameter of a spherical particle with a density of unity with the same terminal velocity as an aerosol of interest. The relationship between the aerodynamic diameter of an aerosol and the volumetric equivalent diameter is expressed in its most simplified terms by Equation Equation 3. Here, *da* is the aerodynamic diameter as reported by the APS®, d^{ve} is the diameter of an equivalent sphere with the same volume

as the aerosol being measured, ρ_p is the density of the particle, ρ_0 is the unit density or the density of water (1 g/mL under standard conditions) and χ is the dynamic shape factor (Hinds, 1999; Sturm, 2012). Aerodynamic measurements are made in the APS® by accelerating an aerosol through a nozzle with two laser beams located at the exit. As a particle passes through each laser beam, the scattered lights by the particle are measured by photomultiplier (PMT) tubes. The time between each scattering event is then used to determine the average velocity of the particle. Larger particles do not accelerate as rapidly as smaller particles, which follow the velocity of the air stream more closely. The time to travel between the two laser beams is used to determine the aerodynamic diameter of the aerosol (Hinds, 1999).

$$d^a = d^{ve}\sqrt{\frac{\rho_p}{\rho_0 \chi}} \qquad \textbf{Equation 1}$$

The UV-APS uses the same aerodynamic sizing technique as the APS®, but also measures the fluorescence of each particle when excited at 355 nm between 420-575 nm. After the particles pass through the sizing optics, the size measurement made is used to predict when the particle will arrive at an additional laser located downstream of the sizing lasers and triggers the fluorescence laser to fire at the particle. The fluorescence from the excitation is then measured with another PMT and reported in

64 channels. By combining the size measurement with the fluorescence measurement, it is possible to use the UV-APS to measure size distribution of fluorescence particles in the aerosol. The UV-APS has been widely used for measuring fluorescent biological aerosol particles (FBAP) for atmospheric studies (Pöhlker et al., 2012; Huffman et al., 2010; Treutlein and Pöschl 2007). For example, using the criteria that FBAP were particles that fluoresce in channels 3-64 and >1 µm when measured by the UV-APS, Huffman et al, (2010) reported that FBAP concentrations varied from 1.2E3 to 1.4 particles/cm^3 of air, accounting for a range of 0.09 to 67% of the total coarse aerosols measured over a four-month period in Central Europe.

Another commercially available on-line particle spectrometer is the wide issue bioaerosol sensor (WIBS). The WIBS combines fluorescence in bands from 310-400 nm and 420-650 nm when excited at 280 nm and 420-650 when excited at 370 nm. The most recent version of the WIBS utilizes xenon lamps and optical filters to fire the two desired wavelengths at aerosols as they pass through an interrogation region and report the fluorescence in the three fluorescence channels (F1, F2, and F3). The WIBS has become more popular in recent years to due to the discontinuation of production of the UV-APS by TSI Inc. Numerous studies have utilized the system for measurement of FBAP in atmospheric studies (Toprak and Schnaiter 2013; Pohlker et al., 2012). Toprak and Schnaiter (2013) measured seasonal and diurnal variations in FBAP in a semi-rural site in South Western Germany and identified a correlation between FBAP concentrations and relative humidity. In the study, the authors reported good

discrimination between FBAP and other non-biological aerosols using the two excitation wavebands provided by the WIBS.

The Single Particle Fluorescence Spectrometer (SPFS) was developed by the Army Research Laboratory and is a custom instrument that has been used for multiple studies characterizing the fluorescence properties of aerosols when excited at 263 and 351 nm (Santarpia et al., 2012, Pinnick et al., 2004, Yong-Le Pan et al., 2010; Yong-Le Pan et al., 2014; Yong-Le Pan et al., 2003; Ratnesar-Shumate et al., 2012). The most current version of the SPFS operates by first drawing an aerosol through a sheath nozzle that focuses the aerosol into a ~300 nm laminar jet stream. Particles first past through the intersection of two-diode laser beams and the associated scattering is detected using two PMTs and used to trigger downstream measurements. After passing through this triggering region, the particles are then exited by a single pulse light provided by either a 263 nm or 351 nm laser and the fluorescence spectrum measured using an Image-Intensified Charge-Coupled Device (ICCD). A diode laser at 705 nm coupled with an additional PMT is used downstream to measure the particle size based on elastic scattering. Pinnick et al., (2004) measured the spectra from coarse aerosols in Adelphi, MD with the SPFS over the span of 3 months and using a hierarchical clustering determined that 92% of the particles measured could be clustered into eight template spectra representing a range of organic compounds including humic and fulvic acids and trytophans such as those associated with biological aerosols.

LIF based optical systems like the UV-APS, WIBS, and SPFS utilize the same two (or one in the case of the UV-APS) wave regions of ~280nm and 360 nm (Pöhlker

et al., 2012, Huffman et al, 2010) because they are the most associated with fluorescence molecules present in FBAP. Fluorescence at 280 nm is generally attributed to amino acids (such as tryptophan) and other protein structures while at the higher wavelengths around 360 nm, biological fluorophores such as NADH and flavins are known to contribute to the fluorescence. Some of the non-biological particles known to fluoresce similar to FBAP including secondary organic aerosols and polyaromatic hydrocarbons and may potentially be a source of error in measurement of total FBAP in the atmosphere (Pöhlker et al., 2012).

When biological particles are released into the atmosphere, they have the potential to interact with free radicals, volatile organic, semi-volatile organic and inorganic gas-phase compounds. Meteorological conditions such as ultraviolet (UV) light, relative humidity and temperature may also cause changes to biological aerosols. These interactions can lead to modification of the aerosol properties that may inactivate the biological component and may affect the ability to detect or sense the presence of these aerosol using different technologies. Signatures used for detection such as LIF, antibody/antigen chemistries, and polymerase chain reaction (PCR) may be altered by atmospheric processing and may impact the ability of current and fielded equipment to detect biological aerosols that have been exposed to the elements. Growth of bioaerosols due to the presence of water vapor can lead to shifts in the size distribution, which may affect respirability, infectivity, and transport in the environment.

In order to enumerate biological aerosols released into the atmosphere and distinguish them from other ambient aerosols, it is important for detection technologies

to have the ability to discriminate between biological and non-biological aerosols. Sensors that are to be used outdoors for detecting and enumerating hazardous biological aerosols need to be able to operate in environments with complex aerosol profiles. The ability to test these sensors with hazardous pathogenic biological aerosols is limited in outdoor studies. For this reason, it is important to be able to recreate such profiles in a controlled laboratory setting. Additionally, physical and chemical changes to biological aerosols in the environment due to atmospheric processing may hinder the ability for sensors to access the presence of biological species present as suspended particulates due to changes in detection signatures.

The transport of biological aerosols is largely dependent upon physical size. Changes to transportability may affect the respirability and infectivity of a biological aerosol as well as sampling efficacy. Accurate assessment of the hazard posed by a population of biological aerosols is contingent upon knowing the size distribution and potential change in size due to atmospheric properties.

The objective of this dissertation is to access the environmental factors that affect the physical and chemical properties and measurement of aerosolized biological aerosols.

Chapter 2: Sensor Characterization and Development for Measurement of Biological Aerosols in the Environment

2.1 Background

2.1.2 Defining Performance of Biological Sensors in the Presence of a Background Aerosol

The background aerosol encountered in the ambient environment contains naturally occurring biological aerosols that may fluctuate according to meteorological conditions, biological processes, or other factors (Lighthart and Shaffer 1995; Shaffer and Lighthart 1997). Tilley et al. (2001) showed significant fluctuations in the biological aerosol concentration over a period of 4 days at two outdoor sites in Australia using LIF measurements of single aerosols and bioaerosol collection systems. The ratio of biological aerosols consisting of bacteria and fungi to the total aerosol count was shown to vary significantly. Total aerosol counts were shown to range from 2246 to 5708 ppL with the absolute rates of change ranging from 1.05 to 15.51 ppL/min. The percent of bacteria and fungi present in the total aerosol counts was estimated to range from 1.5% to 5.1% for bacteria and 1.5% to 2.0% for fungi.

2.1.3 Evaluating Sensor Performance in a Laboratory

Due to the potential operational impacts, it is critical to understand how the response of a biological aerosol sensor is affected by fluctuations in the ambient environment. Ideally, sensor development and evaluation would occur in operationally relevant environments (Carrano et al. 2005). Factors such as the geographical location

and meteorological conditions can affect the performance capability of a sensor. Transportation, cost, and logistical difficulties associated with field-testing drives the need to re-create realistic field conditions within a laboratory setting to pre-screen technologies being developed. Laboratory test must attempt to represent the ambient aerosol compositions, concentrations, and temporal profiles to those in which the sensor is required to operate to evaluate the potential performance a sensor in an operational environment. These tests can then be used to characterize both the detection capability of the sensor for pathogenic and or other biological aerosols of interest, and the ability to reject false positives due to fluctuations in the ambient background. Test and evaluation of biological aerosol detection systems typically occurs in several phases. Initially, it is important to understand the sensitivity of the sensor to both intentional challenges of biological aerosols and to ambient or background aerosol. Sensors may be tested under conditions where the concentration of a challenge aerosol (biological pathogen, pathogen surrogate, or other) or background aerosol particles is increased from virtually no particle (<1 ppL) to high concentrations of aerosols (~10^3 ppL) (Semler et al. 2004; Ho 1989; Ho et al. 2001). This can measure the fundamental sensitivity of the sensor to an aerosolized material, but it does not directly evaluate how a sensor might perform in the field. Another level of evaluation incorporates a constant background aerosol concentration, such as a dust, non-biological material, or mixtures of biological and non-biological aerosol, against which a challenge material is generated (Wilson and Brady 2004). This type of test requires an aerosol wind tunnel or continuous-flow aerosol delivery system; it allows

the evaluation of sensor performance against a simple background, but it does not capture natural fluctuations in the ambient aerosol that may affect sensor performance.

2.1.4 Introduction to the Dynamic Concentration Aerosol Generator (DyCAG)

A novel test system was developed that re-creates natural fluctuations in biological and non-biological aerosol concentrations in a controllable laboratory setting. The Dynamic Concentration Aerosol Generator (DyCAG) provides a means for sensor evaluation by generation of challenges of biological aerosols of interest at specific concentrations in the presence of various levels of environmentally relevant aerosols using a unique aerosol generation and test system. By utilizing the dynamic capability of the DyCAG system in combination with measured concentrations and temporal profiles of naturally occurring aerosols from ambient data, test scenarios can be re-created in a contained laboratory setting that provides simulated ambient conditions for sensor evaluation. The DyCAG can generate up to seven independent aerosols, four of which can vary in concentration independently, before combining and mixing in an airstream for delivery to sensors being evaluated. This type of testing is very important for the development of sensor systems that are to be utilized for detecting pathogenic biological aerosols, such as those that may be utilized as a weapon of mass destruction against the homeland or military assets. For a deployed sensor, not detecting the presence of an infectious biological aerosol during an attack can have significant ramifications (disease and potential loss of life of large populations). However, the converse of this, falsely detecting the presence of a biological attack can

also be problematic, as it can lead to unnecessary response and hazard mitigation (distribution of prophylaxis or wide-area decontamination) that is costly and a waste of resources.

In this dissertation, the capability of the DyCAG system to generate a background aerosol, within a controlled laboratory setting, that fluctuates similar to those observed from outdoor measurements was demonstrated. Surrogates for pathogenic bioaerosol challenges were overlaid above these background aerosols to exhibit how this testing technique could be used to evaluate sensors being developed for measurement of biological aerosols in the ambient environment.

2.2 Materials and Methods

2.2.1 Description of the Aerosol Test System

The DyCAG (Figure 1) consists of three main control regions: an aerosol generation and injection region, a mixing region, and an isokinetic sampling region. The DyCAG aerosol generation and injection region can combine aerosols from up to four ultrasonic generators and two aerosol materials from Collison nebulizers (Table 1) and the exhaust of a diesel engine. Individual aerosol components are generated and conditioned independently from one another and then mixed to form the desired complex imitation of an ambient environmental aerosol mixture.

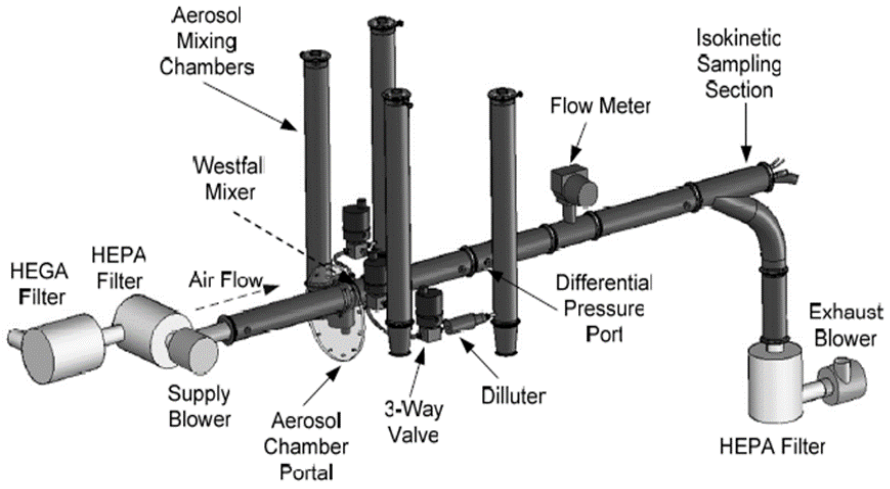

Figure 1 - Overview of Dynamic Concentration Aerosol Generator (DyCAG). The Aerosol generation and injection section consists of four Aerosol Capacitance Chambers (ACCs) used as a reservoir for drying the aerosols created using ultrasonic nozzles. The ACCs are used for charging the aerosol concentration prior to entering into the main DyCAG air stream. Dry clean air is provided upstream of the aerosol injection and used to carry the generated aerosols downstream to the sampling region. A Westfall mixer is used upstream of the sampling region to provide a well-mixed aerosol profile downstream. Isokinetic sampling ports designed specifically for each sensor/collector being tested ensures no bias in the concentration and uniformity of the delivered aerosols.

To allow newly generated aerosols time to dry (if necessary) and to allow the concentration of aerosol to become consistent before it is introduced into the DyCAG flow stream, Aerosol Capacitance Chambers (ACCs; Figure 2) are used to divert the aerosol before it enters the DyCAG. The ACC provides a reservoir of high-concentration aerosol from a single source that can then be metered into the bulk airflow and mixed with aerosols from other sources.

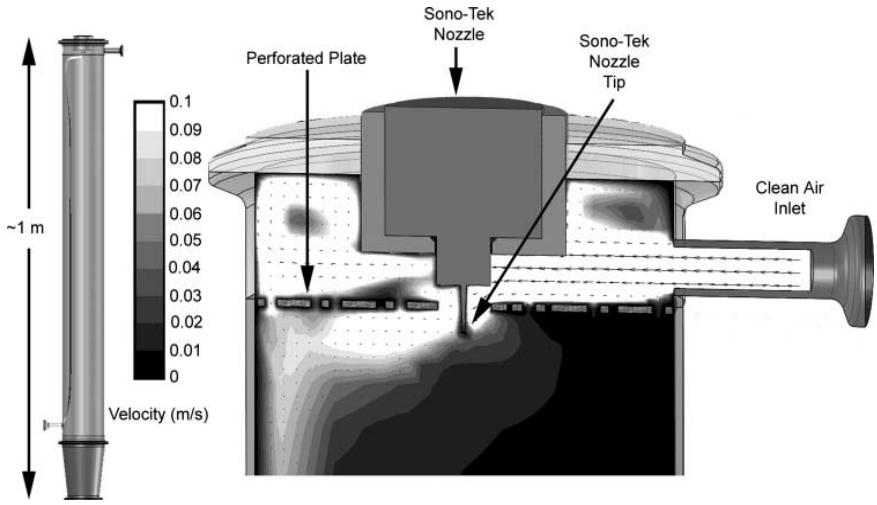

Figure 2 - Computational Fluid Dynamics Simulation of Final ACC Design. (A) CFD analysis shows that 5 µm particles generated via Sono-Tek are introduced at the top of the ACC and have approximately 55 seconds of drying time when the air inlet is at 5.0 Lpm. Particles greater than 30 µm fall to the bottom of the ACC to prevent carryover and non-aerosolized liquid from entering into the DyCAG. (B) Velocity profile of aerosol generation using Sono-Tek nozzles orientated vertically in the ACC.

2.2.2 Aerosol Generation in the DyCAG

Sono-Tek ultrasonic atomizers are used for aerosol generation and are the primary source of aerosols for the DyCAG system. Liquid is fed to the Sono-Tek nozzle (Table 1) using a dual-feed syringe pump (Table 1). A Broadband Ultrasonic Generator (BUG) (Table 1) generates high-frequency vibrations that disrupt the liquid flow at the nozzle tip and atomize the liquid. These atomizers allow for the discrete control of the injection rate of aerosol mass into the ACC and do not increase the air pressure within the ACC. The dry particle size of the aerosol generated by the Sono-Tek is controlled by the concentration of the solute in the liquid being atomized (Hinds 1999). By

varying the rate of liquid injection, the amount of material generated can be modified and used to control the concentration of material introduced into the test chamber. Droplets generated by the Sono-Tek require drying time before introduction to the mixing region to allow solvent evaporation. The ACC design uses the Sono-Tek nozzles pointing downward into the capacitance chamber, parallel to a flow of dry compressed air entering the ACC at flow rates variable between 1 and 15 Lpm (Figure 2). To produce a well-controlled aerosol within the ACC, the source of the liquid being delivered to the nozzle must be a well-mixed suspension of material. A stir bar is placed within the syringe and a magnetic stir plate is held in place above the syringe to mix the suspension before it is pumped to the nozzle. Computational fluid dynamics (CFD) simulations, using Cosmos FloWorks (Structural Research and Analysis Corp., Los Angeles, California) of the ACC show that a 5 μm particle has approximately 55 seconds of drying time when the compressed air inlet is at 5.0 Lpm. According to the model, particles 30 μm or greater will fall to the bottom of the ACC, out of the airflow, preventing carryover between runs. In this way, non-aerosolized liquid from the Sono-Tek nozzles and agglomerated particles larger than 30 μm are collected at the bottom of the ACC, while the test aerosol travels down the ACC and exits through the small tube in the side of the wall with sufficient time to dry.

A Collison 3-Jet nebulizer (Table 1) can be used to generate a background aerosol that does not pass through an ACC. Clean, dry particle free air is supplied directly to the Collison nebulizer using a filtered air supply (Table 1) at 20 psi. The Collison nebulizer is attached to a mini-stir bar plate running at full speed with a 1-inch

stir bar placed inside the nebulizer reservoir to maintain the suspension and minimize settling of the material to the bottom of the container.

2.2.3 Aerosol Delivery and Sampling in the DyCAG

Aerosols are uniformly mixed with filtered air using a modified Westfall injection mixer (Westfall Manufacturing Co., Bristol, RI). The injection module consists of a modified orifice with injection ports situated just downstream of the Westfall mixer (Figure 1). Computational models from Cosmos FloWorks (not shown) indicate that the velocity profile across the tube is uniform and that 1 μm aerosol particles introduced at the injection ports are mixed throughout the cross-section at 10-tube diameter downstream of the mixing element. Two Ametek blowers (Table 1) are used to provide the bulk mixing flow in the DyCAG system. Air is drawn from the room through a high-efficiency particulate air (HEPA) filter and a high-efficiency gas abatement (HEGA) filter to remove particulate and gasses that may complicate the test process. Flow is exhausted through another HEPA filter to prevent the aerosolized test material from escaping into the surrounding laboratory. The peak airflow using this arrangement is ~2500 Lpm, which allows for a wide variety of sensors and reference equipment to sample isokinetically and without influencing one another. Bulk flow is measured immediately upstream of the sensor sample location to ensure accurate measurement of the system flow and calculations of the volume concentration. A flow meter (Table 1) with a sampling inner diameter that equal that of the DyCAG delivery tube is used for flow measurement. This eliminates any

additional parts that may protrude into the aerosol flow. An Omega X differential pressure sensor (Table 1) is used to set the system to an operating pressure of –0.1 in. H2O to allow the DyCAG to perform as the primary aerosol containment barrier.

The aerosol concentration and composition in the DyCAG delivery tube is controlled and varied by regulating the flow from each of the four ACCs with Omega mass flow control (Table-1).

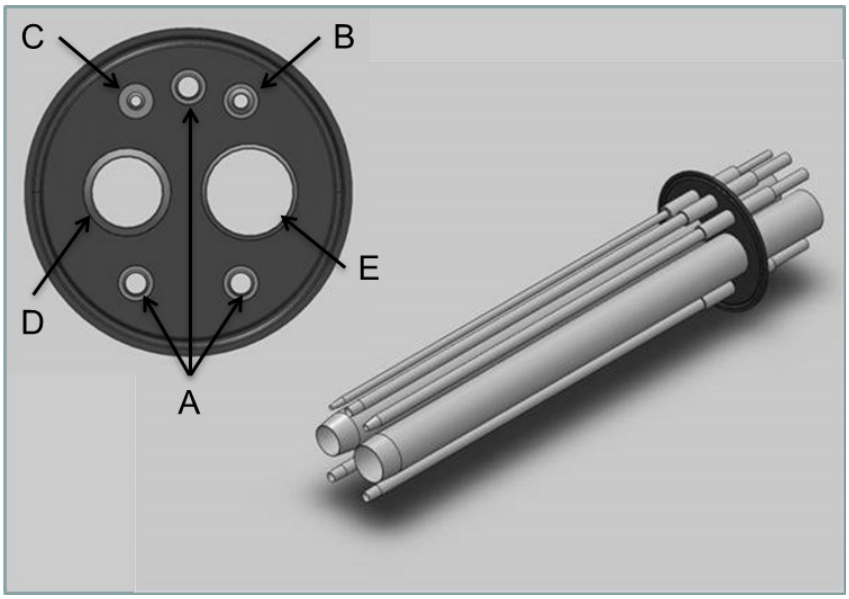

Figure 3 - Example DyCAG Isokinetic Sampling Port. The inset image shows the arrangement of isokinetic sampling ports: three ports for reference filters or impingers (A: 9-12.5 lpm), a port for the UV-APS (B: 5 lpm), and several ports designed for other instrumentation that samples at a variety of flow rates (C: 1.5 lpm; D: 200 lpm; E: 400 lpm). The (A) ports were used to study the uniformity of aerosol in the DyCAG.

Multiple biological aerosol sensors can be evaluated simultaneously in the DyCAG, along with reference measurements, using isokinetic sampling probes for

each unit to sample from the bulk flow after mixing (Figure 3). The designs of the sampling probes for each sensor or reference measurement are generated based on the cross-sectional air velocity of each sensor inlet (calculated from manufacturer-specified flow rate) against the entering air velocity of the DyCAG delivery system (2500 Lpm) to optimize particle sampling and to avoid any sensor-to-sensor sampling bias (Baron and Willeke 2001). These calculations are used to predict the sampling tube size that will allow for the velocity at each sampling tube to be equal to the velocity in the mixing and delivery tube, which ensures that all sensors will sample the same aerosol concentrations. Inlet ends are tapered to knife-edges to minimize the frontal area of the sampling tubes. The cross-sectional area of the tube that is obstructed by the sampling probes during these experiments is approximately 20% of the cross-sectional area of the main airflow tube. Unsampled air continues past the sample probes and leaves the DyCAG main flow tube through a T-Y coupling into a HEPA filter (Figure 1).

Table 1- DyCAG Components			
No.	**Part**	**Model No.**	**Manufacturer**
1	Nozzle	06-04010	Sono-Tek Corporation, Milton, NY
2	Dual-feed Syringe Pump	11-01061	Sono-Tek Corporation, Milton, NY
3	Broadband Ultrasonic Generator (BUG)	06-05108	Sono-Tek Corporation, Milton, NY
4	Collison 3-Jet Nebulizer	CN24	BGI Inc., Waltham, MA
5	Filtered Air Supply	3076	TSI Inc., Shoreview, MN
6	Injection mixer	–	Westfall Manufacturing Co., Bristol, RI
7	Blowers	119105E	Ametek Inc., Paolie, PA
8	Flow Meter	600-9	Thermal Instrument Co., Trevose, PA
10	Mass Flow Controller	FMA 5400-5500	Omega Engineering Inc., Stanford, CT
9	Omega X Differential Pressure Sensor	PX653-2.5BD5V	Omega Engineering Inc., Stanford, CT
10	Ultraviolet Aerodynamic Particle Sizer (UV-APS)	3314	TSI Inc, Shoreview, MN
11	All-glass Impingers	7540	Ace Glass Inc., Vineland, NJ
12	Autoplate 4000 Spiral Plating System	4000	Spiral Biotech, Inc.
13	QCount System Colony Counter	–	Spiral Biotech, Inc.

2.2.4 Summary of Experiments

2.2.4.1 Characterization of DyCAG Cross-Sectional Mixing

The DyCAG was characterized to ensure that it could deliver well-mixed aerosol to multiple sensors being evaluated and reference instruments equivalently. A SonoTek nebulizer was used to generate 3.1 μm green fluorescent polystyrene latex spheres (Catalog# GO300, Thermo Scientific, Waltham, MA) through one of the ACCs. This aerosol was sampled at three locations in the isokinetic sampling port (Figure 3) using Isopore filters with a 0.8 μm pore size (Catalog # ATTP04700, Millipore, Billerica, MA) sampling at 9 Lpm for 20 min, during 5 separate experiments. The filter flow rate was controlled continuously throughout the 20 min sampling period using a flow controller (Model # MCR-250SLPM-D/5M, Alicat Scientific, Tucson, AZ). The filters were recovered by submerging each filter in 20 mL of 0.22 μm sterile-filtered deionized water (SFDI H_2O) in a 50 mL conical tube and placing it on an orbital shaker for 20 min. The fluorescence intensity of the beads in suspension was measured using a Trilogy 7200 fluorimeter (Turner Designs, Sunnyvale, CA). The mean and standard deviation of the fluorescence intensities from the three reference filters were calculated for each experiment. The standard deviations from each experiment indicate that the variation in aerosol concentration between the three locations was between 1.3% and 5.3%, with a mean of 3.1% for all 5 experiments.

2.2.4.2 Demonstration of Dynamic Aerosol Generation

A series of experiments were conducted that demonstrated the capabilities of the DyCAG system to recreate aerosol profiles with varying rates "ramps" representative of outdoor aerosol. The repeatability of the ramp testing was evaluated for two series of designed ramps. For these experiments, *Bacillus thuringiensis* kurstaki (Btk), a bacterium similar to the infectious pathogen *Bacillus anthracis*, the causative agent of the disease anthrax, was released into the DyCAG to simulate an intentional biological release of a pathogen and to demonstrate the potential use of the DyCAG for evaluating the detection capabilities of biological sensors. The Btk spores were obtained directly from Dugway Proving Grounds (DPG), U.S. Army, Salt Lake City, Utah, and rehydrated at 10 mg/mL in sterile filtered deionized water (SFDI H2O) for at least 24 h and stored at 4°C until ready for use. The rates calculated from data reported in Tilley, et al., (2001) are very slow (~10 ppL/min) and proved to be difficult to quantify reproducibly with the available reference equipment and sampling arrangement. Therefore, the ramps were designed to produce fluctuations in the test aerosol that are representative of the types of fluctuations observed in ambient aerosol but at rates that are more easily generated and measured in the DyCAG (Figure 4). A constant background aerosol of Arizona Road Dust (ARD; Table 2) mixed in a 1:1 ratio with $CaCO_3$ aerosol was generated using one of the Sono-Tek nozzles. This mixture is intended to reproduce the ionic composition of dust collected in Saudi Arabia (U.S. Army Environmental Hygiene Agency 1994). Two other background aerosols, one biological and one non-biological, were ramped up and down. The non-biological

background consisted of a mixture of Atlantic seawater, rayon flock, and kaolin (Table 2). The non-biological mixture is intended to represent other non-biological aerosol often found in the environment in areas of human activity such as sea-salt aerosol, material from clothing, and clay material that is prominent in many soils. The biological background aerosol consisted of Gram-positive *Bacillus subtilis* bacterial spores, *Penicillium brevicompactum* fungal spores, and Gram-negative *Yersinia rhodei* mixed in a ratio (~50% gram-positive, ~45% gram negative and ~5% fungal; Table 2) that is representative of biological aerosol that has been collected in Laurel, MD (Santarpia et al. 2010). Initially dry materials were prepared for aerosolization by hydration in SFDI H_2O, at the concentrations listed in Table 2, and were mixed by vortex. After preparation, all materials were stored at 4◦C until needed. Each ramp cycle design consisted of two-hour experiments broken into 40-minute cycles (Figure 4)

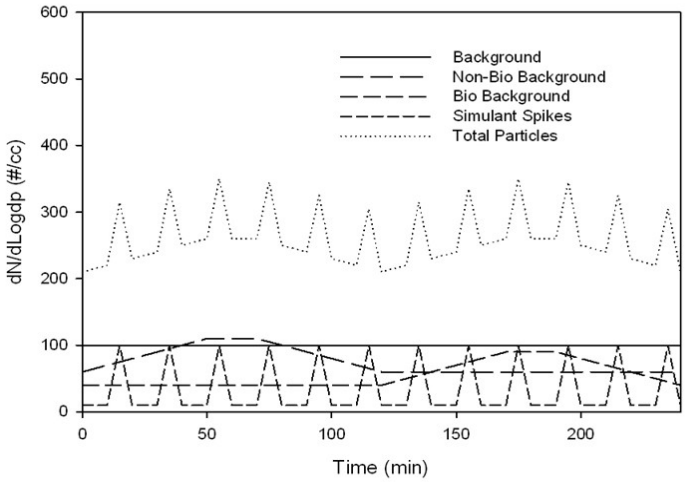

Figure 4 - Illustration of Ramp Aerosol Challenges. The background material that ramped alternated from one ramp cycle to the next. During each 40-minute cycle, sensors were exposed to two 15-min periods of background aerosol followed by a 5 minute Btk challenge. The Btk challenges reach their peak concentration in 10 sec and are maintained until the end of the 5-minute challenge. By overlaying the Btk challenges throughout the ramp cycle, the sensors were challenged to detect simulant while the background was increasing, held constant, and decreasing.

Table 2 - Background Aerosol Components and Corresponding Generation Techniques

Testing Description	Name	Concentration of Stock Material	Vendor Information	Generation Method
Background Aerosol	Arizona Road Dust/$CaCO_3$	1 mg/mL	PTI, Catalog # ISSO 12103-1, A1 Sigma Aldrich, CAS 471-34-1	Sono-Tek
Non-Bio Background	Atlantic Sea Salt	Stock Concentration	Atlantic Seawater, OSIL, UK	Sono-Tek
Non-Bio Background	Kaolin	0.5 mg/mL	Sigma Aldrich, Catalog # 1512	Sono-Tek
Non Bio Background	Rayon Flock	0.5 mg/mL	WR200Z, International Fiber Corporation	Sono-Tek
Bio Background	*Yersinia rhodei*	9.1E06 cfu/mL	American Type Culture Collection #43380	Sono-Tek
Bio Background	*Bacillus subtilis*	1.0E7 cfu/mL	Dugway Proving Grounds	Sono-Tek
Bio Background	*Penicillium Brevicompactum*	1.1E6 spore/mL	Research Triangle Institute	Sono-Tek

During each 120-min ramp cycle, one of the background aerosols was held constant at the minimum concentration, while the other was increased over a 40 min period to the maximum concentration, held at the maximum concentration for a 40min period, and ramped down to the minimum concentration for 40 min. The background material that ramped alternated from one ramp cycle to the next. Each 40 min cycle consisted of two 15-min periods of background aerosol followed by 5-min *Btk*

challenges. The *Btk* challenges reached their peak concentration in 10s and were maintained until the end of the 5-min challenge (Figure 4). By overlaying the *Btk* challenges throughout the ramp cycle, sensors could be challenged to detect the surrogate for the bioaerosol pathogen while the background was increasing, held constant, and decreasing. Each ramp experiment was repeated twice for demonstration of repeatability. Controlling the compressed air flowrate for each ACC produced the fluctuations in aerosol concentration in the DyCAG. For these experiments, the non-biological aerosol ramps were created by changing the compressed air flow rate linearly over a period of 40 min from 1 to 14 Lpm. After reaching the peak concentration, the flow rate was maintained at 14 Lpm for 40 min, and then ramped back down to 1 Lpm over a period of 40min. The biological background flow rates were ramped from 1 to 8 Lpm and back down to 1 Lpm in a pattern similar to the ramps described for the non-biological background. Two instruments were used to quantify the aerosol challenges in the DyCAG. A UVAPS (Table 1) was used to quantify the aerosol concentration, aerodynamic size distribution, and fluorescent size distribution continuously with a sample time of 10s. Reference samples were collected using sterile all-glass impingers (AGI-30; Table 1). The AGI-30s sampled the airflow at 12.5 Lpm into 20 mL of SFDI H_20. Samples were plated in triplicate on Tryptic Soy Agar via the Spiral Biotech Autoplate 4000 Spiral Plating System (Table 1) and then enumerated via the Spiral Biotech Q-Count System (Table 1). Samples with expected concentrations greater than 1×10^5 colony-forming units per milliliter (cfu/mL) were serially diluted with SFDI H_20 to achieve an approximate concentration of 1.0×10^3 cfu/mL and then plated.

Plated samples were allowed to dry before they were inverted and incubated overnight (14–18 h) at 37°C. The average concentration (cfu/mL) of the three plates was reported for each sample. The starting volume in each AGI-30 was 20 mL of SFDI H_2O.

3.0 RESULTS

3.1 Aerosol Profiles during Testing

A series of experiments were performed that demonstrated the ability of the DyCAG to generate dynamic aerosol populations that simulate ambient aerosols populations in a controlled laboratory environment. Particle concentrations measured with the UV-APS® during these experiments were comparable to particle counts observed by Tilley et al. (2001). By gating the fluorescence of particles measured in the UV-APS using a relative fluorescence value of 3 to discriminate between non-biological and biological particles (Huffman et al. 2010), the biological aerosol, the non-biological aerosol, and the combined aerosol concentrations were calculated and plotted (Figure 5). The actual total counts for both ramps 1 and 2 ranged from about 7 × 103 to 1.5 × 104 ppL with the average at approximately 7.8 × 103 ppL. For particles greater than 1 μm the range of total counts was from 6 × 103 to 1.2 × 104 ppL. During the second ramp of each experiment, the biological background was observed to contribute to an increase in the baseline biological aerosol concentration of particles greater than 1μm at about 4.3 × 103 ppL. By separating the two types of aerosols based on relative fluorescence, the Btk spikes were easily observed during each of the ramps.

The Btk aerosol concentrations were measured by the UV-APS to be approximately 2.5 × 103 ppL for both experiments.

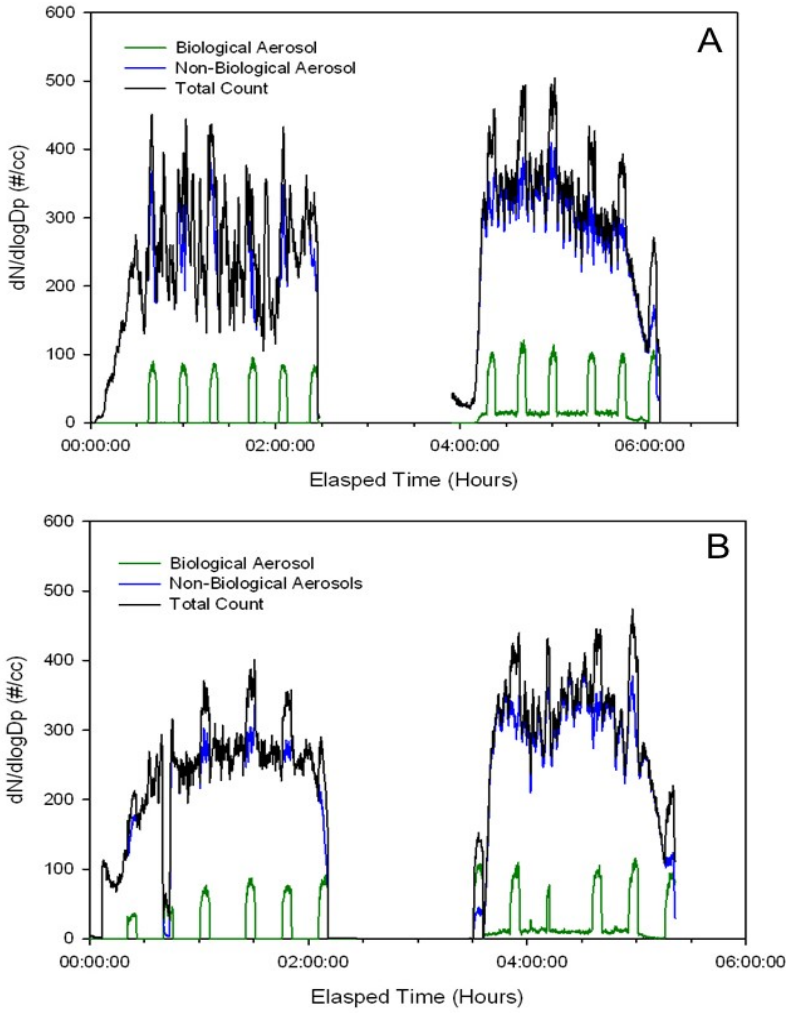

Figure 5 - Example of UV-APS Data Showing Ramp Experiments Created Using the DyCAG. The green trace depicts biological aerosol (relative fluorescence >3), the blue trace shows non-biological aerosol, the black trace shows combined aerosol concentration. Two ramp cycles were performed per experiment. Two experiments were performed on different days are shown (A and B). The first ramp was created by changing the non-biological background while holding the biological background constant. During the second ramp, the biological background was ramped while the non-biological background remained constant. During each ramp six spikes of Btk were released. Between reach ramp cycle, the DyCAG aerosol is allowed to baseline to zero and then restarted. Approximately 45 minutes into the first ramp of the second experiment, communication between the DyCAG and the control computer was lost causing aerosol generation to stop briefly.

3.2 Repeatability of Ramp Aerosol Profiles between Experiments

The UV-APS data indicated that the overall aerosol behavior in the DyCAG was consistent with the experiment design during both ramps on both days of experiments; however, the behavior of the aerosol over short timescales and apparent inconsistencies in the aerosol concentration, despite maintaining control over aerosol generation control parameters, were obvious from the data. Two primary features in the recorded UV-APS data indicated areas where control over the aerosol concentration in the background aerosol was problematic. Beginning around 1:45 h into the first ramp and at approximately the same time in the second ramp during the first day (5:45 h into the experiment; (Figure 5a) there was an unplanned decrease in the aerosol concentration. During these periods, the operating parameters of the Sono-Tek nozzle remained the same and the rate of change of the airflow in the ACC remained consistent (Figure 6) however, in both cases the aerosol concentration in the DyCAG dropped unexpectedly (Figure 5a). This occurred again, to a lesser degree, during the biological ramp on the second day of experiments at approximately hour 4:00 to 4:30 (Figure 5b). The reason for these unexpected changes was not apparent, but it may be due to changes in the uniformity of the suspension in the syringe (despite the continuous stirring of the suspension throughout the experiments). On the second day of experiments, different anomalies were observed despite identical control parameters. During the second day (Figure 5b) there was an initial lag in the increase of background aerosol in both the non-biological and biological background ramps. Despite this, the shape of the non-biological ramp was more representative of the experimental design than the non-

biological ramp during the first day. It was also notable that there were various spikes within the overall aerosol concentrations (Figure 5). These spikes appeared more prominent in the non-biological ramp than in the biological ramp during the first experiment (Figure 5a) and more prominent in the biological ramp during the second experiment (Figure 5b). This may indicate that the suspension used to produce the more irregular aerosol was less uniformly mixed in the syringe prior to aerosolization than the other one. The aerosol flow rate profiles (Figure 6) were virtually identical on both days of testing (not shown) indicating that the source of these anomalies is likely in the aerosol generation process. Spikes in aerosol concentrations are often observed in ambient data and while these spikes were not a part of the designed experiment, and compromise experimental reproducibility, they are consistent with the types of temporal variability in aerosol concentrations that are observed in the ambient environment.

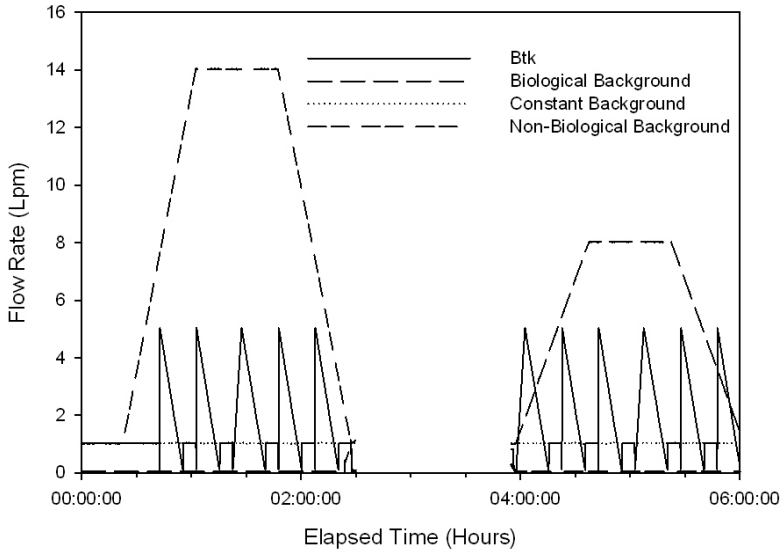

Figure 6 - Flow rates Recorded for ACC Carrier Flow During the First of the Two Ramp Experiments. Since the Sono-Tek aerosol, generators are run with the same parameters into each ACC the aerosol concentration in the DyCAG from each ACC is controlled primarily by changing the flow rates. Note the small step function in flow rate in the Btk channel. This is used to clear out the ACC between challenges. During these periods, aerosol is sent out through a HEPA filter rather than through the DyCAG. This flow rate data is virtually identical between the two days of experiments.

3.3 Concentrations of Bioaerosols During Ramp Testing

The average *Btk* concentration for the 5 min challenges determined via culture of the samples collected with the AGI-30 during the ramp testing was $1.2 \times 10^3 \pm 5.1 \times 10^2$ during the first set of two ramps and $1.3 \times 10^3 \pm 8.2 \times 10^2$ cfu per L of air during the second set (Table 3). The *Btk* aerosol challenge concentrations were estimated from the AGI-30 samples by assuming a liquid evaporation rate from the impinger of 20.0–0.2*t* (where *t*=sampling time) for 5 min (Lin et al. 1997) a collection efficiency of 50% and a particle retention efficiency of 95% (Kesavan et al. 2010). The reported assay values account for these losses and are reported as the calculated airborne concentration

of *Btk* for each challenge. The aerodynamic size distribution for the non-biological, biological, and combined distributions were generated by using the same gating of fluorescence for each ramp cycle (Figure 7). The size distribution of *Btk* aerosol, best represented by the first ramp of each experiment due to lack of other fluorescent particles, (Figure 7a) showed a peak size at approximately 3.3 μm. Given the ratio of culturable *Btk* to the UV-APS measured biological aerosol concentration and the physical size of bacterial spores of *Btk* ranging from 1.07–1.99 μm (Carrera et al. 2007), it was likely that the biological aerosols consisted of a mixture of multiple spores per particle, as well as dry media and buffer. It is also likely that as many as 50% of the fluorescent aerosol did not contain viable spores. When the biological background was present at a high concentration during a ramp (Figure 7b, distribution recorded during the second ramp cycle of the first experiment) the biological aerosol size distribution showed a broad tail in the fine mode due to the presence of the biological background (a mixture of bacterial and fungal spores and bacterial cells). The non-biological portion of the aerosol is a mono-modal with a peak ranging from 0.84 to 1 μm (Figure 7b). When the size distribution of biological aerosols with biological background present and absent is compared, a broader distribution is observable when the biological background is present with a larger concentration of particles occurring between 1 to 3 μm due to the presence of the biological background mixture (Figure 8). Figure 8a–d shows a 10s fluorescence distribution of each type of aerosol challenge, non-biological background, non-biological background when *Btk* is present, biological background, and biological background when *Btk* was present. In the case of the non-biological

background ramp, when no *Btk* was present, a broad distribution of aerosols with multiple peaks was observed, the addition of *Btk*, shows a single mode biological component, but the non-biological background distribution remained relatively similar to the distribution observed in the absence of *Btk*. This suggests that biological fluorescence information could be used to discriminate between biological and non-biological aerosols, and allows for a semi-quantifiable measure of the biological aerosol component that may be correlated to other biological measurements techniques. For the second ramp, a broader distribution of the biological aerosols with a higher concentration of particles between 1 and 3 μm was present due to the biological background (Figure 7b). These particles are observable in the fluorescence distribution shown in Figure 8c when *Btk* was not present.

Table 3 - *Btk* Concentration Determined by Culture for Ramp Experiments (cfu/L-air)

Release Number	Cycle 1	Cycle 2	Cycle 3	Cycle 4
1	3.05E+01	1.07E+03	1.31E+03	4.57E+02
2	1.65E+03	1.07E+03	1.99E+03	8.88E+02
3	1.07E+03	1.26E+03	2.17E+03	7.62E+02
4	1.92E+03	1.19E+03	3.36E+03	1.25E+03
5	1.62E+03	9.78E+02	7.35E+02	1.07E+03
6	1.86E+03	9.46E+02	1.07E+03	7.31E+02

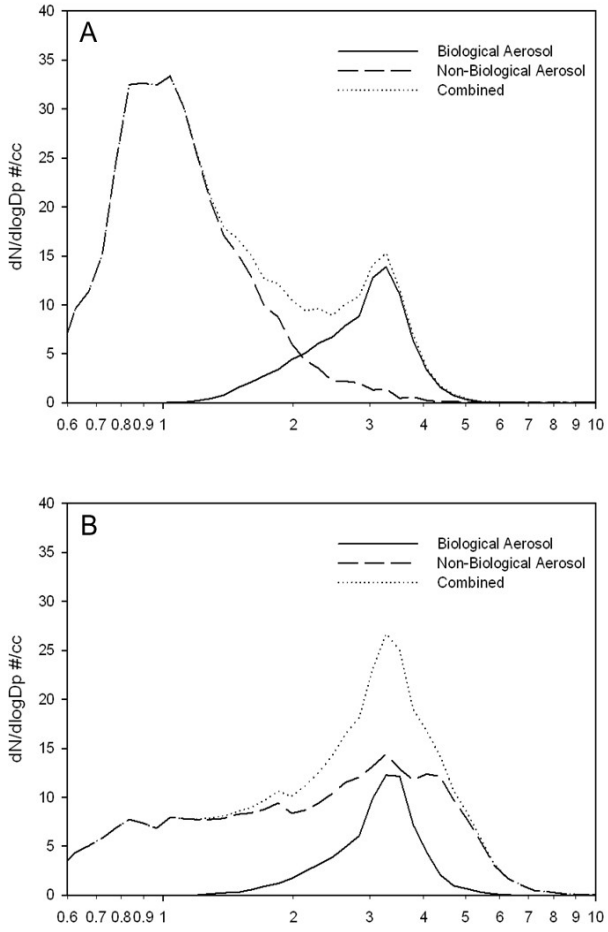

Figure 7 - Comparison of Size Distributions for Biological Aerosols With Biological Background Present and Absent. A broader distribution is observable when the biological background is present with a larger concentration of particles occurring between 1 to 3 µm due to the presence of the biological background mixture.

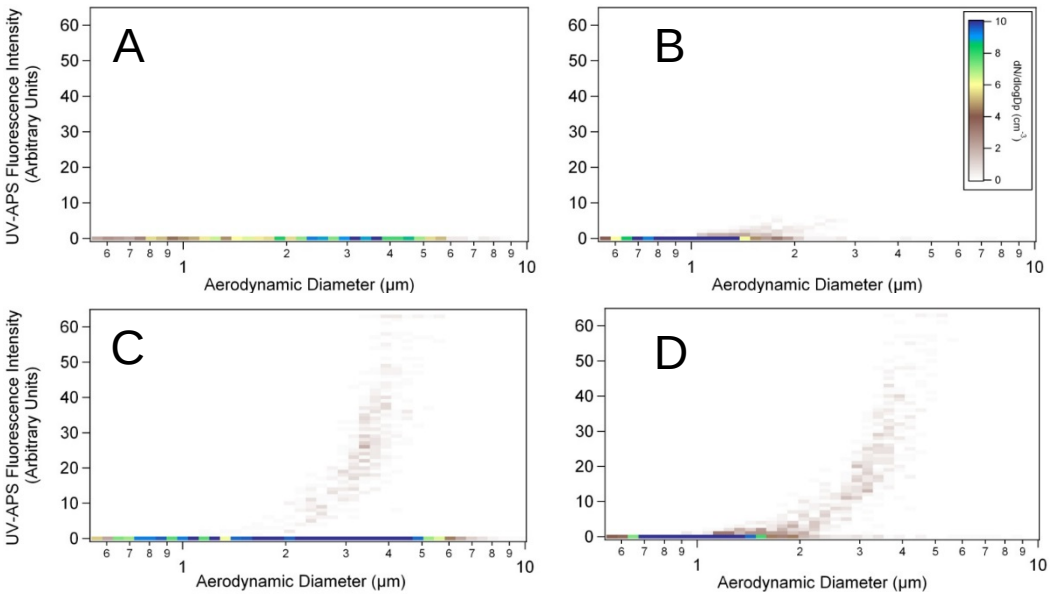

Figure 8 - Fluorescence Properties of Aerosol During The First Two Cycles of Ramps as Measured by the UV-APS. (A) shows the size-resolved fluorescence distribution when only the non-biological background was generated, while (B) shows the same measurement when Btk was generated on top of this background aerosol. (C) shows the size-resolved fluorescence distribution when only the biological background was being generated, while (D) shows the same measurement when Btk was generated on top of this background aerosol.

4.0 Summary and Discussion

Various biological sensors have been developed that utilize multiple detection technologies to measure the presence of biological aerosols. It is not possible to test these sensors for the ability to detect and identify biological aerosols of interest, such as those that cause disease and may be harmful in outdoor environments. Therefore, sensors need to be tested in a laboratory setting that is representative of the operationally relevant environments in which they are required to perform. Real-time information about ambient aerosol concentrations, size distributions, and chemical and biological makeup can be used to recreate these scenarios in a laboratory setting. A

limited amount of this type of data has been generated that demonstrates the fluctuations of the aerosol populations. Traditional sensor testing is often static, consisting of pulse aerosol challenges with little to no manipulation of the background aerosol. To evaluate the performance of biological sensors under conditions that are representative of real-world environments there exists a need to recreate ambient aerosols populations within a controlled laboratory setting. The DyCAG system is capable of generating a dynamic range of aerosols fluctuating in concentration and composition. Ramping experiments, in which the background aerosol concentration was dynamic, were performed during two series of tests. Single particle biological fluorescence measurements and microbial culture were used to quantify the biological, nonbiological, and total aerosol concentrations during testing. These experiments demonstrated the ability to simulate representative ambient aerosol fluctuations within a controlled laboratory setting; however, improvements to the airflow control are needed to reproduce the slow rates of change that have been observed in available ambient datasets (Tilley et al. 2001). The apparent difficulty in maintaining the consistent aerosol generation needed to produce the background ramps for greater than 1.5 h demonstrates the need for improved methods for generating consistent aerosol over long periods. In addition, more detailed data on the composition, fluctuations, and biological diversity of ambient aerosol at various geographic locations and seasons is needed to build a stronger data set for experimental challenges. These datasets could be used to better define the shape and composition of fluctuations in laboratory test

aerosols in order to provide more realistic backgrounds to evaluate emerging biological aerosol sensors in the laboratory.

The potential for biological aerosols to remain aloft in the environment for long periods due to various forces such as wind and turbulence allows for potential modifications by exposure to atmospheric processes such as water vapor, solar radiation, or oxidants or other chemicals. The testing approach described this far does not account for adulteration to the particulates due to the various processes that may change the spectral or physical signatures. However, very little data exists as to what these changes may be and how they affect detection signatures or the physical properties of the aerosol. In the two next chapters, the potential for these factors to change the signatures of biological aerosols as well as the physical properties is discussed.

Chapter 3: EFFECT OF ATMOSPHERIC PROCESSING ON THE SPECTRAL MEASUREMENT AND VIABILITY OF BIOLOGICAL AEROSOLS

3.1 INTRODUCTION

3.1.1 Background

There are many other mechanisms by which bioaerosol particles may undergo chemical or physical changes in the atmosphere (Deguillaume, et al., 2008) including chemical reactions with nitrogen oxides, OH radicals, uptake of water or desiccation due to fluctuations in relative humidity (RH), solar irradiation initiated photochemical reactions, agglomeration with other aerosols and interactions with secondary aerosol forming precursors. In addition, bioaerosols may also cause changes to other aerosols or chemicals in the atmosphere through metabolic interactions with organic compounds (Deguillaume, et al., 2008; Ariya and Amyot, 2004; Sun and Ariya, 2006). The effect of these mechanisms on and the roles of bioaerosols in the atmosphere is an ongoing topic of study.

3.1.2 Previous Studies Investigating Open Air Factor

Vegetative bacterial bioaerosols (e.g. *Escherichia coli, Serratia marcescens, Francisella tularensis, Brucella suis,* and *Staphylococcus epidermidis)* (May, Druett, & Packman, 1969) and viruses (Benbough and Hood (1971) have been shown to be

sensitive to components, known as “open air factors” (OAF), in outdoor environments (Cox et al., 1973). Other types of bacteria have been shown to be insensitive to OAF including *Bacillus subtilis* and *Bacillus anthracis* spores and *Micrococcus radioduran (*May, Druett, & Packman, 1969, Cox et al., 1973). OAF is hypothesized to be the result of exposure to ozone, olefins, and ozone-olefin reaction products (May, Druett, & Packman, 1969). De Mik and DeGroot (1977) showed inactivation of the φX174 bacteriophage due to damaged proteins when exposed to either ozone or to cyclohexane. In combination, ozone and cyclohexane resulted in inactivation via damage to both proteins and DNA.

3.1.3 Review of Biological Aerosol Sensing and Characterization Methods

Several kinds of sensors have been developed to detect and characterize bioaerosols. Identification of microbes to the genus or species level is accomplished using antibodies to specific proteins on cell or viral surfaces or via DNA/RNA identification using sequencing or PCR. Rapid reagentless detection methods based on intrinsic fluorescence of certain fluorophores have been developed and are commercially available (Wilson and Defreeze, 2003; Schroder et al., 1999; Eversole et al., 2001; Hill et al., 1999; Tilley et al., 2001). Cells and most proteins contain tryptophan, which when excited by UV light, emits fluorescence peaking between 310 to 350 nm. Additionally, cells contain NADH, which emits light in the 400 to 500 nm range (Hill et al., 1995; Hill et al., 2013) when excited by near-UV light. Chemical changes to bioaerosols caused by interactions with constituents in the atmosphere may

diminish detectability in cases where specific molecules (e.g., tryptophan, nicotinamdides, flavins, surface antigens, DNA) that are used for identification are modified (Santarpia et al., 2012, Pan et al., 2014). The spectroscopic signature detected by a sensor is dependent upon the wavelength used for generating the fluorescence (excitation wavelength), the emitted fluorescence (spectrally resolved or in one or more bands occurring over some wavelength range) as well as the ratios of the fluorophores within the bioaerosol being interrogated. In many cases, light scattering from the particle is also used to infer size and shape information, which may aid in discrimination. Changes in detectability could result in misinterpretation of measurements and underestimation of bioaerosol concentrations in the environment.

3.1.4 Oxidation of Biological Fluorophores Used for Biological Aerosol Sensing

Effects of ozone on the fluorescence properties of tryptophan in solution have been reported (Ignatenko, et al., 1982; Ignatenko, 1988, Mudd et al., 1969). Santarpia et al. (2012) showed significant fluorescence decreases in the 330 nm peak emission of *Yersinia rohdei* and MS2 bacteriophage aerosols, when excited at 263 nm in the presence of high concentrations of ozone (>300 ppb) at relative humidity 35-43%. Further, a more rapid decrease in the emission spectra was observed when relative humidity was increased by less than 7%, indicating that uptake of water by bioaerosols may be important in the facilitation of atmospheric changes to the spectral properties. Effects were seen before the product of time and concentration reached the 8-hr Environmental Protection Agency (EPA) limit for exposure to ozone. The observed

changes in fluorescence in the 300 nm peak are in agreement with the effects of ozone on tryptophan fluorescence in solution previously reported by Ignatenko et al. (1982). However, these experiments were performed at higher than typical ozone levels in the United States and with limited control over RH. Pan et al., (2014) measured changes in spectra of eight-amino-acid-peptide aerosols containing one tryptophan, one tyrosine, and one phenylalanine per molecule, at atmospherically relevant ozone concentrations (0 or 150 ppb) at different RH levels (~20%, 50%, or 80%). The 263 nm fluorescence of the peptide in the 280-560 nm band was shown to decrease with time of exposure to ozone while the 351 nm-excited fluorescence between 430 and 700 nm was shown to increase. Both of these changes are consistent with the oxidation of tryptophan to N'-formyl kynurenine (NF) and kynurenine (KY) (Ignatenko, et al., 1982; Ignatenko, 1988, Mudd et al., 1969). These results indicated that there exists a potential for changes to the spectral properties of bioaerosols when exposed to atmospheric constituents, potentially affecting the ability of sensors to accurately detect them. These changes need to be understood for different detection modalities. Current testing and evaluation strategies, such as those discussed in the previous section, utilize biological aerosols generated from freshly grown cultures. The development or measurement of signatures for different pathogenic aerosols is largely performed in a laboratory setting where the adulteration of these signatures due to atmospheric aging is not currently considered. As in the case of background and interfering aerosols, the inability to accurately detect a biological aerosol that is infectious or being used as weapon, can have significant ramifications for affected populations. It is critical

therefore, to understand the signatures of these pathogens following an initial release, before changing in the atmosphere, but also after these pathogens have been transported in the environment for some period.

3.1.5 Objective of Experiments

To understand the limitations of fluorescence-based measurements for detection and characterization of biological aerosols and to develop improved instrumentation and methods for making measurements, changes that may occur due to atmospheric exposure to ozone and water vapor need to be fully understood. This chapter reports the spectral properties of ultra-violet laser-induced fluorescence (UV-LIF) of two types of biological aerosols, *Bacillus thuringiensis* Al Hakam (Bt Al Hakam) spores and MS2 bacteriophage when excited at 263, 351, and 355 nm after exposure to ozone at different RH. In addition, changes in the biological activity of these bioaerosols as a function of the exposure conditions were attempted in order to correlate with loss in spectroscopic signatures.

3.2 Materials and Methods

Rotating Drum Aerosol Exposure Chamber

The test system (Figure 9) used for these experiments utilized a rotating drum reaction chamber, an aerosol generator, an UV-APS, a single particle fluorescence spectrometer (SPFS), and equipment to generate, monitor and control the ozone and RH. Rotating drum aerosol test systems can maintain particles in the aerosol state for

long periods of time (depending on particle size, drum diameter, and rotational speed) by decreasing gravitational settling in the chamber due to centrifugal forces (Goldberg et al., 1958, and Ashagarian and Moss, 1992). The rotating drum chamber used in this study consisted of a 400 L stainless steel cylindrical chamber rotating at one RPM with a chemically inert Teflon coated interior. Each end cap had three Acryltie OP4 windows to allow for penetration of UV light for simulated solar exposure (not utilized in these experiments). The drum rotated around a center axel, consisting of a perforated tube, containing sampling lines in which the aerosol and ozone were introduced and samples were drawn. The axel is fixed allowing the drum to rotate around it using a sealed bearing system attached to the end-caps of the drum. The interior surface of the drum is coated with a layer of Teflon to prevent the steel from reacting with gas-phase species. Sealed ports made of Roxtec seals were used for the inlet and outlets. The inlet into the drum was used to provide the aerosol, air and water for an RH generator, and electrical and data connections to probes inside the drum. The outlet ports were used for drawing samples into the UV-APS, the SPFS, the ozone monitor, and All-Glass Impingers used for sampling. The concentration of ozone and the relative humidity were autonomously controlled to observe the corresponding changes in the aerosol. Water vapor was generated using a small piezo-electric water generator (Model # 50-1011.1, APC International Ltd.) housed in a custom made acrylic tube and placed directly inside the drum chamber. RH and temperature were monitored in the drum using a probe mounted along the center (Model # HMP110, Vaisala Inc.). Ozone was generated into the drum by passing laboratory air at 50 mL/min over a small

mercury pen lamp (<220 nm, Pen, Ray, 97-0067-01) housed within a Teflon enclosure. Air exiting the Teflon enclosure containing photolyzed oxygen converted into ozone was then delivered into drum until the desired concentration was achieved. The concentration of ozone in the drum was measured using an ozone monitor (Model 106-L, 2B Technologies Inc.) sampling at 1 Lpm with a range of 0 to 100 ppm and a resolution of 0.1 ppb. Aerosol was generated and transported into the drum using an ultrasonic nozzle aerosol generation system consisting of a 120 kHz nozzle, broadband ultrasonic generator, and syringe pump (Models # 06-04010, #06-05108, 11-01061, Sono-Tek Corp.). The ultrasonic nozzle was housed in an ACC system (Ratnesar-Shumate et al., 2010). Characterization experiments with the drum showed that 20% of the injected aerosols between 1-2 μm in the drum remained suspended in the chamber for up to 4 hours.

A UV-APS (Model #3312, TSI Inc.) was used to measure the size distribution and fluorescence of biological aerosols during experiments. The UV-APS measured the integrated fluorescence (430-580 nm) of aerosols excited at 355 nm and reported the aerodynamic size of the aerosol between 0.523 and 20 μm. Air was sampled into the UV-APS at 1 Lpm directly from the rotating drum with 4 Lpm of sheath air being drawn from the surrounding laboratory.

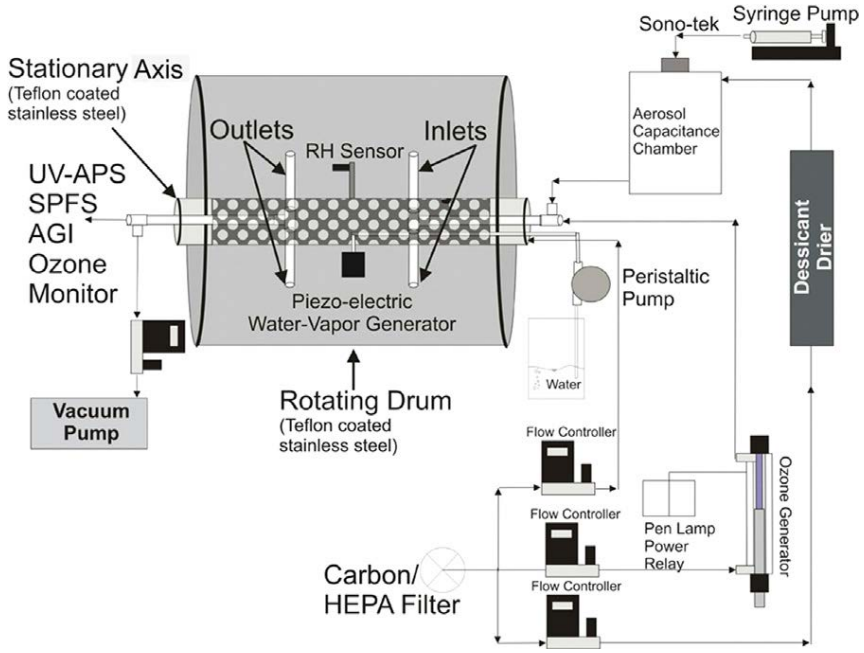

Figure 9 - Schematic of the rotating drum aerosol exposure chamber. **Biological aerosols are maintained aloft in the chamber for long periods due to centrifugal and gravitational forces and are exposed to varying ranges of atmospheric conditions to simulate atmospheric aging.**

3.2.2 Single Particle Fluorescence Spectrometer (SPFS)

A single-particle fluorescence spectrometer (SPFS) was used to measure the LIF of individual bioaerosol particles from the rotating drum as a function of exposure to RH and ozone (Pan et al., 2014). Aerosol was drawn into an 18 in3 airtight chamber at 1 L/min from the drum, and then focused into a laminar jet of around 300 μm in diameter by a sheath nozzle within the chamber. Any aerosol particles larger than 1 μm flowing through a trigger volume (~100 μm×100 μm defined by the intersection of two diode-laser beams at 650 nm and 685 nm) were detected by two photomultiplier tubes (PMT) and illuminated by a single pulse of 263-nm or 351-nm laser. Emitted

fluorescence was collected by a reflective objective and dispersed by a spectrograph. Two long-pass filters with cut wavelengths at 280 nm and 365 nm installed in a filter wheel mounted on the front of the spectrograph were used to block the elastic scattering of the laser at 263 nm and 351 respectively. Both filters have about 95% transmission 3 nm above the cut-off wavelength, and have a very steep cut-off at the indicated wavelength. An Image-Intensified Charge-Coupled (ICCD) camera recorded the dispersed spectrum. A third PMT and a diode laser at 705 nm were used in measuring the particle size. The near forward scattering (10-40 degrees) was detected by the PMT, amplified, sent to a data acquisition board and digitized with the outputs recorded by the computer. A photodiode was used to measure the energy of each laser pulse. The particle size, pulse energy of the illuminating UV laser (263-nm or 351-nm), and the fluorescence information were all recorded for each particle simultaneously. The sizing of each detected aerosol particle was calibrated using National Institute of Standards and Technology (NIST) traceable polystyrene latex (PSL) microspheres aerosolized by a Royco aerosol generator (Model 256, Royco Instruments Inc). Calibration PSL particles were distinguished from surfactant, dust and aggregate particles, by the associated UV-LIF data from the ICCD. The particle size distribution was also validated by an APS® (Model # 3321, TSI Inc.) during the calibration process.

Understanding the changes of fluorescence from Bt Al Hakam and MS2 aerosols due to aging in a rotating drum was complicated by the fact that the size distribution of the aerosol typically changed during the exposure period. Changes in the aerosol size distribution were due to different sized particles being removed

physically (by gravitational, inertial, and centrifugal forces) at different rates inside the rotating drum, with larger particles being removed faster than smaller particles. For a given material, the fluorescence intensity is dependent on the particle size (represented here by d, the diameter of a volume-equivalent sphere), particle shape, and the particle orientation relative to the excitation beam and collection optics. For all the particles and fluorescence emission wavelengths used in this paper, it was assumed that the fluorescence is proportional to absorption by a particle to within a few percent because re-absorption within the particle is small (Hill et al., 2001; 2013). Then, the absorption by a particle and the fluorescence intensity is approximately proportional to particle volume (d^3), i.e., to the number of fluorophores in a homogeneous particle, under the conditions where: (i) the particle diameter is sufficiently small relative to the wavelength (van de Hulst, 1981, 6.13 and 6.31); (ii) or the real refractive index is near one and the absorptivity is small so that the particle is in the Rayleigh-Gans regime (van de Hulst, 1981, 7.12); or (iii) the particle (sphere or non-sphere) is not small, but the imaginary component of the refractive index is sufficiently small that a plane wave propagating through the material could propagate many (e.g., 10) particle lengths L (where L is the maximum length of the particle) and not decrease in intensity (W/m^2) more than a few percent, and the absorption is averaged over a range of sizes or wavelengths sufficient to smooth out the morphology-dependent resonances (MDRs), also known as whispering gallery mode resonances, in the absorption cross section (Hill, 2003). In contrast, the absorption by a particle and fluorescence intensity is approximately proportional to particle cross-sectional area (proportional to d^2) in cases

when the particle is highly absorbing so that a plane wave decreases to a small percentage (e.g., 4%) of its initial value when it propagates through a distance comparable to a particle diameter (or the smallest semi-axis of an ellipsoid). Particles between these two limiting cases are sometimes normalized by d^y, where y is some value typically between 1.9 and 3.2 (Sivaprakasam et al., 2011; Pan et al., 2014). For the data presented here, the fluorescence intensity for each particle was normalized for 263-nm excitation by dividing the fluorescence by $d^{2.05}$, and was normalized for 355-nm excitation by dividing the fluorescence by $d^{2.8}$, where the 2.05 and 2.8 were estimated from calculations of fluorescence verse diameter for dry homogeneous spherical particles which had concentrations and optical parameters similar to those obtained in Hill et al., (2013). If the concentrations and optical properties of the molecules in biological particles (Hill et al., 2013) are used to estimate fluorescence verses size, these approximate exponents appear useful, especially if the 263-nm excited particles contain a negligible amount of water.

3.2.3 Growth and Preparation of Biological Aerosol Materials

Bt Al Hakam spores were obtained from MRI Global Inc. Bt Al Hakam spores were spread-plated on New Sporulation Medium (NSM) Agar, consisting of 0.3% Tryptone (Benton Dickinson and Co., Product # 211705), 0.3% yeast extract (Benton Dickinson and Co., Product # 212750), 0.2% agar (Benton Dickinson and Co., Product #214010), 2.3% Lab-Lemco agar (Oxoid Ltd, Product # CM0017), and 0.001% $MnCl_2$ (Sigma-Aldrich Inc. Product # M8054) (w/v), and incubated for seven days at 37°C

(Cliff et al., 2005). The resulting bacteria lawn, which sporulated as nutrients were exhausted, was then scraped into 0.22 μm sterile-filtered deionized (DI) water, and heat-shocked for ten minutes at 70°C, to kill any remaining vegetative cells. The suspension was pelleted once by centrifugation at 4500 RPM for 25 minutes (Model # Allegra X-22R, Beckman-Coulter Inc.), to wash away any residual media and cellular debris, and then resuspended into sterile filtered DI water. The suspension was further diluted in sterile-filtered DI water to achieve an aerosol particle diameter of approximately 2 μm. The final concentration of Bt Al Hakam spores in the aerosol suspension used for experiments was determined by culture to be 1.7E8 colony forming units per mL (CFU/mL).

Male-specific bacteriophage (MS2) (ATCC # 15597-B1) production and plaque assays utilized *Escherichia coli* (*E. coli)* str. C-3000 (ATCC # 15597) as the host organism. The recommended media, EM 271, was prepared by combining and autoclaving 1% tryptone (Benton Dickinson and Co., Product #211705,), 0.1% yeast extract (Benton Dickinson and Co., 212750), and 0.8% NaCl (Sigma-Aldrich Inc., Product # S7653) (w/v). Agar (Benton Dickinson and Co., 214010) was added for solid medium at 1.5%, and the resulting autoclaved medium was supplemented with 0.1% glucose (Sigma-Aldrich Inc., Product # G5767), 0.0294% $CaCl_2$ (Sigma-Aldrich, Product # C7902), and 0.001% thiamine (Sigma-Aldrich Inc., Product # T5941) w/v, all of which were 0.22 μm sterile-filtered. *E. coli* C-3000 host cultures were propagated from glycerol stocks by overnight incubation on EM 271 agar at 37°C. Individual colonies were picked, placed into EM 271 broth, and incubated (37°C, 200 RPM) until

log-phase culture (spectrophotometric absorption between 0.2 and 0.5 at 520 nm) was achieved, as monitored by spectrophotometer (Model # Ultraspec 2100 Pro, Amersham Biosciences Corp). Lyophilized MS2 stock was resuspended in EM 271, with 100 μL used to inoculate the log-phase *E. coli*. Incubation of the suspension continued for eighteen hours, after which point the culture was centrifuged for 25 minutes at 4500 RPM (Beckman Coulter Allegra X-22R) to remove any residual *E. coli*. As a final cleanup, the MS2-containing supernatant was filtered using a 0.22 μm filter to finish removing any large cellular debris. The resulting stock was further diluted in sterile-filtered DI water, in order to achieve a mean particle size of two μm during aerosol experiments. The final concentration of MS2 used for aerosolization was determined to be 7.8E9 plaque forming units (PFU/mL).

The final suspensions of Bt Al Hakam and MS2 were loaded daily into 30 mL syringes with magnetic stir bars for aerosolization.

3.2.4 Experimental Design

Each measurement period lasted four hours, with additional time required for ozone conditioning. Prior to the test, the drum was pre-conditioned to an RH 5% below the desired value, to allow for additional moisture that was introduced into the drum by the wet-disseminated aerosol. Aerosols were generated and introduced into the chamber for ten minutes, to reach a particle concentration 300 particles/cm^3 or above. Once the aerosol had reached the desired concentration, initial measurements were made with the UV-APS and SPFS. An all-glass impinger (AGI-30, Ace Glass Inc.)

operated for five minutes at 12.5 Lpm, collecting the bioaerosols into phosphate buffered saline. If the test required ozone conditioning, ozone was added to the drum for approximately 20 minutes after the initial measurements, until the ozone reached a concentration of ~150 ppb. The four-hour measurement period thus began with UV-APS and SPFS measurements taken every hour. UV-APS samples were collected for three minutes every hour using a 30-second sampling cycle in the Aerosol Instrument Manager (AIM) software (AIM, TSI Inc.). The pump for the UV-APS was remotely powered off when not sampling. The SPFS was used to sample 200 particle spectra every hour. During the measurement period, ozone and RH generation systems were used to maintain the ozone and RH at their set points. For ozone, this control system was turned on for two minutes every ten minutes to maintain ozone levels during high ozone trials. Air lost during sampling for the AGI-30, UV-APS, SPFS, and ozone monitor were balanced with particle and vapor free, filtered dry air that was sent into the drum using a mass flow controller (Model # MCR-250SLPM-D, Alicat Scientific Inc.). Between each measurement, while the aerosol was being aged, no air was introduced or withdrawn from the drum. Each time a sample was drawn from the drum chamber, the aerosol population was effectively diluted due to the influx of the clean particle free air to maintain pressure. In order to maintain a representative population for the four-hour experiments, AGI-30 samples were only taken at the start and end of each experiment due to the high flow rate (12.5Lpm) required for sampling. At the end of the four-hour measurement period, final measurements were taken with the UV-APS and SPFS, and the final sample was collected by AGI-30. The drum was then purged

at 55 Lpm for about 30 minutes, until the aerosol concentration was below 1% of its starting value.

Bt Al Hakam spores and MS2 bacteriophage in *E.coli* lysate (described previously) were generated into the drum using suspensions that achieved a mean particle size of ~ 2 μm. Submicron particles are difficult for the light-scattering sizing of the SPFS to measure, and particles greater than 3 micron are more rapidly lost in the drum physically over the 4-hour period. In order to assess the changes in the biological activity of the aerosols, samples taken with the AGI-30 were enumerated via culture and q-PCR immediately following aerosolization into the drum and at the end of each experiment. Due to the physical losses of particles during experiments, culture alone could not be used to determine the changes in biological activity, because a perceived decrease in viability/infectivity could simply have been a drop in the number of sampled particles. Instead, the ratio of culturable organisms to genomic equivalents was used as an indicator of biological activity, assuming that the number of genomic equivalents per organism would not change during the course of the experiment.

Using three RH (~80%, 50% and 20%) and two-ozone concentrations (~0 and 150 ppb), the fluorescence changes of the aerosol due to exposure to RH and ozone were measured independently and in combination. An exposure at 150 ppb for 4 hours in the drum represents the integrated EPA exposure limit for ozone during an 8-hr period and therefore represents a worst-case scenario in an urban environment for which a biological aerosol could theoretically be exposed to aging for up to eight hrs. Each experimental condition was repeated three times.

3.2.5 Measurement of Bt Al Hakam and MS2 Phage Biological Activity

The genomic content of samples containing Bt Al Hakam was determined using q-PCR on an existing assay developed at the Johns Hopkins Applied Physics Laboratory (JHU/APL) for the rpoB gene on *Bacillus anthracis*. The probe uses a Quasar 570 fluorophore on the 5' end, with a BHQ-2 black hole quencher on the opposite 3' end. DNA isolations were accomplished via a five-minute bead beat using 100 μm glass silica beads (MP Biomedicals LLC, Product #116911100), followed by a rapid gel cleanup using Bio-Spin 30 columns (Bio-Rad Laboratories Inc., Product # 732,). The assay was evaluated using a three-step PCR reaction on a Cepheid SmartCycler II system. Mastermix was developed using TaqMan Universal PCR Master Mix (Roche Diagnostics, Product # 4304437), with a ten minute 95°C activation followed by 47 cycles consisting of 95°C melting, 47°C annealing, and 60°C extension temperatures. The primers and probe set were added to the Master Mix at concentrations of 300 nM and 250 nM respectively, and brought to a volume of 20 μL with molecular biology grade water. The remaining 5 μL of the reaction was reserved for the samples, which were analyzed in triplicate along a negative control, a standard curve dilution (based on the original aerosol stock), and no template controls for the DNA extraction process.

Bt Al Hakam samples from the AGI-30s were additionally enumerated in triplicate by plating on Tryptic Soy Agar (TSA) plates using a Spiral Biotech Autoplate (50 μL exponential setting), and incubated overnight (sixteen hours) at 37°C. A Spiral

Biotech Q-Count calculated the number of colonies and resulting viable concentrations (CFU/mL).

The infectious concentration of MS2 phage samples was determined by a plaque assay utilizing the same C-3000 strain of *E. coli* used in propagation. Single colonies of *E. coli* were inoculated into EM 271 and incubated (37°C, 200 RPM) until reaching the log-phase. The *E. coli* was co-inoculated with 0.5 mL of serially diluted MS2 into EM 271 containing 0.5% agar, and kept melted in a 46°C water bath. The tube was then emptied onto EM 271 plates, incubated overnight at 37°C, and counted in the morning.

MS2 phage sample RNA concentrations were determined by quantitative real-time fluorescent reverse transcriptase polymerase chain reaction (RT-PCR). RNA from MS2 drum samples was isolated using a QIAamp viral RNA kit (Qiagen Inc., Product # 52904) and isolated in parallel with a standard curve based on serial dilutions from the original stock. Reverse transcriptase and PCR were accomplished in 20 μL reactions, using an EXPRESS One-Step qRT-PCR Universal Mastermix (Life Technologies Inc., Product #11781). Primers and probes, targeting an assembly protein gene, were based on a set published by O'Connell et al. (2006); FAM was the target dye, attached opposite of a TAMRA quencher on the 5' end, with ROX serving as a passive reference at a concentration of 500 nM. Molecular biology grade water was added until the volume per well reached 15 μL, with the remaining 5 μL reserved for the sample. Complementary DNA synthesis occurred during a fifteen minute hold at

50°C, followed by an activation at 95°C for 20 seconds, and 50 cycles of 95°C melting and 60°C annealing and extension temperatures. All samples were run in triplicate on an ABI StepOne Plus, with no template controls for the PCR and RNA isolation processes, and a standard dilution curve.

The active fractions for both Bt Al Hakam and MS2 were determined by dividing the number of viable/infectious organisms measured by the total genomic equivalents, with the initial aerosol stock used as a baseline, measured using qPCR.

3.3 Results

3.3.1 Environmental Conditions in the Rotating Drum Chamber

Five experimental conditions were tested for each type of aerosol: RH Low, RH Medium, and RH High (20, 50, and 80%), with ozone at either Low or High (0 and 150 ppb). The effects of temperature were not the focus of this study but were monitored to ensure that temperature was consistent. The temperature in the drum chamber during experiments was stable at 20-21°C with 3% variation across all experiments (Figure 10 and Figure 11). During experiments where a low RH was desired, the average RH across all experiments was 24 ± 5% with the RH slightly increasing during experiments. For experiments in which a medium RH was desired, the average RH across all experiments was 52 ±3%. The average high RH was 81±3%. The average low and high ozone concentrations once target levels were achieved inside the drum were 6 ±3 ppb and 144±11 ppb respectively.

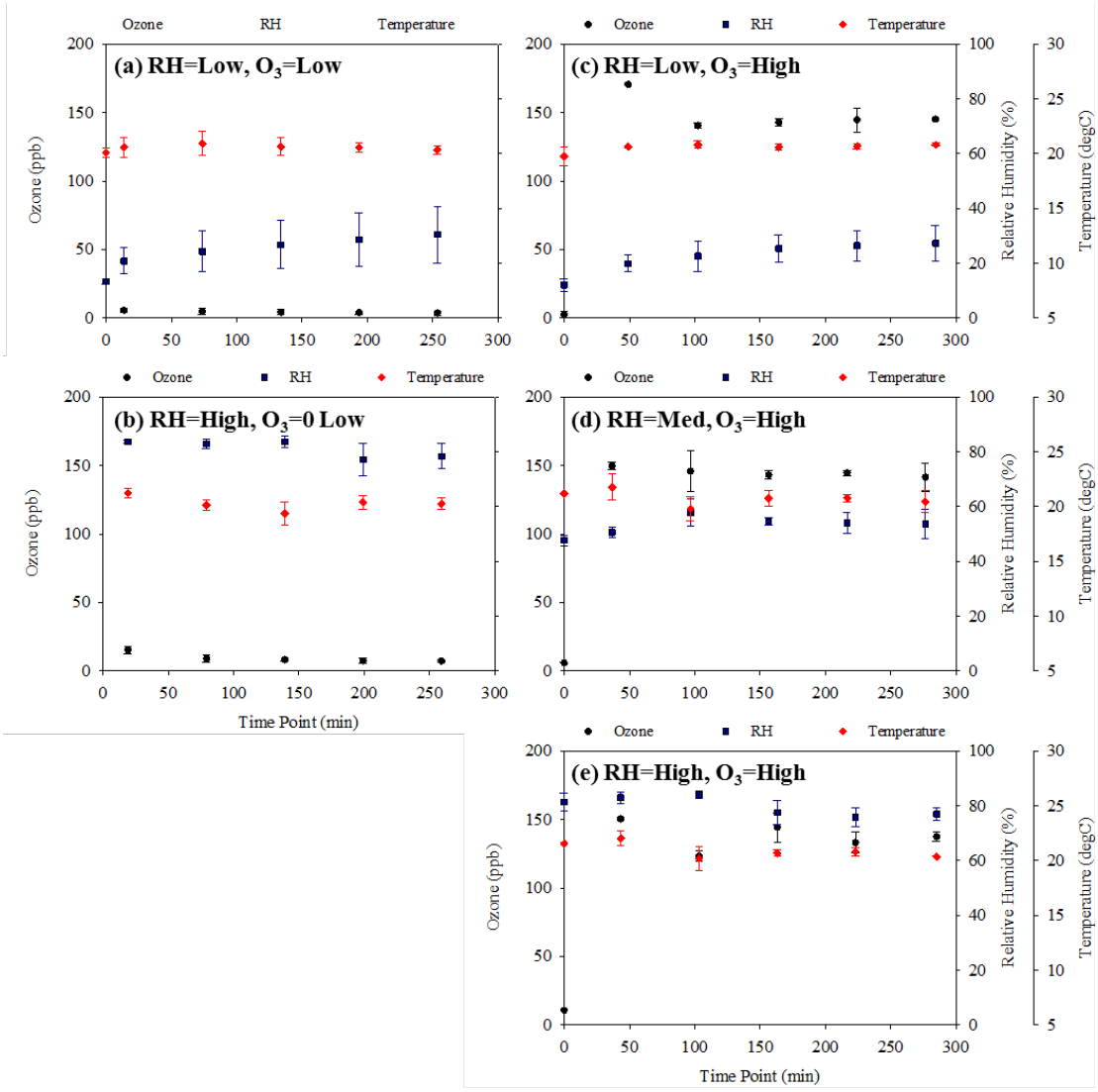

Figure 10 - Average Environmental Conditions in Rotating Drum During Bt Al Hakam experiments. Where RH is Low=24±5%, Med=52±3%, High=81±3%, and O_3 is Low=6±3 ppb, and High=144±11 ppb.

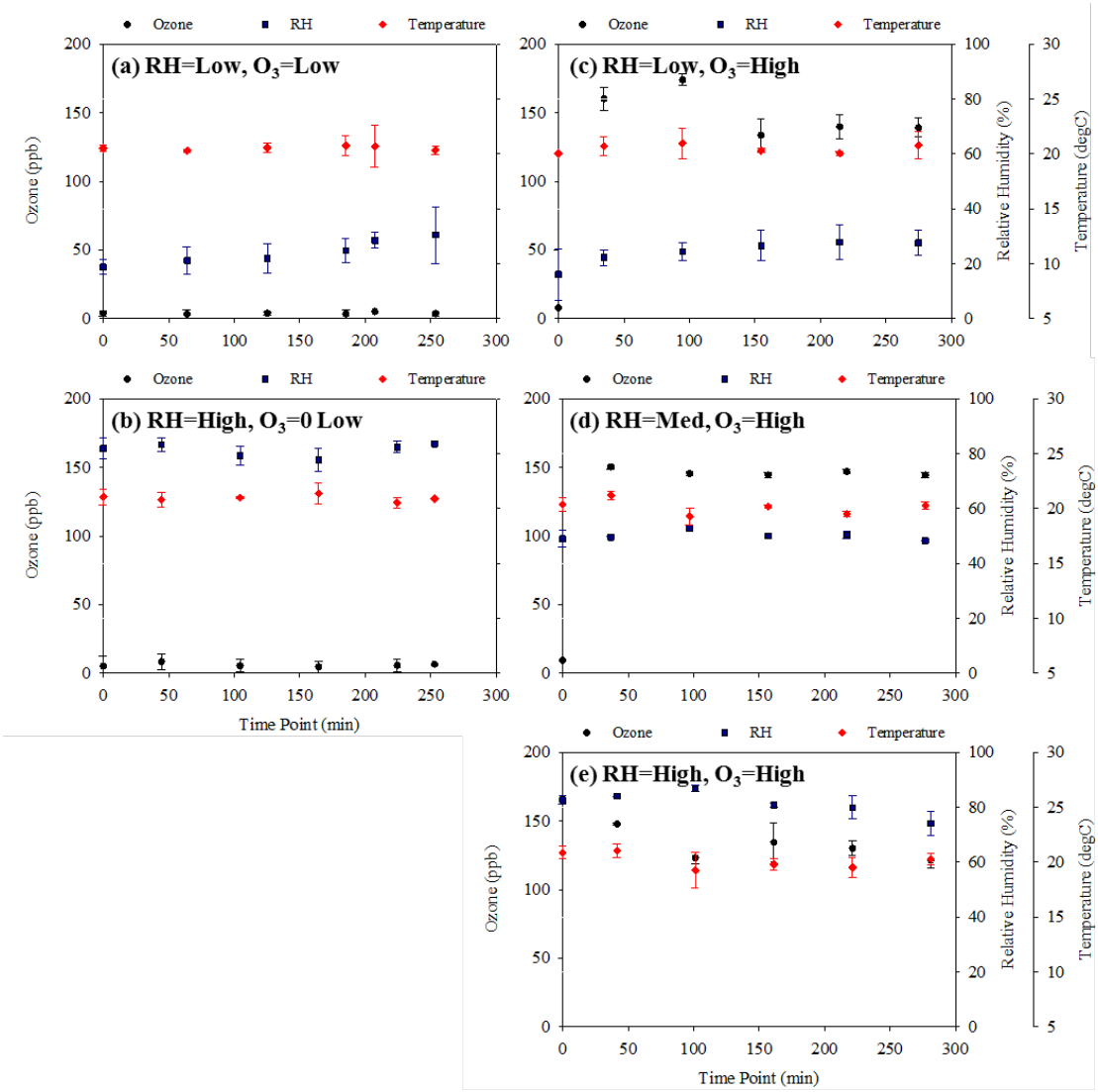

Figure 11 - Average Environmental Conditions in Rotating Drum During MS2 Phage Experiments. Where RH is Low=24±5%, Med=52±3%, High=81±3%, and O_3 is Low=6±3 ppb, and High=144±11 ppb.

3.3.2 Aerosol Size Distributions During Experiments

The average size distribution of Bt Al Hakam spore aerosols was multimodal for all experiments with a peak mode diameter of 1.8 μm. During the 4-hr period, the

peak mode shifted to a smaller diameter (~ 1.6 μm) as larger particles in the drum were lost faster than the small size particles due to physical decay. Figure 12 shows the average starting and ending size distributions of Bt Al Hakam spores during experiments performed at each type of environmental condition. All distributions are very similar at the start of experiments with the higher RH distributions being slightly less broad after 4-hrs in the rotating drum, potentially due to particle uptake of water. Uptake of water would have resulted in larger particles, and subsequently larger physical losses in the drum, a phenomenon that will be discussed further in the following chapter.

The initial size distribution of MS2 phage aerosol varied more prominently as a function of RH than did the Bt Al Hakam. The mode size at low RH was approximately 1.8 μm, similar to that of the Bt Al Hakam spores Figure 12(a). At the medium and high RH, the mode sizes started at 2.2 and 2.5 μm. These differences in the starting mode size indicate uptake of water by the MS2 aerosols in the rotating drum. EM271 media contains a large amount of NaCl that likely dominates the hygroscopic properties of the MS2 phage aerosol used for these experiments. The deliquescence relative humidity (DRH), defined as the RH in which an aerosol will begin to uptake water and the efflorescence relative humidity (ERH), the RH in which an aerosol will return to a crystalline state for NaCl are 73% and 45% respectively (Seinfeld and Pandis, 2006). It is probable that the aerosol introduced into the drum was under slightly wet conditions after passing through the ACC and never fully reached the ERH in order to dry completely to a crystalline state. Given the average

RH in the drum during the medium RH experiments was 52%, and the known ERH for NaCl is 45%, the MS2 phage aerosol was likely in transition phase, which explains the mode size of 2.2 μm that falls between the low and high RH mode sizes. For experiments performed at the high RH (>80%) the slightly wetted aerosol entering into the drum likely continued to uptake water to achieve a mode size observed at 2.5 μm causing larger particles to be lost in the drum rapidly. As shown in Figure 12 (b and d) the mode size at high RH after 4 hours in the rotating drum is considerably shifted from about 2.5 to 1.1 μm during a 4-hr experiment. While in relative low RH conditions, the mode size remains at approximately 1.7 μm throughout the 4-hr period.

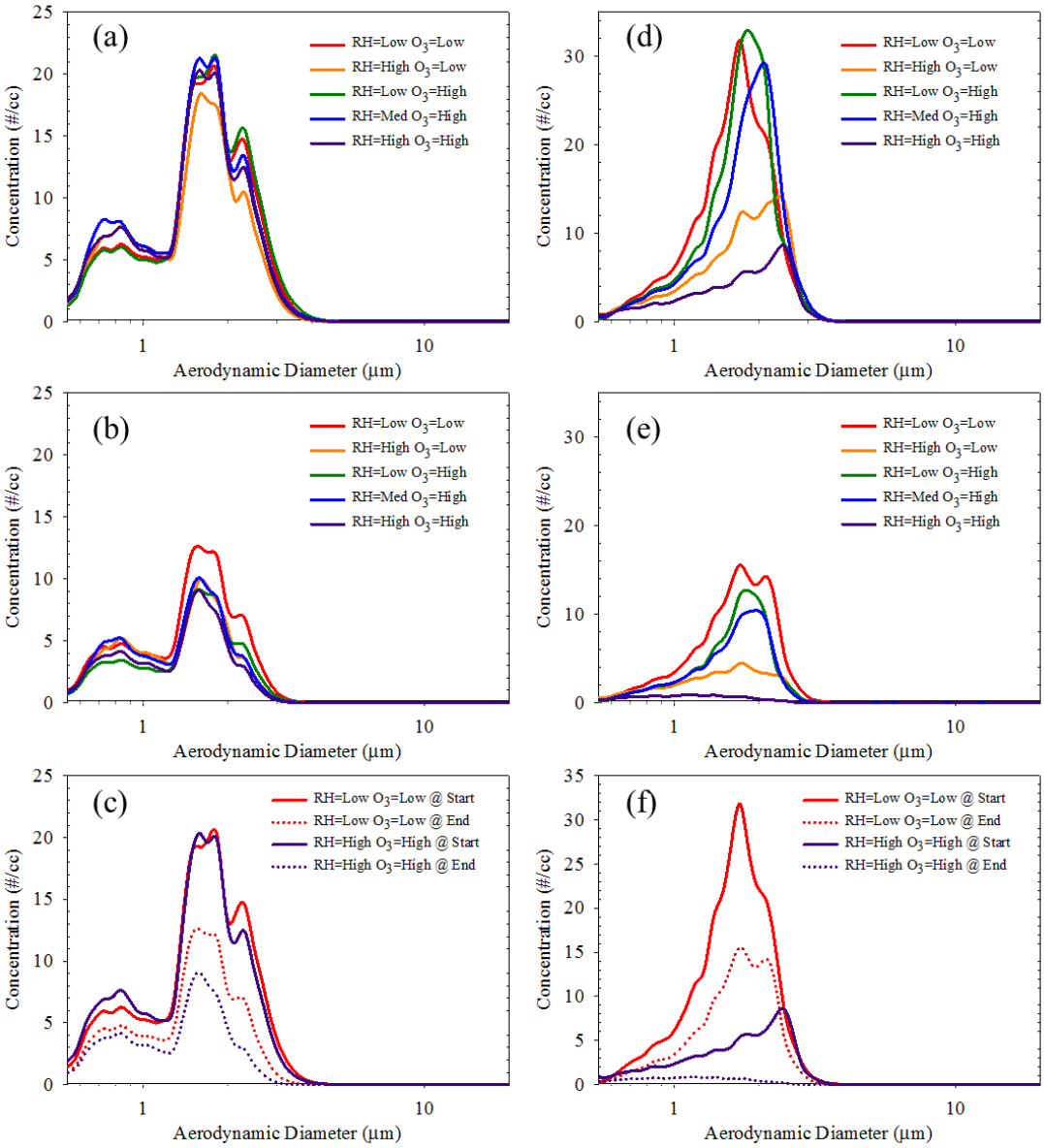

Figure 12 – Size Distributions in Rotating Drum During Experiments (a) Bt Al Hakam size distributions at the start of experiments (b) Bt Al Hakam size distributions at the end of experiments (c) Bt Hakam size distributions for two cases at the start and end of experiments for direct comparison (d) MS2 size distributions at the start of experiments (e) MS2 size distributions at the end of experiments (f) MS2 size distributions for two cases at the start and end of experiment for direct comparison. Where RH is Low=24±5%, Med=52±3%, High=81±3%, and O_3 is Low=6±3 ppb, and High=144±11 ppb.

3.3.3 Fluorescence of Bt Al Hakam and MS2 Phage Measured with SPFS

The SPFS was used to measure the fluorescence at excitation wavelengths 263 and 351 nm of Bt Al Hakam and MS2 aerosols during the 4-hr experiments. The results are shown in Figure 13 through Figure 16. The data sets shown are the averages from three experiments and each plot represents 600 UV-LIF spectra from 200 individual aerosol particles during each of the three experiments. The fluorescence intensities were normalized by $d^{2.05}$ or $d^{2.8,}$ for fluorescence excited at 263 and 351 nm, respectively, in order to reduce the effects of the decrease in the average particle size, over the course of an experiment.

The integrated fluorescence over each emission band, plotted verses time for each experiment (shown in Figure 17 through Figure 18), illustrates more clearly the trends in amplitudes. The UV 263 is the integrated fluorescence band intensity from 280 to 400 nm when excited by 263 nm laser. The Vis 263 is the fluorescence from 400 to 580 nm when excited by 263 nm laser. The Vis 351 is the emission band from 380-700 nm when excited by 351 nm laser.

Table 4 summarizes the measured decreases in integrated fluorescence from the initial time (t=0 min) to the final time (t=4 hrs) for the different emission bands, excitation wavelengths, and type of aerosol. The *p*-values calculated using the *t*-test with unequal variances is shown. It is the probability that the two sets of three measurements, initial and final, are sampled from the same distribution. The overlaps in the standard errors between the initial and final fluorescence intensities are

calculated in order to help in estimating whether the decreases are significant. Decreases in fluorescence intensity are considered significant in the absence of an overlap of the error bars of the intensities measured at the initial and final time points.

Table 4 - Percent Decrease in Fluorescence in Each Emission Band for Bt Al Hakam and MS2 as Function of Ozone Concentration and Relative Humidity.

***Bt* Al Hakam**							
	RH	**Low Ozone**			**High Ozone**		
		Decr. %	**(F_F-F_I) / (SD_F+SD_I)**	**p**	**Decr. %**	**(F_F-F_I) / (SD_F+SD_I)**	**p**
UV263	**Low**	12%	0.51	.22	5%	0.23	.71
	Med	—	—		26%	1.001	.16
	Hi	30%	1.13	.06	45%	2.68	.005
	Avg.	21%	0.82		25%	1.30	
VIS263	**Low**	13%	0.49	.23	8%	0.26	.67
	Med	—	—		17%	0.66	.31
	Hi	17%	0.68	.21	21%	0.77	.17
	Avg.	15%	0.59		15%	0.56	
VIS351	**Low**	17%	0.86	.14	16%	0.71	.21
	Med	—	—		38%	1.89	.02
	Hi	13%	0.72	.097	20%	1.04	.10
	Avg.	15%	0.79		25%	1.21	
MS2 Bacteriophage							
		Low Ozone			**High Ozone**		
		Decr. %	**(F_F-F_I) / (SD_F+SD_I)**	**P**	**Decr. %**	**(F_F-F_I) / (SD_F+SD_I)**	**p**

UV263	**Low**	28%	0.95	.09	31%	1.67	.03
	Med	—	—		56%	2.40	.012
	Hi	38%	1.54	.03	75%	6.13	.001
	Avg.	33%	1.25		54%	3.40	
VIS263	**Low**	23%	0.81	.12	22%	0.94	.11
	Med	—	—		22%	0.89	.13
	Hi	18%	0.90	.08	52%	2.54	.006
	Avg.	21%	0.86		32%	1.46	
VIS351	**Low**	3%	0.13	.77	38%	1.62	.04
	Med	—	—		26%	1.02	.08
	Hi	18%	0.97	.12	45%	1.68	.036
	Avg.	11%	0.55		36%	1.44	

Numbers in red have no overlap of the error bars at the initial and final times, i.e., the difference between the initial and final averages is greater than the sum of the standard deviations, or the case of p values, p is less than 0.1. RH is Low=24±5%, Med=52±3%, High=81±3%, and O_3 is Low=6±3 ppb, and High=144±11 ppb.

For Bt Al Hakam the averaged fluorescence spectra (280 - 580 nm) excited at 263 nm are shown in Figure 13, with two emission peaks, centered near 330 nm and 450 nm. The time-dependence of the integrated intensities over these bands can be seen in the solid lines and the dotted lines in Figure 17. At low RH with low ozone, no large differences in the relative intensity between the two fluorescence bands are observable, and the decrease of the 330-nm band is not monotonic. At high RH the 330 nm bands intensities decrease slightly faster than the 450 nm bands. In Figure 13, the

fluorescence spectra (365-700 nm) with a 351 nm excitation have very slight intensity decreases, as can also be seen in the dashed lines in Figure 17 for VIS 351.

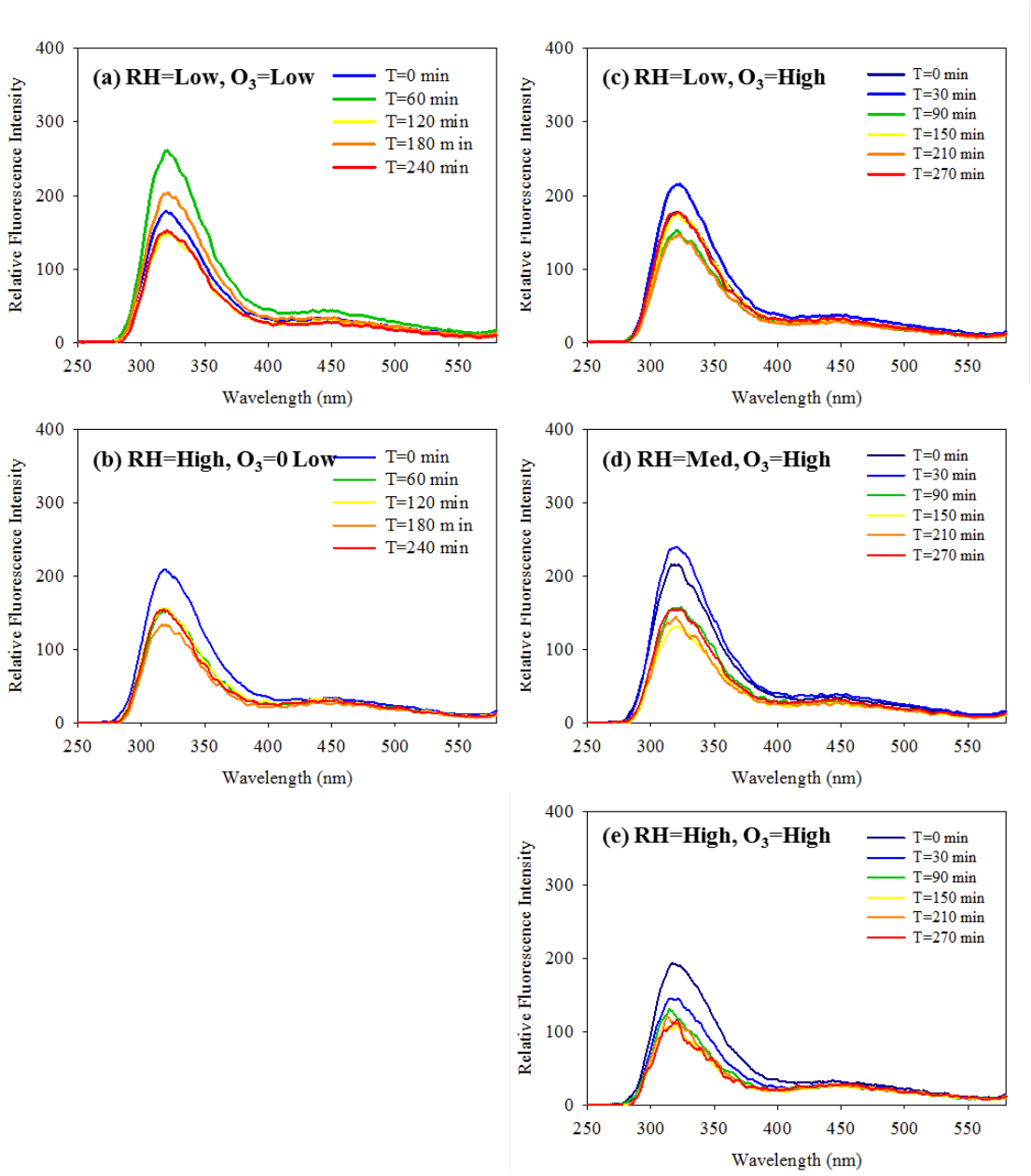

Figure 13 - Bt Al Hakam Emission Spectra as a Function of Time When Excited at 263 nm for Each Exposure Type. Each plot represents the average of 200 particle spectra at each time point for three experiments. **Where RH is Low=24±5%, Med=52±3%, High=81±3%, and O_3 is Low=6±3 ppb, and High=144±11 ppb.**

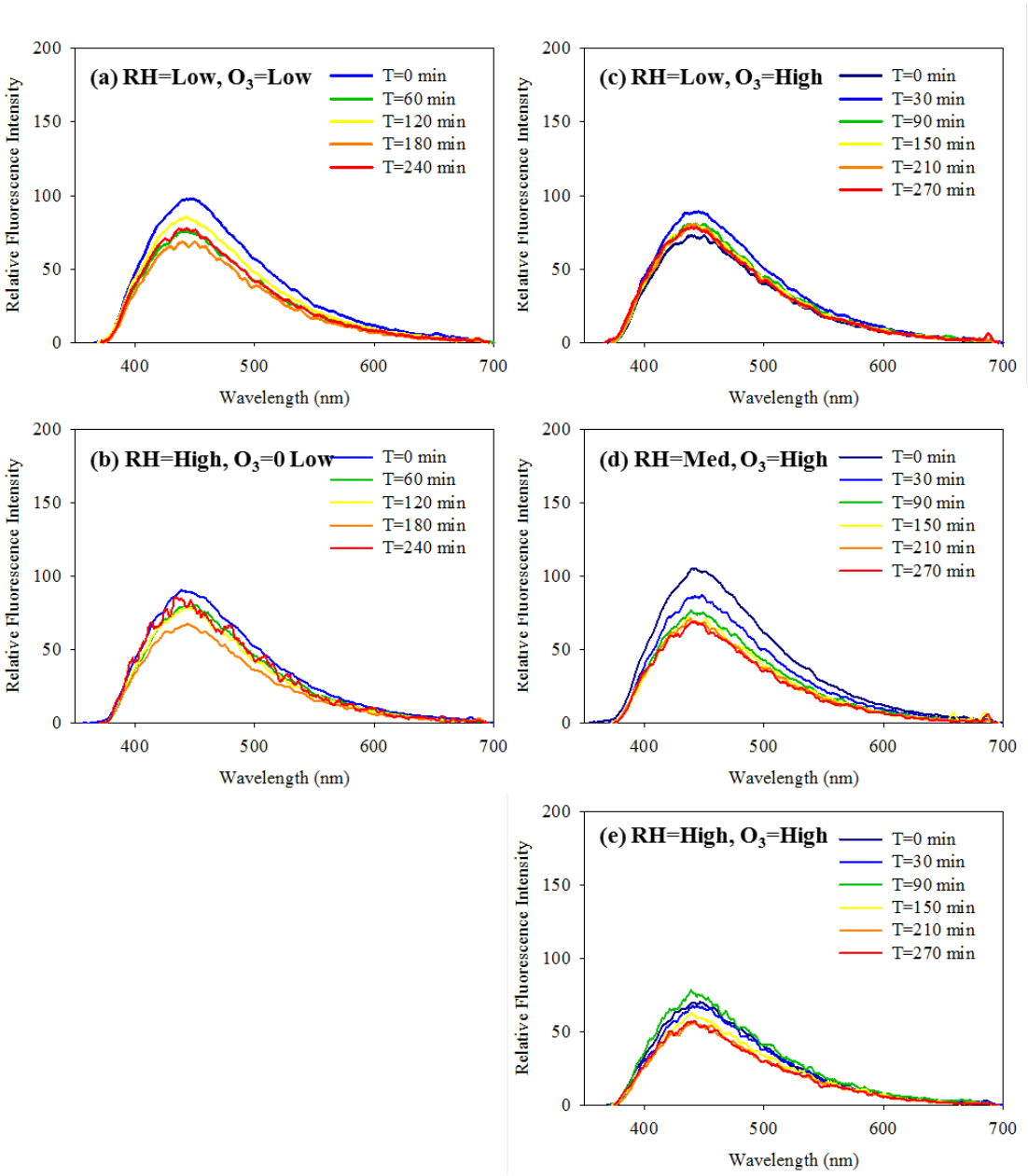

Figure 14 - Bt Al Hakam emission Spectra as a Function of Time When Excited at 351 nm for Each Exposure Type. Each plot represents the average of 200 particle spectra at each time point for three experiments. **Where RH is Low=24±5%, Med=52±3%, High=81±3%, and O_3 is Low=6±3 ppb, and High=144±11 ppb.**

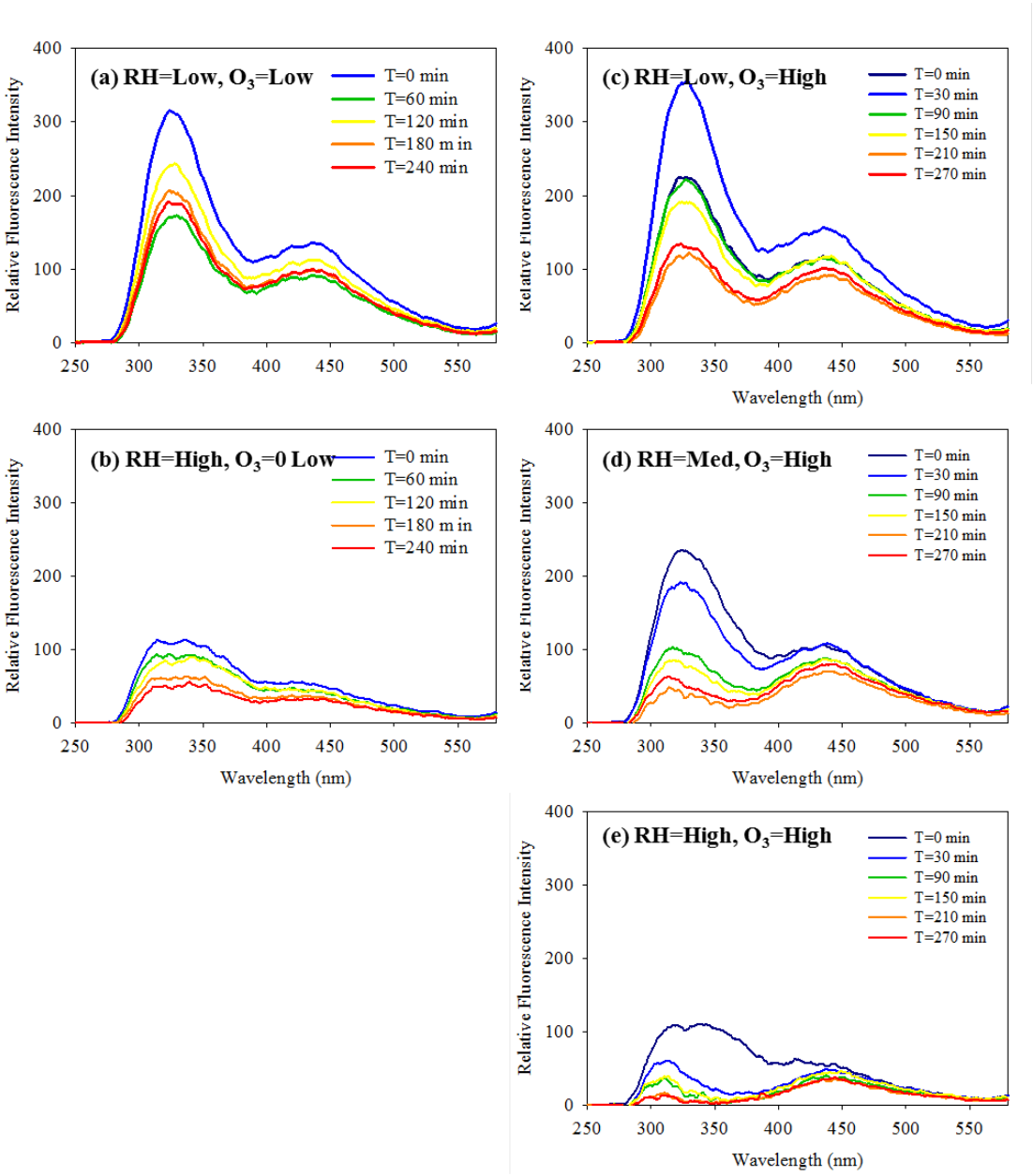

Figure 15 - MS2 Emission Spectra as a Function of Time When Excited at 263 nm nm for Each Exposure Type. Each plot represents the average of 200 particle spectra at each time point for three experiments. **Where RH is Low=24±5%, Med=52±3%, High=81±3%, and O_3 is Low=6±3 ppb, and High=144±11 ppb.**

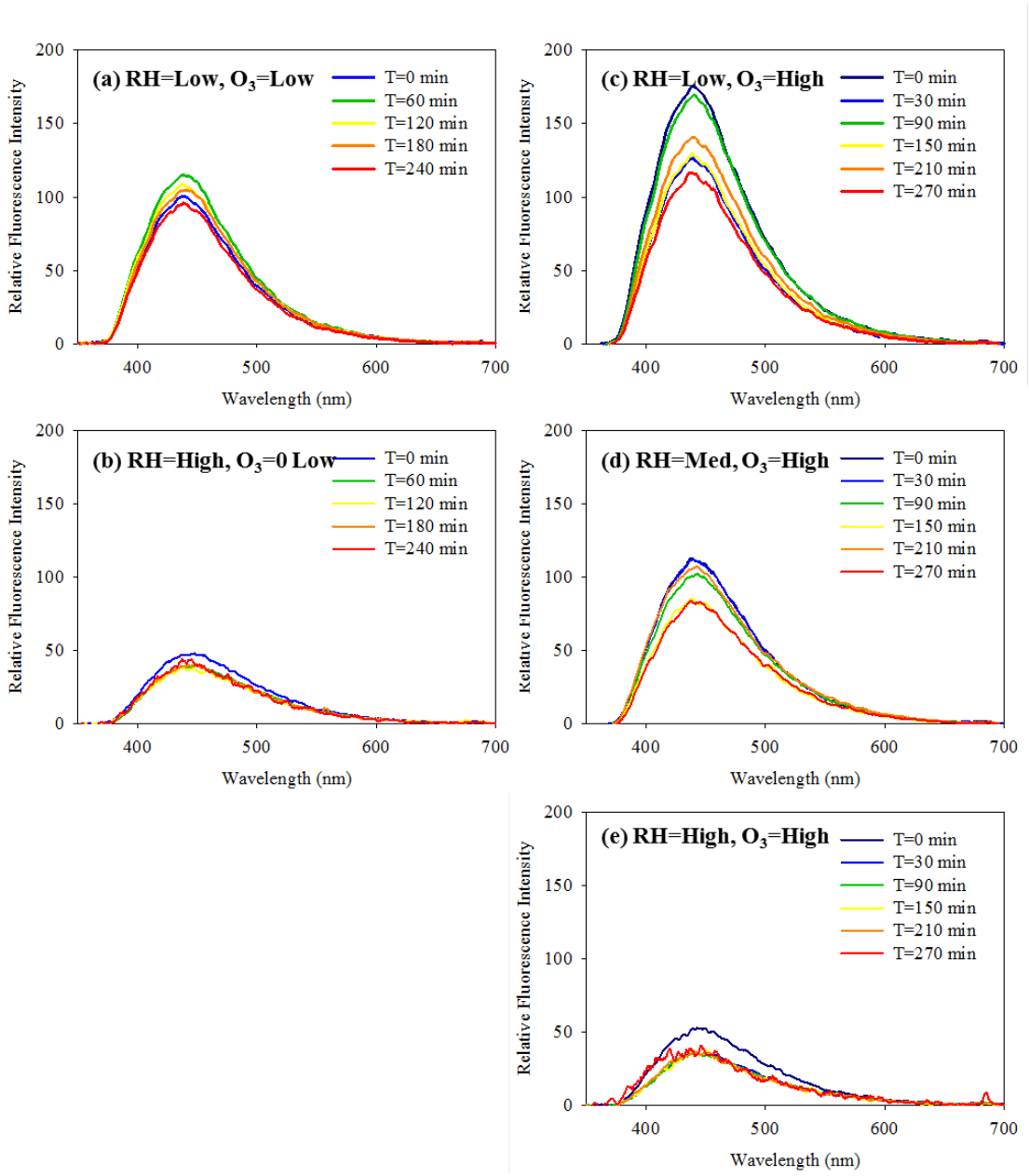

Figure 16 - MS2 Emission Spectra as a Function of Time when Excited at 351 nm for each Exposure Type. Each plot represents the average of 200 particle spectra at each time point for three experiments. **Where RH is Low=24±5%, Med=52±3%, High=81±3%, and O_3 is Low=6±3 ppb, and High=144±11 ppb.**

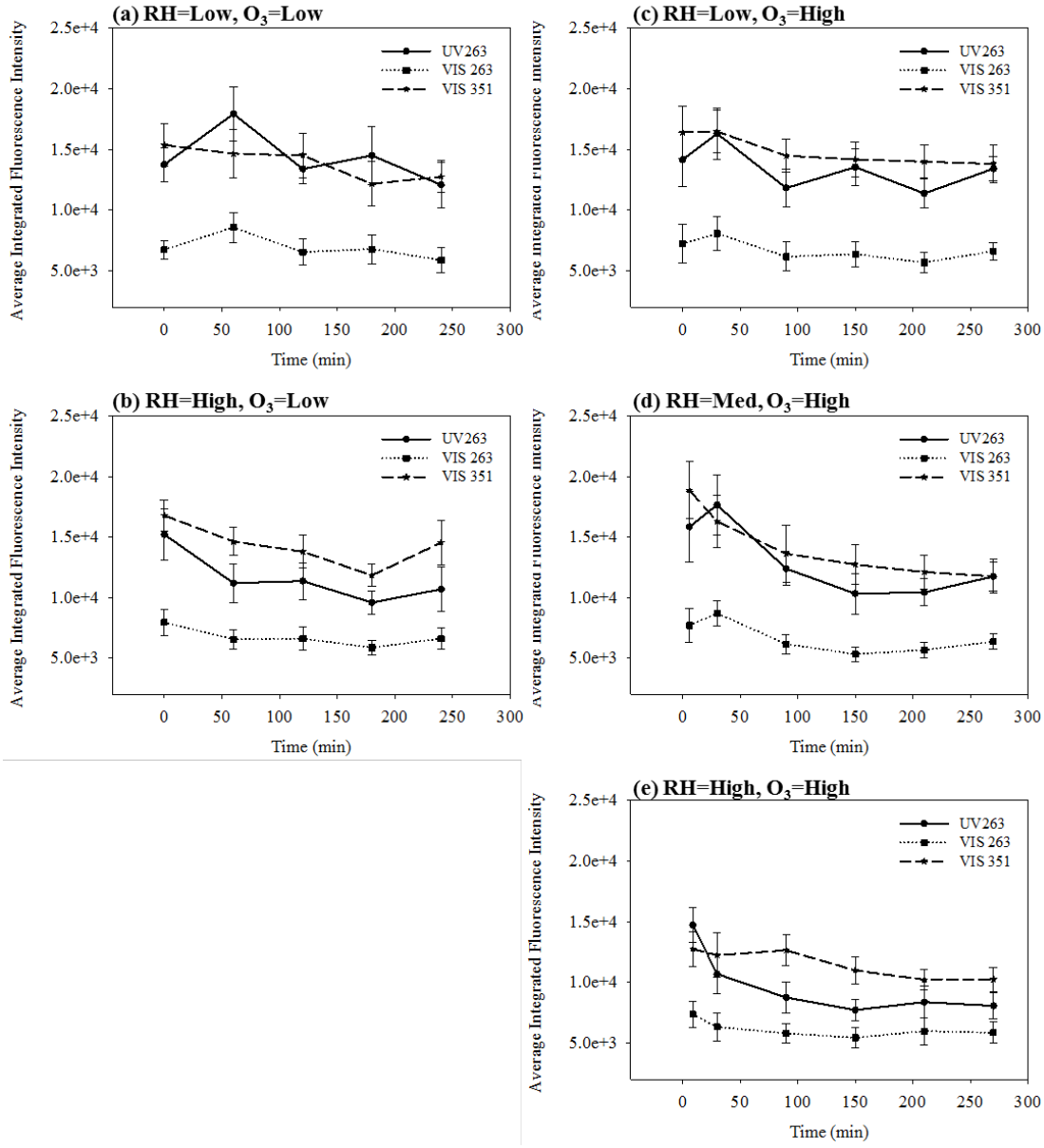

Figure 17 - Integrated Fluorescence of Bt Al Hakam Aerosols in Each of Three Emission Bands When Excited at either 263 or 351 nm. UV 263 band =280 to 400 nm at excitation 263 nm, Vis 263 =400 to 580 nm at excitation 263 nm, Vis 351=380-700 nm at excitation 351 nm. **Where RH is Low=24±5%, Med=52±3%, High=81±3%, and O_3 is Low=6±3 ppb, and High=144±11 ppb.**

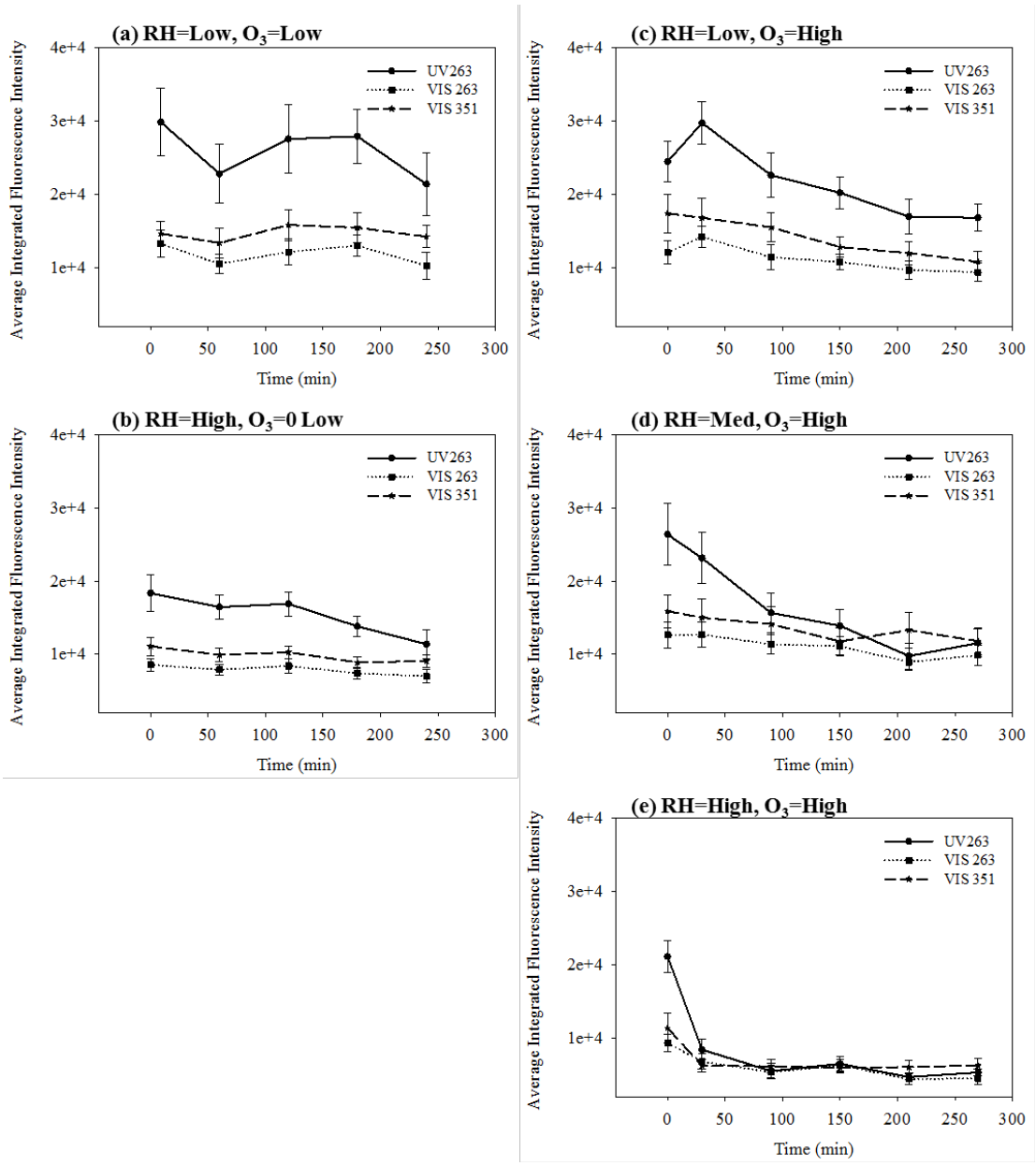

Figure 18 - Integrated Fluorescence of MS2 Aerosols in Each of Three Emission Bands When Excited at either 263 or 351 nm. UV 263 band =280 to 400 nm at excitation 263 nm, Vis 263 =400 to 580 nm at excitation 263 nm, Vis 351=380-700 nm at excitation 351 nm. **Where RH is Low=24±5%, Med=52±3%, High=81±3%, and O_3 is Low=6±3 ppb, and High=144±11 ppb.**

For MS2 phage with 263-nm excitation, the fluorescence peak around 330 nm decreases more than that from Bt Al Hakam as shown in Figure 15 and the solid line in Figure 18. For MS2 phage, at low RH and low ozone, the relative fluorescence intensities between the UV and visible bands changed little over the 4-hr experimental duration, even though both bands were slightly decreased. At high RH and low ozone, a large decrease over time occurred in both fluorescence bands excited at 263 nm. At low RH and high ozone concentration, large decreases were also observed for both fluorescence bands, with $p \leq 0.06$ in both cases. The rate of decrease in fluorescence increased as RH was increased, particularly for the tryptophan fluorescence band around 330 nm. This suggests that both RH and ozone contributed to the decrease in fluorescence intensity, and that ozone accelerates the decrease of the UV band. Figure 16 shows the fluorescence emission profiles excited at 351 nm for the MS2 phage. The decrease in fluorescence is more notable all in cases where a high concentration of ozone is present. Meanwhile a large blue shift was notable for the UV band at 263 nm excitation especially in the presence of high ozone concentrations.

For low ozone, as shown in Figure 17a and Figure 17b, Bt Al Hakam spores exhibit no significant decrease in the average integrated fluorescence intensity in any of the fluorescence emission bands measured, except for the UV263 at high RH with p=0.06. The average integrated visible fluorescence intensity (VIS263) of Bt Al Hakam spores does not decrease significantly even at high ozone concentrations (Figure 17c through Figure 17e). The VIS 351-fluorescence band of Bt Al Hakam

spores at medium and high RH at the present of high ozone decreases significantly by 38% and 20% respectively. At medium and high RH levels in the presence of high ozone, the UV 263 fluorescence band for Bt Al Hakam decreased significantly, with nearly 45% decrease at high RH (Figure 17e) and close to 26% at medium RH (Figure 17c and Figure 17d). Decreases in fluorescence for Bt Al Hakam aerosols appear to stabilize after about 150 minutes of exposure (Figure 17).

For MS2 at low RH and low ozone, shown in Figure 18a, no decrease in the fluorescence intensity appears significant. At high RH and low ozone, neither of the VIS peaks for MS2 decreases significantly; however, the UV263 appears to be constant for the first 120 minutes then followed by a 38% decrease. The VIS263 nm fluorescence band for MS2 at high ozone does not decrease significantly for low and medium RH, but does decrease 52% in the presence of high RH (Figure 18e). At all RH in the presence of high ozone the UV 263 and VIS 351 all decrease significantly (Figure 18c through Figure 18e). As the RH increased from low to high at the present of high ozone concentration, the intensity decrease of the UV 263 fluorescence band is monotonically increased (31% to 56% to 75 %). The decreases of fluorescence from MS2 are more rapid than that from Bt Al Hakam. The decrease was stabilized after the first 100 minutes in the presence of high ozone and low RH, but changed fast when exposed to high ozone and high RH and stabilized after about 50 minutes.

3.3.5 Fluorescence of Bt Al Hakam and MS2 Measured with UV-APS

Shown in Figure 19a and summarized in Table 5 are the average change in fluorescence intensities of Bt Al Hakam spores for different experimental conditions over time for the 1.8 μm size bin as measured by UV-APS. Unlike the SPFS measurements, the fluorescence increased with time with no apparent change in the rate of increase as function of ozone or RH. In all cases, the fluorescence appears to initially decrease between 0 and 30 minutes (for experiments where ozone was introduced into the chamber) and 0 and 60 minutes where no ozone was present. This difference may be due to the degree of drying of the aerosol in the drum when the first measurement was taken at time "zero" verses the second time point after which equilibrium had been reached. The final fluorescence after four hours in the chamber is significantly greater ($p<0.05$) during experiments with low RH and not significantly different at the high RH conditions, a difference that may be due to more water being present in the particles at higher RH. The rate of increase of fluorescence intensity show little correlation between ozone concentration and RH together.

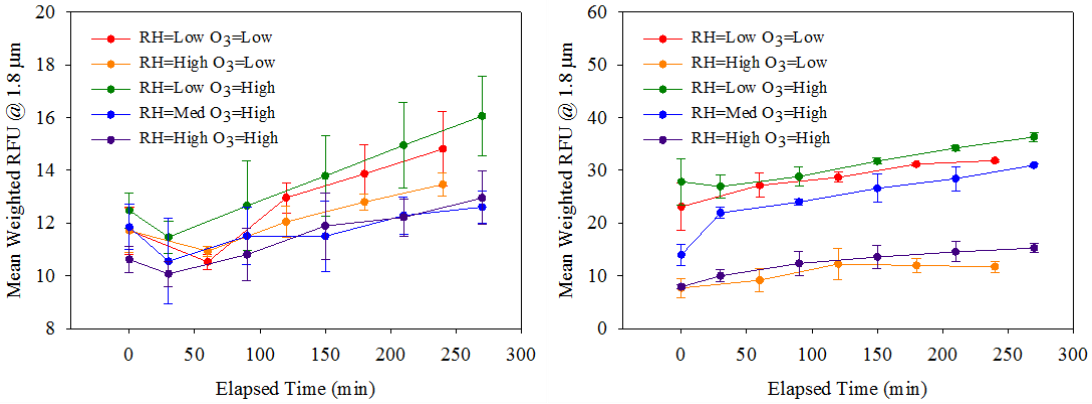

Figure 19 - (Left) Change in Mean Weighted Fluorescence for Bt Al Hakam Spores @ 1.8 microns (Right) Change in Mean Weighted Fluorescence for MS2 Phage @ 2.0 microns. Both with UV-APS @ 355 nm excitation. Where RH is Low=24±5%, Med=52±3%, High=81±3%, and O_3 is Low=6±3 ppb, and High=144±11 ppb.

For MS2 phage aerosol, some fluorescence trends can be seen with the experiment conditions. Shown in Figure 19 are the average fluorescence intensities in the 2.0 µm size bin for MS2 aerosols and summarized in Table 5 are the average increases in fluorescence and the level of significance. RH was anticorrelated with the initial fluorescence. This is likely due to the presence of water in these aerosols affecting the fluorescence intensity. One possible explanation for the differences in the starting fluorescence of both Bt Al Hakam and MS2 aerosols could be that particles entering the drum under wet conditions grow almost instantaneously before being measured by the UV-APS. This theory is consistent with the particles in the 1.8-2.0 µm bins being much smaller when initially injected into the drum and then growing to that size at the higher RH. Particles entering the drum under dry conditions (at low RH) were likely 1.8-2.0 µm to start and therefore grew little, if at all. Therefore, a particle

with a certain size (2.0 μm) at high RH would contain less fluorescent material and more water than a particle of the same size at low RH, which would have started at 2.0 μm and grew little by adsorption of water. Under all conditions tested, the change in fluorescence during four hours was statistically significant ($p<0.05$) with the changes in fluorescence at 50% and 85% RH in the presence of ozone having the most significant changes followed by the low RH no ozone condition.

Table 5 - Fluorescence changes in Bt Al Hakam and MS2 aerosols as measured with the UV-APS®

Condition	Bt Al Hakam		MS2	
	% Increase $(F_f-F_i)/F_i$	p-Value	% Increase $(F_f-F_i)/F_i$	p-Value
RH Low, O_3=Low ppb	26%	0.02	38%	0.002
RH High , O_3=Low ppb	15%	0.06	53%	0.02
RH Low, O_3=High ppb	20%	0.05	23%	0.007
RH Med, O_3=High ppb	4%	0.06	103%	0.0002
RH High, O_3=High ppb	15%	0.07	84%	0.002

*p-values calculated using a two sample T-test assuming equal variances. Where RH is Low=24±5%, Med=52±3%, High=81±3%, and O_3 is Low=6±3 ppb, and High=144±11 ppb.

3.3.6 Changes in Biological Activity of Bt Al Hakam and MS2 Phage

The change in biological activity (viability for Bt Al Hakam and infectivity for MS2) during experiments was measured to determine what effects exposure to ozone and RH may have on the functionality of the aerosols. The approach taken for these experiments was to measure the biological activity against the total genomic equivalents present in the aerosol samples. In theory, if there is no change in biological activity (biological decay), then the ratio of active units to genomic equivalents should stay the same regardless of physical losses. Culture of samples taken with AGI-30 at the start and the end of each experiment were compared with q-PCR to determine if any biological decay could be observed. Figure 20 shows the arithmetic mean log change in biological activity at different experimental conditions. In the case of MS2 phage, a 2-3 log loss in infectivity (of *E.coli* cells) was observed for medium or high RH in the presence of high ozone concentration. The change in Bt Al Hakam is less straightforward. These experiments showed an apparent increase in viable fraction under high ozone conditions. It is not feasible that the Bt Al Hakam was replicating during the 4-hr experiments in the aerosol state, and therefore, the number of genomic equivalents must be decreasing. The decrease in infectivity of MS2 phage is consistent with the decrease in fluorescence intensity measured by SPFS.

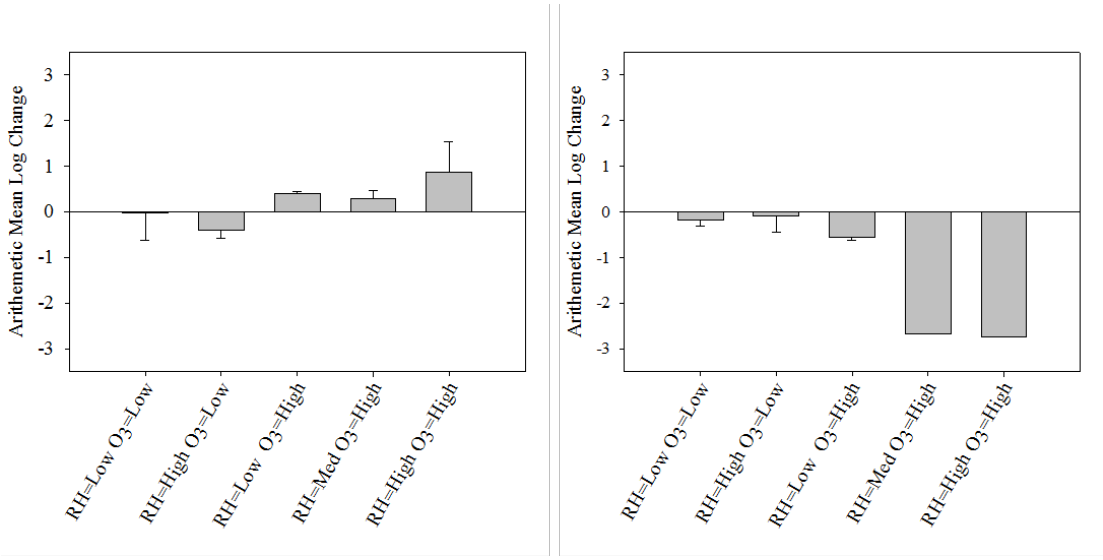

Figure 20 - (Left) Change in Measured Viability for Bt Al Hakam Spores During Experiments (Right) Change in Measured Infectivity for MS2 Phage.

4.0 Discussion

4.1 Fluorescence Shifts During Experiments

Fluorescence between 320 to 350 nm in bacteria and proteins is attributed to the presence of tryptophan when excited by light between 250 to 290 nm (Santarpia et al., 2012, Pan et al., 2014, Hill et al., 2013). When oxidized by ozone in liquid solution and in animal tissues, tryptophan fluorescence at ~ 330 nm decreases as oxidation and reaction with water results in the formation of NFK and NK (Pryor and Uppu, 1993) both of which fluoresce between 400 to 420 nm (Santarpia et al., 2012; Pan et al 2014). Previous studies performed by Santarpia et al., 2012 with MS2 and *Yersinia rhodei* aerosols show similar results to these experiments in which treatment with ozone leads to a decrease in the 330 nm band relative to the 400-580 nm band, especially in the case

of MS2 phage aerosols at high RH and high ozone concentration. However, in these experiments no increase in fluorescence was observed that would indicate the production of kynuerine products. Given the complexity of the molecular composition of bioaerosols and the possible oxidation products, it is possible that while some fluorophores are being oxidized and their fluorescence intensity is decreased in the visible band by 351 nm excitation, fluorescence intensity may be increased from the generation of new fluorophores by products of oxidation, and result in a net effect that has little change in fluorescence intensity by 351 nm excitation.

It was expected that similar fluorescence spectral profiles and intensity would be produced by the excitation of similar molecules if the two fluorescence spectrometer systems, the SPFS and UV-APS, have similar excitation wavelengths (only 4 nm difference). In particular, the SPFS VIS351 emission covers the fluorescence from 365 to 700 nm, which decreases for Bt Al Hakam and MS2 phage, with the largest decrease at high RH and high ozone concentration. The fluorescence emission (430-580 nm) observed by UV-APS increased over time for both Bt Al Hakam and MS2 (with the exception of Bt Al Hakam in the first 60 minutes) for all conditions tested. We could not find significant evidence for the hypothesis that the difference in the detection wavelength range for SPFS (365-700 nm) and UV-APS (430-580 nm) could explain this observed difference in the trends in fluorescence over time.

The data in Figure 13 through Figure 18 and Table 4 indicate that greater fractions of the fluorophores are modified by ozone in MS2 than in Bt Al Hakam spores. The different rate of decrease observed for Bt Al Hakam spores verses the MS2

phage indicates different kinetics are involved within the oxidation process for the two types of aerosols during exposure to ozone. *Bacillus* spores contain a protective exosporium that likely shields the bacterium from oxidative stresses and slows the uptake of water. *Bacillus* spores are hydrophobic, and so in the absence of media or other material that might attract water molecules to the surface, the observed chemical changes due to ozone are expected to take longer with less intense reaction. Conversely, for MS2 phage, several factors may have contributed to the more rapid reactivity. MS2 phage aerosol preparation was filtered with a 2-µm filter, but would have contained residual lysate from the *E. coli* cells (the parts of the lysate small enough to pass through the filter) and the now-spent EM271 media, containing NaCl, in which it was grown. Therefore, a large fraction of the biological material in the MS2 aerosol is bacterial material that is not protected by a cell membrane. The NaCl in the media likely resulted in large uptake of water and therefore a higher probability of hydrolysis and oxidative damage during the aging process. Second, the MS2 phage does not contain the same protective factors as a spore (spore coat, calcium dipocolinate, or special soluble proteins) to protect it from oxidative or other chemical reactants allowing more opportunity for the fluorophores in the MS2 aerosols to react and at a faster rate.

The loss in infectivity of MS2 appears to follow the same trend as the loss in fluorescence when excited at 263 nm for MS2 phage. This result is consistent with the protein degradation, which causes the decrease in the fluorescence, being the cause, or one of the causes, of the decrease in infectivity, but it could also be consistent with

ozone damage to DNA being more responsible for the decrease in infectivity. The apparent increase in Bt Al Hakam viability during high ozone experiments was initially perplexing. Untreated spore preparations have been shown to contain significant amounts of extracellular DNA, which in the absence of cell lysis treatment prior to assay may result in amplification of DNA during PCR (Johns et al., 1994). DNA is known to react with ozone (Cataldo, 2006, Theravathu et al., 2001). It is possible that extracellular DNA was oxidized and destroyed during experiments and resulted in a lower genomic material available for q-PCR. This would result in the ratio between culturable spores and genomic equivalents to decrease, regardless of changes in viability. These results indicate that the use of q-PCR (measurement of total genomic equivalents in a sample) as a method of normalizing for physical loss, in these types of experiments, may not be the most appropriate method for determining biological decay of *Bacillus* spores.

The results presented here also suggest that research studies or sensor technologies that use PCR based detection for enumeration may be skewed if ozone or other atmospheric constituents destroy extracellular DNA more rapidly than intracellular materials (such as those in the core of a Bt Al Hakam spore). The viability (infectivity of *E.coli* cells) of MS2 phage decreased by 100 fold while the average fluorescence intensity measured by the SPFS decreased by no more than 75% and the fluorescence intensity measured by the UV-APS increased by 30 to 45%. These results suggest additional studies are need to understand of the effects of atmospheric air on the ability of other detection modalities, such as antibodies to detect specific antigens

of biological particles to correlate with biological activity and fluorescence. To determine whether the results observed in this study for Bt Al Hakam were actually due to loss in extracellular genomic material, additional studies need to be performed. One approach may be to utilize DNA-modifying Propidum monoazide (PMA™) dye for staining extracelluar DNA or DNA not housed within a live cell. PMA dye selectively binds with DNA either outside of a cell or DNA within a cell with a compromised membrane. The dye then prevents further amplification of the DNA to which it has reacted, allowing for the distinction between enclosed DNA in a live cell and that of free-floating or available DNA. Experiments could be performed using this dye to measure the amount of "extracellular" DNA in samples prior to and after aging by coupling the PMA measured population (when compared to culture) before and after lysing and extraction of the intact DNA in the cells.

The changes in fluorescence observed in the presence of different RH and ozone indicate that biological aerosols can be significantly altered while remaining aloft in the ambient environment. Laboratory studies, related to the characterization of biological aerosols and to the development of new sensor technologies, typically utilize aerosols measured shortly after aerosolization. The results of the studies shown in the present paper indicate that the fluorescence amplitudes and spectral profiles may be considerably different for freshly generated aerosols as compared with those that have been in the environment. The different conditions tested were intended to be representative of EPA standards for ozone exposure during an 8-hr period. The results suggest that at these levels, which often exist in urban areas, the changes observed may

occur between 30 minutes to 3 hours following the emission of a biological particle into the atmosphere. Fluorescence based technologies used for measurement or detection of biological particles may therefore be misrepresenting actual atmospheric bioaerosol concentrations. For example, instruments that rely on tryptophan fluorescence (excitation in the range 260 to 290 nm and measured fluorescence between 320 to 350 nm) may not accurately measure many bioaerosols that have been exposed to ozone and humidity. Additionally, the loss of extracellular genomic material on *Bacillus* spores during exposure may be an indication of a loss in sensitivity for sensors that utilize PCR based assays for detection and also be indicative of the potential for other extracellular components used for detection (such as antigen/antibodies) to be diminished.

5.0 Summary

The measurement and detection of biological aerosols in the atmosphere continues to be a topic of great interest in the scientific community. Most sensors for detecting biological aerosols rely on the presence of specific molecules in the biological particles, e.g., as antigens on the surface, DNA sequences, or molecules more common to all living cells such as tryptophan, flavins, or NADH, which can be detected in the intrinsic fluorescence of biological materials. In developing and testing bioaerosol detection methods, researchers should account for the potential changes in the physical and chemical properties of bioaerosols caused by various atmospheric conditions. This paper describes experiments performed to measure the changes in light-induced

fluorescence spectra and viability of two types of biological aerosols, Bt Al Hakam and MS2. The aerosols were exposed for 4 hours in a rotating drum chamber to high and low RH at two ozone concentrations. Changes in fluorescence and viability were measured using an SPFS, UV-APS, cell culture, and q-PCR. For both Bt Al Hakam and MS2 bioaerosols (i) the decrease in fluorescence intensity was larger when excited at 263 nm than when excited at 351 or 355 nm; (ii) the fluorescence of *Bt Al Hakam* decreased more slowly, and with a much smaller net decrease, than did the fluorescence of MS2; (iii) the decrease in fluorescence of MS2 or Bt Al Hakam was typically largest in the UV263 emission band, smaller in the VIS 351 band, and smallest in the VIS 263 band. Most of the decrease in fluorescence occurred in the first 100 to 150 minutes with *Bt Al Hakam* spores, and in the first 50 to 100 minutes with MS2. The UV-APS fluorescence increased during experiments, but the SPFS fluorescence in the VIS 351 band decreased. This may be due to differences in the way the two instruments measure particle size, the differences in excitation wavelength or the range over which the fluorescence is integrated, however, not enough information was available to draw any specific conclusion. An approximately 2-log loss in viability was observed for the MS2 phage when it was exposed to ozone in the presence of medium at high RH. The Bt Al Hakam viability was skewed by the destruction of extracellular DNA and was therefore not quantifiable during experiments. This observation suggests that utilization of PCR based detection for *Bacillus* spores, may be limited if the spores have been exposed to atmospheric oxidizing agents. The results of these experiments indicate that the fluorescence spectra and viability (of Bt Al Hakam) and infectivity (of MS2) of

biological aerosols exposed for up to 4 hr to ozone at medium and high RH, which are not uncommon in the atmosphere, are different from those of freshly generated bioaerosols.

Chapter 4: Measurement of the Growth Factors of Biological Aerosols and Associated Media using an Aerodynamic Hygroscopic Growth Analyzer (AHGA)

4.1 Introduction

4.1.1 Background

As discussed in the previous chapters, the atmospheric conditions in which a bioaerosols is present can affect the physical and chemical properties. In the previous chapter, relative humidity and ozone were show to change the spectral properties of two biological aerosols, *Bacillus thuringiensis* Al Hakam spores and MS2 Phage. The largest shift in these spectral properties was noted at high relative humidity and high concentration of ozone. Observations were also made regarding shifts in the size distribution as a function of relative humidity. The degree of affinity for a biological aerosol to uptake water may play a very critical role in how the aerosol itself may change physically and chemically in the presence of water vapor.

4.1.2 Changes in Bioaerosols Size Distributions Due to Uptake of Water

Several studies have shown that depending on the hygroscopicity of the organism, changes in relative humidity can lead to shifts in size distributions of biological aerosols (Dua, 1996; Lee, et al., 2002; Reponen et al., 1996; Westphal, 2002). Shifts in size distributions can lead to increased or decreased deposition

efficiency within the respiratory system (Hinds, 1999). In addition, understanding the hygroscopic nature of biological organisms can help to predict whether bioaerosols may result in size changes within the human respiratory system due to the high local relative humidity (Dua, 1996; Lee, et al., 2002; Reponen et al., 1996). Reponen et al., 1996 showed that the size distribution of fungal spores did not change significantly at RH between 30 and 90%, but saw in an increase when RH approached 100%. Lee et al., (2002) predicted an increase in respiratory deposition based on the observed growth factors for *Escherichia coli* and *Bacillus subtilis* aerosols at RH of 85% of 1.34 and 1.16 respectively. Westphal et al., (2002) showed swelling of *Bacillus thuringiensis* spores using automated scanning microscopy and predicted that two mechanisms controlled the diffusion of water into spores, diffusion into the spore coat and cortex followed by uptake of water into the spore core, both of which occurred on differing timescales. However, very little is understood regarding the hygroscopic nature and size distribution shifts of pathogenic biological aerosols, including spores, vegetative bacteria, viruses and toxins. While the sizes of many of these organisms are known, the aerosolized size distribution, and possible shifts due to the relative humidity of the environment in which they are released are unknown. The effects of media composition, culture, and aerosolization technique may also affect the hygroscopicity and subsequent shift in size distributions of these aerosolized biological organisms.

4.1.3 Potential Role of Bioaerosols to Serve as Ice Nuclei or Cloud Nuclei

Approximately 0.01% of organic carbon found in the water contained in atmospheric precipitation such as clouds or rain can be attributed to the presence of bacteria. Fungal spores have been found contribute to a much larger fraction of organic carbon of 1.5 % (Bauer et al., (2002). Motazavi et al., (2008) found eight additional bacterial isolates, not inclusive of the commonly known ice nuclei bacteria of *Pseudomonas* or *Erwinia* genera to be present in snow, showing the potential for a range of types of bacteria to serve as CNN or IN. Incorporation of aerosolized biological aerosols into CCN or IC could lead to potential transport and mobility of these microorganisms within the environment. A study performed by Franc and Demott (1998) of plant pathogens from the *Erwinia* genera showed that 25-30% of the aerosolized bacteria serve as CCN and participate in precipitation processes and vertical transport into the atmosphere. Fuzzi et al., (1997), identified a two-fold increase in the number of culturable bacteria in fog clouds and surmised that the chemical composition of fog droplets serve a culture media for bioaerosols and a source of secondary biological aerosols (SBA) in the atmosphere.

4.1.3 Role of Relative Humidity on Bioaerosol Activity

Relative humidity can also influence the viability and virulence of aerosolized organisms. For example, the survivals of influenza and corona viruses have been shown to be dependent on relative humidity and temperature. Lowen et al., (2007) indicated that lower temperatures and lower relative humidity increased the viability of influenza

virus aerosols and transmission from person to person. Viruses with lipid envelopes generally can survive at low RH values <30% while non-lipid enveloped viruses survive at higher RH values >70% (Tang, 2009). Kim et al., (2007) reported viability and sampling efficiency for porcine corona viruses were lowest at 90% RH and highest at 30% RH and surmised that enveloped viruses were less susceptible to stresses from RH than enveloped viruses. Bacterial aerosol survival has also been shown to increase with decreasing RH. Differences between the sensitivity to RH for Gram-positive verses Gram-negative bacteria have been observed (Tang, 2009). In addition, the method of aerosolization, dry verses wet, as well as suspension medium, all may contribute to variances in the sensitivity of an organism to RH (Cox, 1989, 1998). The effectiveness of various toxic gases on spores has also been shown to be dependent on RH. Whitney et al., (2003) showed that prehumidification of *Bacillus anthracis* spores led to 100% kill rates with chlorine dioxide gas verses incomplete kill at RH values of 20 and 40%. Ozone has been demonstrated to be more effective at killing spores in the presence of high relative humidity (Ishizaki, 1986; Currier et al., 2001). Santarpia et al., (2010), and Pan et al., (2013) showed significant differences in the autofluorescence of biological aerosols when in the presence of high relative humidity. Ratnesar-Shumate et al., (2013) demonstrated significant differences in the autofluorescence, size distribution, and culturability of spores and phages at high relative humidity in the presence of ozone.

The effects of relative humidity on the various physical and chemical properties of biological aerosols is important in order to understand the risks associated with the

release of infectious biological aerosols both unintentionally, such as the natural spread of viruses such as influenza or the common cold, but also intentionally, such as those utilized in an attack by an adversary as a weapon of mass destruction. Knowledge of the hygroscopic properties for given biological aerosols as a function of relative humidity, as well as its impact on the size and virulence, can be used to inform further studies for measuring the stability and transport of these aerosols in the environment.

4.2 Objective of Experiments

Very few studies have attempted to distinguish between the hygroscopic growth of pure bioaerosols and those with buffer or media present which are more commonly used in laboratories. Much is known about the hygroscopicity of various salts such as sodium chloride and ammonium sulfate (Tang and Munkelwitz, 1993; Hu et al., 2010). However, the effects of salts on biological aerosols has yet to be understood. In this study, the hygroscopicity of several types of biological aerosols was measured, both in the presence of aerosolization media such as buffers, and in pure form. For comparison, the hygroscopic properties of the media alone was used to determine whether any observed growth could be attributed to soluble salts present on the surface of the organisms.

The objective of this research was to develop and utilize a new method for measurement of the hygroscopic properties of biological aerosols and media components including the growth factors and deliquescence and efflorescence behavior.

4.2 Materials and Methods

4.2.1 Aerodynamic Hygroscopic Growth Analyzer (AHGA)

To determine the hygroscopic nature of biological aerosols of interest, a test apparatus has been developed that allows for the measurement of aerosols before and after humidification. Using this test setup, the hysteresis behavior of aerosols to be tested can be measured. Several different methods have been employed for measurement of hysteresis for aerosols (Radar and McMurry, 1986, Santarpia, et al., 2004; Kaku et al., 2006; Rubel, 1997; Lee et al., 2002). These methods relied on the changes in particle size as measured by Tandem Differential Mobility Analyzers (TDMA), which are intended for measurement of fine aerosol growth and not growth of particles in the size range of respirable biological aerosols. For this study, the growth factors of test aerosols were measured by monitoring changes in the aerodynamic particle size distribution using an APS® as a function of relative humidity in a new test system developed called the Aerodynamic Hygroscopic Growth Analyzer (AHGA). A schematic of the system is shown in Figure 21.

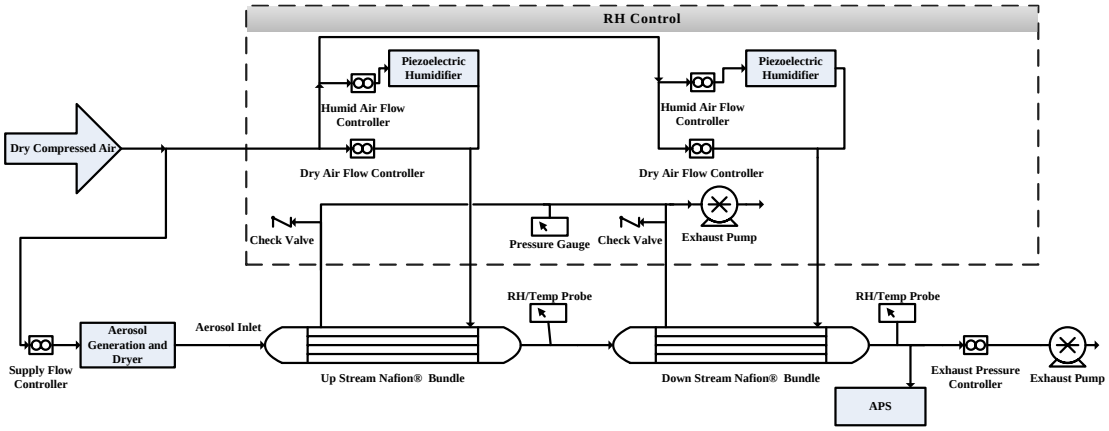

Figure 21 - Schematic of Aerodynamic Hygroscopic Growth Analyzer

4.2.2 Aerosol Generation

Test aerosols were generated using a Sono-Tek aerosol generation system. Liquid suspensions or solutions of the bulk material to be tested were loaded into 30 mL syringes (Model 309650, Luer-Lok Tip, Benton-Dickinson Worldwide) and the syringes were loaded onto a syringe pump (Model # 12-05-00144, Sono-Tek Corporation). A mini-stir bar was placed inside the reservoir of the syringe and a small stir plate (Catalog # 1151050, Thermo-Fisher Scientific Inc.) was inverted and held in place above the syringe and operated at medium speed in order to maintain material homogeneity throughout the syringe by reducing settling of solid material in the syringe reservoir for the duration of the experiments. Liquid mixtures were transferred from the syringe at 100 uL/min into a 120-Hz Sono-tek Ultrasonic Atomizing Nozzle (Model # Nozzle 120, Sono-Tek Corp.) located at the top of an ACC as previously described by Ratnesar-Shumate, et al., (2010). Compressed HEPA and HEGA filtered air (Model

3074B, TSI Inc.) was fed into the ACC at 15 pounds per square inch (PSI) and 10 Liters per minute (Lpm) using a standard rotameter. The clean air was used to push the aerosol through a diffusion dryer (Model # 3062, TSI Inc.) followed by an aerosol neutralizer (Model # 3012A, TSI Inc.), and into the test system as shown in Figure 21.

Aerosol introduced to the inlet of the AHGA was diluted to optimize the particle concentration. Only a portion of the total aerosol generated was allowed to enter the AHGA. This was done by regulating the total flow through the AHGA and by adding filtered air to the inlet of the AHGA to displace the air containing the aerosol. An exhaust pressure controller (Model # PC-15PSIA-D, Alicat Scientific Inc.) at the end of the AHGA test system was set to about 14.4 to 14.6 PSI to maintain the AHGA exhaust pressure at approximately 0.2 PSI below the system inlet pressure, which varied depending on atmospheric pressure. With the system pressure differential maintained, the AHGA test system only allowed a minimal amount, approximately 5 to 10 Lpm, of air to enter. Clean filtered air at a rate of approximately 5-8 Lpm was used to regulate the flow of aerosol entering the AHGA system. An increase in the clean airflow at the inlet decreased the amount of aerosol-laden air allowed to enter from the aerosol generation system. Excess aerosol laden air from the aerosol generation system was vented into the room through a HEPA filter.

4.2.3 Humidification System

Relative humidity in the AHGA was controlled within two Nafion® tube bundles (Model # PD07018T-24MSS, Perma Pure LLC) housed in stainless steel shells. The main sample air stream inside the Nafion® tube bundles was conditioned with a countercurrent air stream outside the Nafion® tube bundles but inside the shells. Water molecules permeated through the Nafion® tube walls because of water concentration gradients between the two gas streams. In the case of humidification, water permeated into the Nafion® bundles, and in the case of desiccation, water permeated out of the Nafion® bundles. The two Nafion® systems were located in series as shown in Figure 21.

Mixing dry and humid air at different proportions controlled the water content of the conditioning air stream. The dry air component was created by passing compressed air through HEPA and HEGA filters (Model # 3074B, TSI Inc.) and a diffusion drier (Model # 26800, WA Hammond Drierite Co. Ltd.) before entering the Nafion® shell. The humid air component was generated using a small piezo-electric water generator (Model # 50-1011.1, APC International Ltd.) housed in a custom made acrylic tube. Air flowing through the acrylic piezo-electric tube picked up water vapor and water droplets. The air stream was directed into a plastic bottle to allow the larger water droplets to fall out before entering the Nafion® shell. The water level in the piezo-electric acrylic tube was maintained at about 2” by using small peristaltic pumps (Model # 3386, Control Company Inc.) to recirculate water in and out of the acrylic tubes, into the same bottle used for trapping the large water droplets. The conditioned dry air and humid air streams were mixed prior to entering in the Nafion tube bundles.

The pressure of the conditioning stream, with respect to the inside of the Nafion® tubes, was kept negative to avoid collapsing any of the individual Nafion® tubes. A Nafion® tube, which already has a diameter less than 1 mm, in a collapsed state would hinder the flow of aerosol through the system, thus a vacuum source maintained at approximately 2.5 PSI was connected to the outlet of the Nafion® conditioning stream. Additionally a check valve was placed prior to the vacuum source to allow conditioning air to escape in the event of a vacuum malfunction and allow the vacuum source to pull directly from the conditioning air stream.

Relative humidity and temperature of the main sample air stream immediately downstream of the US and DS Nafion® tubes was monitored in real-time every second and the average recorded every 10 seconds using two RH/temperature probes (Model # HMP60, Vaisala Inc.) located perpendicular to the air stream. Temperatures at four critical points throughout the test system were monitored using thermocouples (Model # SA1-RTD-B, Omega Engineering Inc.) located at the exit of both Nafion® systems as well as the inlet of the APS® (described in the next section). The temperatures were monitored and recorded in order to ensure that there was sufficient thermal uniformity in the AGHA to avoid the generation of cold spots that might introduce spontaneous condensation.

LabVIEW (LabVIEW 2011, National Instruments Inc.) was used to read and record the RH, temperature, and pressure in the various sections of the AHGA via a data acquisition device (Model # NI USB-6229, National Instruments Inc.). The moisture content of the conditioning air stream and the RH of the main aerosol sample

stream was achieved by controlling the dry and humid generation airflow component via electronic flow controllers (Model # MC-10SLPM-D-PVC90, Alicat Scientific Inc.), two per Nafion® or four total. Each Nafion® (US and DS) was connected to a dry and humid flow controller using the same LabView system. The flow output of the controllers was set to always combine to 10 Lpm so that the conditioning air entering the Nafion® shell was always 10 Lpm. Depending on the desired RH of the aerosol stream, the software adjusted the ratio of the dry and humid component airflow. The software used a PID feedback control algorithm to maintain the humidity within the Nafion® tubes at the desired point. The software had a script function that allowed the user to input a schedule of RH set points, for each Nafion® system in order to automate experiments and reduce human error.

4.2.4 Measure of Growth Factors

Experiments were performed by starting all functions of the test system and allowing both the US and DS Nafion® systems to reach a baseline RH of 20%. The aerodynamic aerosol size distribution at this condition was measured continuously for ten minutes. After ten minutes, during the deliquescence leg of the experiment, the DS Nafion® system RH was increased to 30% and held for another ten minutes. This process was repeated at 10% intervals until a final RH of slightly less than 85% was achieved and was used to calculate the deliquescence relative humidity and growth factor of the test aerosol. After reaching the condition in which the US Nafion® was at 20% and the DS Nafion® was at the 85% target the RH in the US Nafion® was

increased to RH 85% during the efflorescence leg of the experiment and held for ten minutes. The DS Nafion® was then reduced to 70% and held for ten minutes, with the same process as the deliquescence leg being repeated for efflorescence with decreasing RH at 10% intervals as shown in Figure 22.

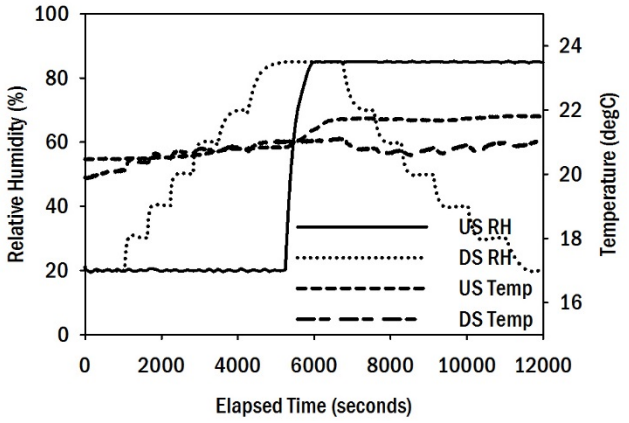

Figure 22 - Example of RH Profile and Temperature Stability During Experiments in the AHGA.

APS® samples were taken every ten seconds and recorded by LabVIEW along with RH, and temperature at the US and DS Nafion® systems. It was determined during system validation that at RH >85%, measurement of size distributions of an APS® unit was not possible due to clogging and that supersaturation of water vapor and condensation may be occurring randomly throughout the test system. The data streams used for analysis were parsed by selecting acceptable ranges of RH values for each target Nafion® system RH (i.e. RH 30±2%) and outputting the average size distribution across all 52 bins of the APS® for the 10 minute time interval in which the RH values fell within these ranges. Along with the size distribution for the intervals selected, the

average RH was reported. The first bin of the APS® data files (<0.523 μm) was discarded during further data analysis. As depicted in Figure 22, each step region represents the time intervals in which data was selected from the APS® for calculating growth factors. Temperature was shown to only vary within <1°C during experiments in the US and DS Nafions®.

For several of the aerosols tested, multiple modes were noted in the raw average distributions, a minimization of the sum of least square errors (LSE) between the raw distribution and the sum of multiple parameterized lognormal distributions that resulted in the closest fit to the raw distribution was used to determine and fit multiple modes to each raw distribution (when applicable) as depicted in Figure 23. This was performed in Microsoft Excel by first assuming either one, two, or three modes, assuming the count median diameter (or geometric mean diameter), the geometric standard deviation, and the number concentration, for each mode and using the Solver function to iteratively solve for the parameterized values that provided the best-fit to the raw distribution based on the minimization of the LSE. Once the best fits were determined and the appropriate number of modes and parameters obtained for these distributions, the growth factors for the deliquescence and efflorescence legs were calculated using Equation 3, where d^* is the geometric mean diameter (GMD) measured by the APS® for the mode at RH=20, 30, 40….85%, and d^{20} is the initial starting GMD measured by the APS® at RH=20%. The APS® has 52 equally spaced size bins (on a log scale) ranging from 0.523 to 20 μm. The minimum and maximum bin widths in the size range of interest for these experiments was 0.06 μm for the 0.777 um and 0.22

for the 3.051 µm bin respectively, therefore the smallest theoretical resolvable growth factor across this range of particles in the APS® is 1.07. To determine whether the size shifts observed between the two trials for each aerosol type were significant, two sided paired t-tests were performed using the differences in each mode between the GMDs at RH=20% and 30% and the differences between the GMDs at each subsequent RH and RH=20% during the deliquescence and efflorescence leg. Growth factors less than or equal to 1.07 were not considered statistically significant due to the lower limit of the resolvable growth factors using the APS® measurement.

The residence time associated with generation of the aerosol into the ACC via ultrasonic nozzle and passage through the diffusion dryer and charge neutralizer at 10 Lpm is approximately 22 seconds. The number median diameter generated by a 120 kHz ultrasonic nozzle is 18 µm, which if modeled as a purely aqueous droplet, requires 2 seconds at 85% RH to evaporate completely (Hinds, 1999). The RH in the ACC through the charge neutralizer was likely well below 85% since dry air at approximately RH=20% was introduced into to ACC with the aerosols as they were generated. The residence time in the aerosol generation process should have provided ample time for each droplet to dry to a solid particle before entering into the first Nafion®. In the range of particles utilized in this study, from 0.8 to 3 µm, (as measured by APS® when RH=20%) the equilibration time of an aqueous droplet ranges from 6.4E-2 seconds for 0.8µm at 20% RH to 5.8E-2 seconds for 3 µm at 85% (Hinds, 1999). The theoretical residence time in each Nafion bundle at the maximum flow rate through the AHGA

system of 10 Lpm is 0.103 seconds and therefore should have provided enough time for particles to reach equilibrium in the Nafions® prior to measurement.

$$Growth\ Factor = \frac{d^*}{d^{20}} \qquad \textbf{Equation 3}$$

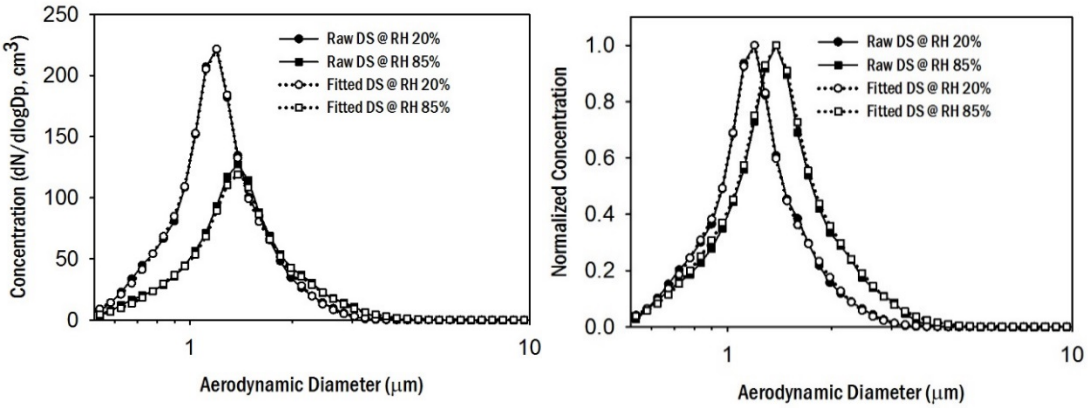

Figure 23 - Example of Fitting Process Used for Data Analysis. (Left) The raw and fitted distribution assuming two modes for the APS measurement at 20% and 85% RH. (Right) The raw and fitted distributions normalized by concentration to shown alignment of the distribution. Growth factors are calculated by comparing the geometric median diameter for each mode at each RH using the APS.

4.2.5 Test Aerosols

The growth factors of several non-biological and biological materials were measured using the AHGA. The final concentrations used during experiments were selected based on trial and error in order to achieve a diameter with a mode between 1 and 2 microns during experiments. This size range was selected in order to reduce

physical losses of aerosols in the system due to inertial and deposition forces in the Nafion® systems.

NaCl, and polystyrene latex spheres (PSLs) were used to validate performance of the system. NaCl (Catalog # S9888 Sigma Aldrich Co.) was mixed with sterile filtered deionized water as listed in Table 6.

Polystyrene latex 3.1μm spheres (Catalog # GA500 and GS300, Thermo Fisher Scientific Inc.) were mixed with sterile filtered deionized water as listed in Table 6.

Two aerosolization additives that may be used with biological organism were tested on the AHGA. Phosphate Buffer Saline (PBS) (Catalog # P5492, Sigma-Aldrich), Cab-osil®M5 (Catalog # 20830, Fluka-Sigma-Aldrich Inc.), were diluted with sterile filtered deionized water to achieve the final concentrations listed in Table 6.

Three types of sterile media were aerosolized independent from the actual biological organisms. Nutrient Broth (Catalog # 234000, Difco™, Becton, Dickinson and Company) was prepared per manufacturer's instructions. EM271 was prepared by combining and autoclaving 1% tryptone (Catalog # 211705, Becton, Dickinson and Company), 0.1% yeast extract (Catalog # 212750, Becton, Dickinson and Company), and 0.8% NaCl (Catalog# S7653, Sigma-Aldrich) (w/v). Modified-Minimum Essential Medium (G-MEM) was prepared as 86% (v/v) Minimum Essential Medium (MEM Gibco # 11095-080), 10% (v/v) Heat-inactivated Fetal Bovine Serum (FBS, Gibco# 10082-147), 1% (v/v) 200 mM L-glutamine (Life Technologies Inc. # 25030-024), 1%

(v/v) 10 mM Non-essential Amino Acids (NEAA, Life Technologies Inc. # 41500-018), 1% (v/v) 100 mM Sodium pyruvate (Gibco # 11360-070), and 1% (v/v) of 100x Antibioltic-antimycotic (Life Technologies Inc., # 15240-096). Each type of media was diluted in sterile filtered deionized water at the concentrations listed in Table 6.

Table 6-Summary of Aerosol Materials, Concentrations, and Sizes.

Material	Concentration	Number of Modes	CMD or GMD (microns)
NaCl	0.82 mg/mL	1	1.98
PSL-3.1 µm	0.02% Solids	1	2.97
Phosphate Buffer Saline	4.8% (v/v)	1	1.72
Cab-osil®M5	0.5 mg/mL	1	1.23
Bacillus thuringiensis Al Hakam Crude	3.9E4 CFU/mL	2	1.39,1.45
Bacillus thuringiensis Al Hakam Clean	7.1E5 CFU/mL	2	0.8, 1.1
Pseudomonas fluorescens Crude	3.0E7 CFU/mL	2	1.29,1.37
Pseudomonas fluorescens Clean	7.9E7 CFU/mL	2	1.35, 1.38
MS2 in *Escherichia coli* Lysate	8.5E10 PFU/mL	2	1.35,1.40
MS2 Filtered in Spent Media	3.6E10 PFU/mL	2	1.37,1.47
Sterile EM271 Media	0.1% v/v	2	1.15,1.18
Nutrient Broth	4% (v/v)	2	1.24, 1.31
MEM	2% (v/v)	2	1.22, 1.29

Several biological aerosols were tested on the AHGA for the hygroscopic properties. *Bacillus thuringiensis* (Bt) Al Hakam spores were obtained from MRI Global Inc., and prepared two distinct ways for aerosolization in order to understand the individual effects on hygroscopic growth. These methods consisted of a sporulated culture in spent media, and the same culture resuspended in water. All stocks of Bt Al Hakam spores were picked from individual colonies that had been incubated overnight on tryptic soy agar (TSA, Thomas Scientific #C996W03) plates at 37°C. Bt Al Hakam stocks were prepared by single colony inoculation in Nutrient Broth Sporulation Medium (NSM) broth, omitting the agar and utilizing Lab-Lemco powder (Oxoid LP0029). These cultures were incubated on a shaking incubator (37°C, 200 RPM) for one week to ensure efficient sporulation, then heat shocked at 80°C for ten minutes to inactivate any remaining vegetative cells (Yezza, 2005). This preparation was split into a dirty stock, kept in spent media, and clean stock, separated by centrifugation at 10,000 RPM for 25 minutes and resuspended in an equal volume of 0.22 μm filter-sterilized deionized water. All stocks were further diluted in 0.22 μm sterile-filtered water to achieve the target particle size to final concentrations as listed in Table 6.

Pseudomonas fluorescens strain 1013 (ATCC/948) originated from frozen glycerol stocks and was grown on nutrient agar (BD 212000) for 48 hours at 25°C. Individual colonies were isolated and propagated in nutrient broth (BD 233000), incubating at 200 RPM and 25°C. The resulting stock was split, with a portion saved for aerosolization as a dirty stock, and the remaining centrifuged at 10,000 RPM for 25 minutes, and resuspended in 0.22 μm filter-sterilized deionized water. This wash served

to prepare a media-free clean stock of the same bacteria. Both stocks were further diluted using 0.22 μm sterile-filtered water to reach the target particle size as listed in Table 1.

Bacterial stocks were enumerated in triplicate by plating on TSA plates using a Spiral Biotech Autoplate (50 μL exponential setting), and incubating at temperatures specific to each organism. Bt Al Hakam incubated overnight (sixteen hours) at 37°C, while the *P. fluorescens* incubated for 48 hours at 25°C. A Spiral Biotech Q-Count calculated the number of colonies and resulting concentration. Since all stocks were diluted to achieve a specific particle size, the final concentration listed in Table 6 is based on the concentration for aerosolization, diluted to achieve appropriate sized particles.

Male-specific bacteriophage (MS2) (ATCC 15597-B1) production and plaque assays utilized *Escherichia coli* (*E. coli*) str. C-3000 (ATCC 15597) as the host organism. The recommended media, EM 271, was prepared by combining and autoclaving 1% tryptone (BD 211705), 0.1% yeast extract (BD 212750), and 0.8% NaCl (Sigma S7653) (w/v). Agar (BD 214010) was added for solid medium at 1.5%, and the resulting autoclaved medium was supplemented with 0.1% glucose (Sigma G5767), 0.0294% CaCl2 (Sigma C7902), and 0.001% thiamine (Sigma T5941) (w/v, sterile-filtered). *E. coli* C-3000 host cultures were propagated from glycerol stocks by overnight incubation on EM 271 agar at 37°C. Individual colonies were picked, placed into EM 271 broth, and incubated (37°C, 200 RPM) until log-phase culture was achieved, as monitored by spectrophotometer (Model # Ultraspec 2100 Pro, Amersham

Biosciences) absorption at 520 nm. The lyophilized MS2 stock was resuspended in EM 271, with 100 μL used to inoculate the log phase *E. coli*. Incubation of the suspension continued for eighteen hours and then divided. A portion was saved for aerosolization as a dirty preparation, while the remaining stock was centrifuged to remove E. coli lysate, centrifuged at 10,000 rpm for 25 minutes, with the resulting supernatant processed using a 0.22 μm sterile-filter. For this clean preparation, the MS2 phage remained in the filtered liquid, with the majority of cellular debris removed.

MS2 concentrations were determined by a plaque assay of stock serial dilutions, utilizing the same C-3000 strain of *E. coli*. Single colonies of *E. coli* were inoculated into EM 271 and incubated (37°C, 200 RPM) until reaching the log phase, considered a spectrophotometric absorption between 0.2 and 0.5 at 520 nm. The *E. coli* was co-inoculated with 0.5 ml of serially diluted MS2 into EM 271 containing 0.5% agar, kept melted in a 46°C water bath. The tube was then emptied onto EM 271 plates, and incubated overnight at 37°C. The triplicate set containing individually countable plaques determined the concentration of the dirty and clean stocks.

4.3 Results

4.3.1 Validation of AHGA Performance

Experiments were performed with two types of aerosols with known deliquescence and efflorescence relative humidities (DRH and ERH), NaCl and PSL spheres. Shown in Figure 24A is the measured hygroscopic properties of NaCl in the AHGA. Significant growth 1.38 ($p<0.05$) was observed for NaCl between 70 and 80%

RH. During the efflorescence leg, the growth factors were observed to be significant ($p<0.05$) at 85% down to 50% RH, decreasing from 1.41 to 1.09 respectively and returning to the original size at 40% (when $p>0.05$). The DRH and ERH values agree with previously reported values of 75% and 45% for the DRH and ERH respectively (Seinfeld and Pandis, 1998, Lee et al., 2002, Tang and Munkelweitz 1993, Wang et al., 2010) demonstrating that the AGHA accurately captured the hysteresis known to occur with NaCl aerosols after uptake of water prior to drying. PSL spheres, known to be hydrophobic (Lee et al., 2002) showed no significant ($p<0.05$) growth in the AHGA at all RH tested (Figure 24C). The observed growth or lack of growth of the NaCl and PSL spheres tested validated the ability of the AHGA to accurately measure particle size changes at the appropriate deliquescence and efflorescence points for different aerosols and to show agreement with previously reported values.

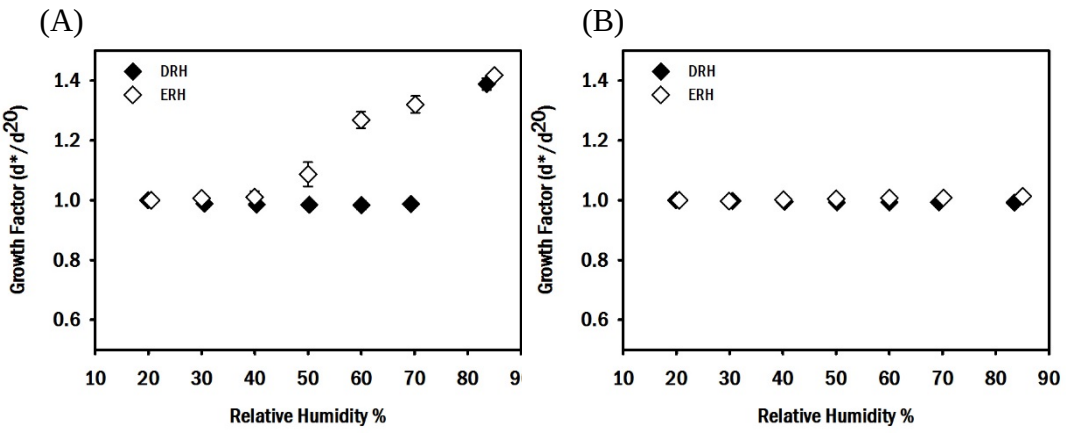

Figure 24 - Growth factors for (A) NaCl (B) PSL Aerosol in the AHGA During Validation Testing. DRH=Growth factors as the aerosols are humidified during the deliquescence leg of the experiment, ERH=Growth factors as the aerosols are dried during the efflorescence leg of the experiment.

The AGHA system design was inspired by traditional Tandem Differential Mobility Analysis that is used for measurement of the uptake of chemical or water vapor for submicron aerosols (Radar and McMurry, 1986). However, biological aerosols, especially those known to be respirable, are in the size range of 1 to 10 μm. The Nafion® systems used in the AHGA contain several small <1mm inner diameter, Nafion® tubes. Losses due to inertial and gravitational settling in the tubes were a concern during experiments. Additionally, there was concern that the tubes may also swell at higher RH leading to an effective smaller inner diameter, increasing losses at higher RH. The loss of larger particles in the system would then potentially skew the distributions observed during measurement in the APS® and lead to errors in the calculated GFs. In order to estimate the transmission losses through the system, and more specifically through each Nafion® a series of experiments was performed with 3.1 μm PSL spheres to determine the transmission efficiency in the system at varying RH. The measurement was performed between an APS® placed upstream of the first Nafion® after aerosol generation and conditioning and the APS® using for measuring the growth factors (inclusive of both Nafion® systems). Given the target-starting diameter of each type of aerosol to be between 1 to 2 μm, it was not anticipated that any growth would be observed beyond 3 microns in the AHGA. As shown in Figure 25, the transmission losses of PSL spheres ranged between 10 to 20% at all RHs measured with the losses being slightly larger at higher RH. Experimental results were were not corrected to account for this effect.

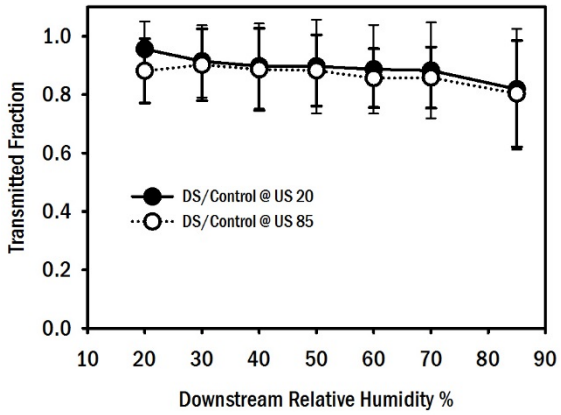

Figure 25 - Transmission Efficiency of AHGA for Three um PSL Beads Between a control APS plased upstream of the two Nafions® and the measurement APS Unit. The mean loss in spheres was observed to be between 10-20 percent across the test system. Higher losses were observed at the highest RH tested, 85%.

4.3.2 Growth of Biological Aerosols

Bacillus thuringiensis Spores

Bt Al Hakam spores were prepared in two ways for aerosolization and measurement of hygroscopic growth in the AHGA. A crude preparation was used to observe the growth of Bt Al Hakam in spent media and a clean preparation was used to see if the spores grew in the absence of media. Shown in Figure 26 are the growth curves for both types of spore preparations. Bt Al Hakam aerosol distributions contained two modes. The crude preparation Mode 1 and Mode 2 average starting geometric mean diameters (GMD) were 1.39 and 1.45 μm while the clean preparation Mode 1 and Mode 2 GMDs were 0.8 and 1.1 μm. Mode 1 and Mode 2 in the dirty and clean preparation showed no significant growth ($p<0.05$) at all RH tested below 80% during both the deliquescence and efflorescence legs of the experiments. Mode 1

showed a statistically significant growth at RH >80% of 1.07, however, this was right at limit of the ability to quantify growth using the APS® and therefore was not considered as actually significant.

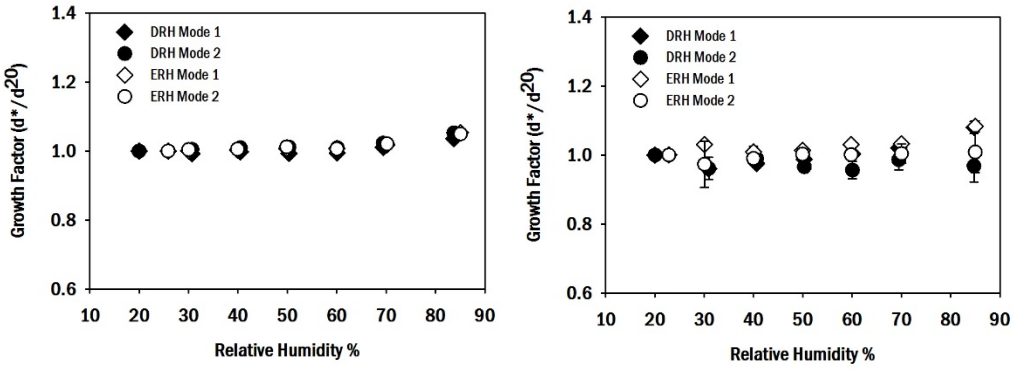

Figure 26 - Hygroscopic Growth of *Bacillus thuringiensis* Al Hakam Spores. (LEFT) represents a crude preparation with spores aerosolized in with spent media and (RIGHT) clean spores resuspended in sterile water. DRH=Growth factors as the aerosols are humidified during the deliquescence leg of the experiment, ERH=Growth factors as the aerosols are dried during the efflorescence leg of the experiment.

Pseudomonas fluorescens

The crude and clean preparation of *P. fluorescens* each had two starting modes at 20% RH with an average GMD 1.29 and 1.37 µm, for the crude, and 1.35 and 1.38 µm, for the clean. The modes in the clean preparation were very close to each other (<40 nm apart), which made it difficult to track and calculate the individual shifts in the GMDs. However, as depicted in Figure 27 when comparing the MSE between using a monomodal lognormal distribution to fit the clean distribution verses a bimodal distribution of two lognormals, the bimodal distribution resulted in the lowest MSE, 3.82 verses 82.3, and so two modes were used to calculate the growth factors. Similar

to the Bt Al Hakam preparations, (Figure 28) neither the dirty nor the clean preparation of *P. fluorescens* showed statistically significant growth ($p<0.05$).

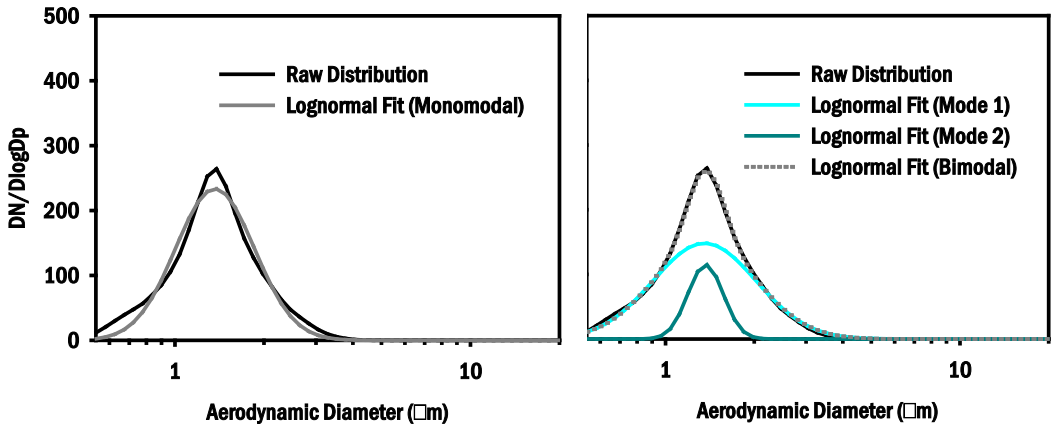

Fit Parameters		
MSE	82.36	
Mode 1		
N	GSD	Dbar
179.7	1.36	1.365

Fit Parameters					
MSE	3.82				
Mode 1			Mode 2		
N	GSD	Dbar	N	GSD	Dbar
149.8	1.5	1.4	39.9	1.1	1.4

Figure 27-Example of Fitting Pseudomonas fluorescence Clean distributions to one or two modes and resulting Mean Square Error (MSE) from parameterized distributions.

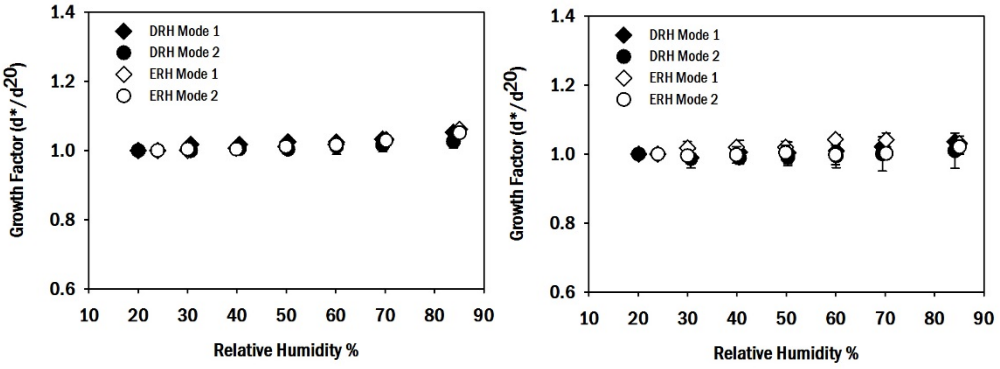

Figure 28 - Hygroscopic Growth of *Pseudomonas fluorescens* Vegetative Bacteria. (LEFT) represents a crude preparation with bacteria aerosolized in with spent media and (RIGHT) clean bacteria resuspended in sterile water. DRH=Growth factors as the aerosols are humidified during the deliquescence leg of the experiment, ERH=Growth factors as the aerosols are dried during the efflorescence leg of the experiment.

MS2 Phage

The hygroscopic growth properties of MS2 phage in spent *E. coli* lysate is shown in Figure 29. For comparison, the same suspension was filtered to remove the lysate and compared with the EM271 media used for growth of the bacteria alone. The GMD of the two modes of MS2 in *E. coli* lysate were 1.35 and 1.40 µm. The filtered sample had two similarly sized modes, 1.37 and 1.47. The average concentrations of the two preparations, 8.5E10 verses 3.6E10 pfu/mL for the unfiltered and filtered and the similar sizes of the two final aerosols indicated the filtration process did not remove a significant portion of large solid materials that would have altered the final distributions. EM271 media had two modes, 1.15 and 1.18 microns. As shown in Figure 29, in all three preparations, the DRH is between 40 and 50% RH with the statistically significant growth factors peaking on average around 1.2 ($p<0.05$). During

the ERH the aerosol of each preparations returns to the original size, ie.no statistically significant difference in the originally diameter vs. those measured between 50 and 40% RH for all three preparations

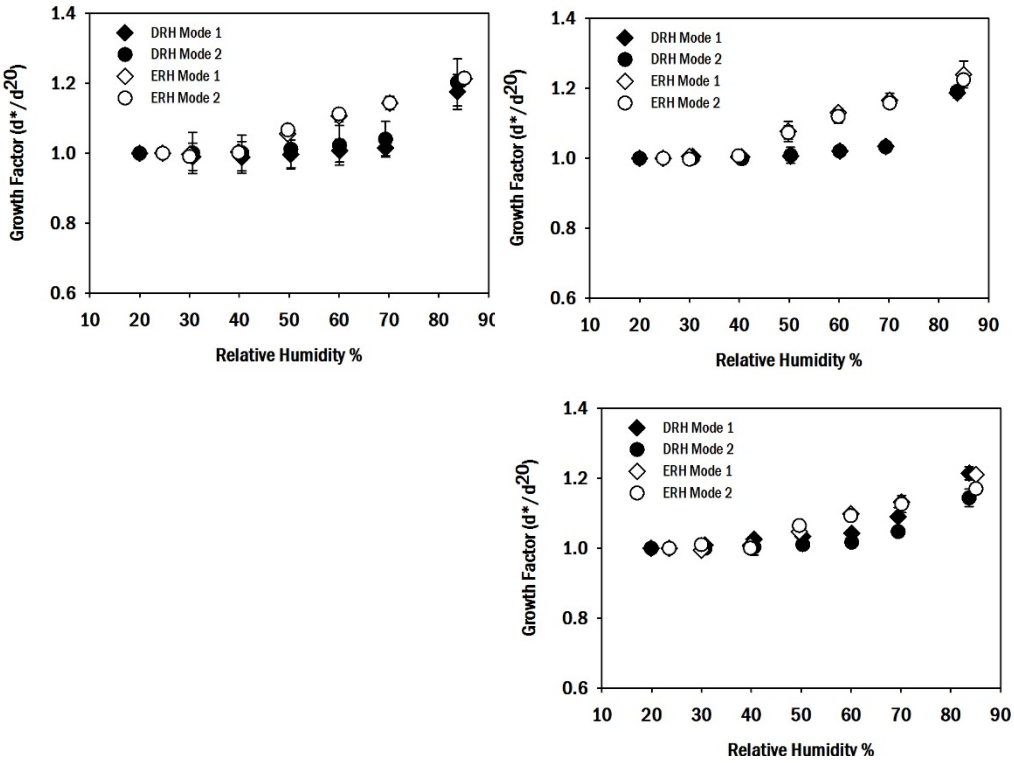

Figure 29 - Hygroscopic Growth of MS2 Phage Aerosols. (LEFT) represents a crude preparation with MS2 phage in E. coly lysate (RIGHT) MS2 phage filtered to remove E. coli lysate (BOTTOM) EM271 media. DRH=Growth factors as the aerosols are humidified during the deliquescence leg of the experiment, ERH=Growth factors as the aerosols are dried during the efflorescence leg of the experiment.

4.3.3 Growth of Media, Buffers, and Additives

The hygroscopic properties NB, MEM, PBS, and Cab-o-sil, were measured in the AHGA as shown in Figure 30. The NB had two modes at 1.24 and 1.31 um and similar to the *P. fluorescens* growth in nutrient broth, showed no significant growth.

The MEM had two similar modes, 1.22 and 1.29 and the largest statistically significant observed growth factor of all the aerosol tested with the AGHA. Between 60 and 70% RH, G-MEM began to uptake water with significant growth factors of 1.09 and 1.10 in Mode 1 and Mode 2 and peaking at 1.24 and 1.26 at RH just slightly below 85%. Differences for G-MEM between the diameters at RH >40% during the efflorescence leg of the experiments were noted, however, these differences were only statistically significant at RH >85% and at 60%, this was due to the large standard deviation between the two replicates for the other RH tested. The PBS aerosols contained one mode when aerosolized in the AGHA at 1.72 μm. PBS deliquescence approached significance ($p=0.053$) between 70 and 80% RH with a maximum of 1.16 at ($p<0.05$) 85% and a statistically significant efflorescence between 50 and 40% RH similar to NaCl. The aerosolized Cab-o-sil had only one mode at 1.23 μm and showed no growth during the experiments as seen in Figure 30C.

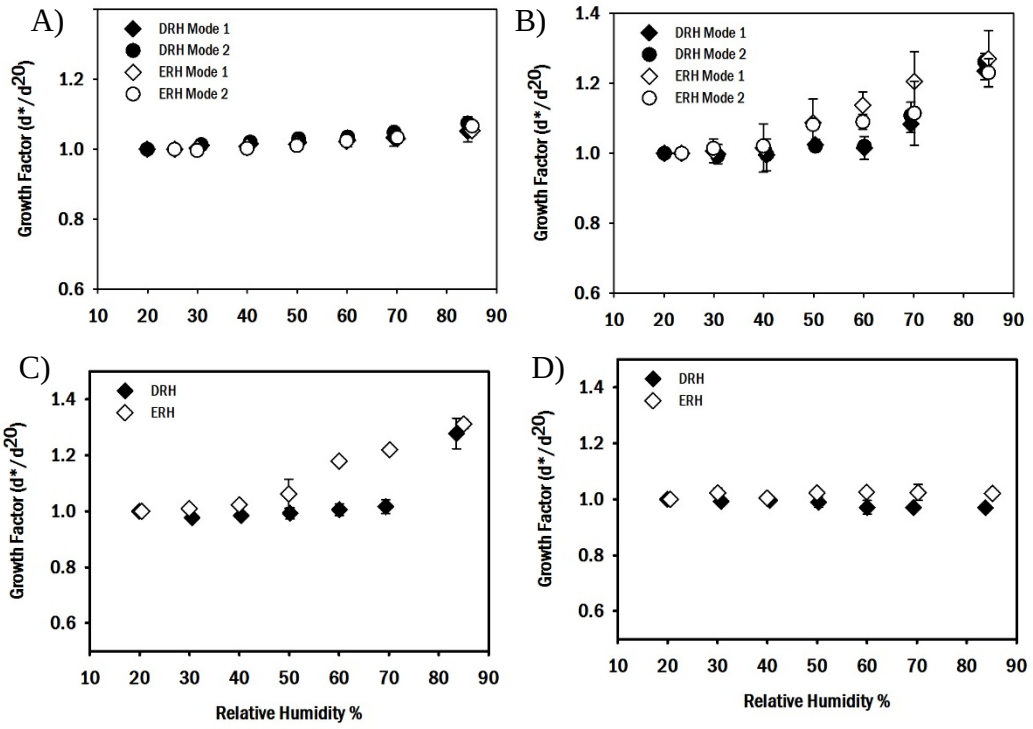

Figure 30- Hygroscopic Growth of Various Media, Buffers, and Additives Commonly Used for Aerosolization of Biological Materials in Laboratory Experiments. (A) Nutrient Broth (B) Minimum Essential Medium (C) Phosphate Buffered Saline (D) Cab-o-sil. DRH=Growth factors as the aerosols are humidified during the deliquescence leg of the experiment, ERH=Growth factors as the aerosols are dried during the efflorescence leg of the experiment.

4.4 Discussion

4.4.1 Aerodynamic Size Growth of Biological Aerosols

The growth factors measured by the AHGA are intended to capture the changes in aerodynamic size, rather than changes in geometric or volume equivalent size of biological aerosols. In theory, depicted in Figure 31, as the bioaerosol may begin to adsorb water, the aerosol hydrates, and the density of the particle, as well as the shape,

approach that of a spherical aqueous droplet. Depending on the original density and morphology of the aerosol prior to uptake or loss of water, the change in the actual size or equivalent diameter may not be easily apparent or captured by the AHGA. For example, the dynamic shape factor of a NaCl aerosols have been reported previously ranging to range 1.1 to 1.5. For a NaCl particle with a starting *dve* of 1 μm and a material density of 2.615 g/mL, the corresponding d^a would be measured by an APS® as ~ 1.24 μm. If the same particle was then hydrated, and grew to a d^{ve} of 1.3, the shape now spherical rather than crystalline and having a density approaching that of water, the d^a would be equivalent to the d^{ve}, however, the calculated GF associated with a volumetric change from 1 to 1.3 μm would not be a factor 1.3, but rather a factor of ~1.05 (1.24 to 1.3 μm). However, as stated previously, the aerodynamic diameter is the physical parameter that is most important to understand with respect to particle transport and deposition in the respiratory track due to inertial forces within the size ranges that represent biological aerosols of interest.

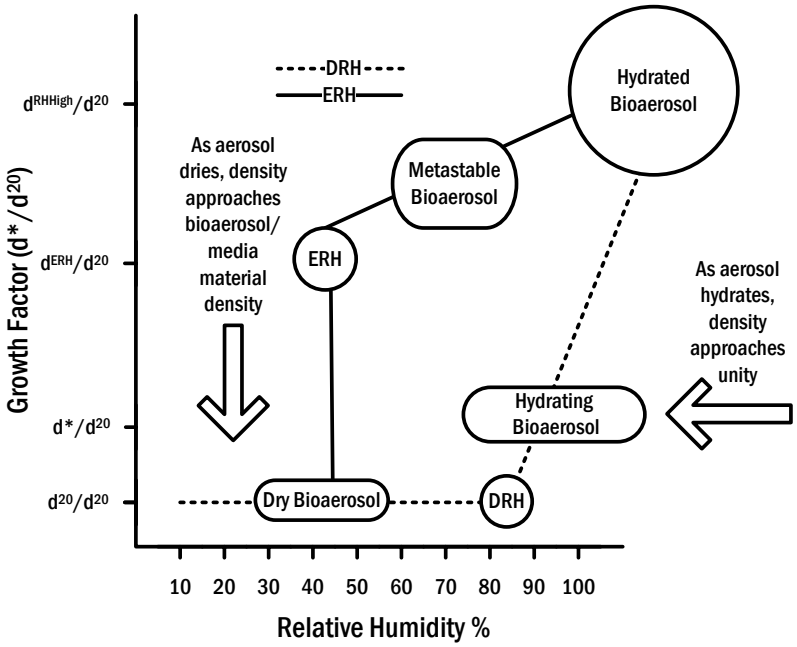

Figure 31- Schematic of the Hygroscopic Changes Occurring for a Bioaerosols in the AHGA During an Experiment.

Growth of Bt Al Hakam

Very little change in the aerodynamic diameters was observed in the Bt Al Hakam spore preparations tested. This lack of growth agrees with previous studies in which other *Bacillus thuringiensis* spores have been observed to by hydrophobic (Doyle et al., 1984; Tomihhiko et al., 1989). The hydrophobicity of *Bacillus thuringiensis* spores, in comparison to other *Bacillus* spp such as *Bacillus subtilis* is thought to be due to the presence of an exosporium thought to contain hydrophobic lipids and proteins (Tomihiko et al, 1989). Westphal et al., (2003) observe the swelling of *B. thuringiensis* spores through microscopy, however, the time and size resolution in which this growth was observed (>1min) and on the order of tens of nanometers are

much longer and much smaller than the residence time and resolution in the AHGA, and therefore the results may not be directly compared. Lee et al., 2002, observed growth of *Bacillus subtilis* spores at RH > 85%; however, the media used for aerosolization of this preparation was not reported. Similarly, Johnson (1999) compared the GF for *B. subtilis* spores as a function of the concentration of PBS used for aerosolization. Changes in the Mass Median Aerodynamic Diameter (MMD) during the study for spores suspended in water with no PBS, showed a GF of ~ 1.2 between 80 and 90% RH which is higher than the GF observed for Bt Al Hakam in the present study. These differences, between Bt Al Hakam and *B. subtilis* are in agreement with the known hygroscopicity of *B. thuringiensis* spores verses *B. subtilis* spores. The growth in Mode 1 for both preparations was likely due to residual spent media still present in the suspension after the cleaning cycle. Nutrient broth alone showed some growth at the higher RH >85% of 1.07, and the sporulation broth used for growing the Bt Al Hakam spores contained Nutrient Broth with some additions including 10% (w/v) potassium chloride which has a DRH at 84.2% (Tang and Munklewitz (1993). Although this media was removed prior to aerosolization in the clean preparation, a small amount of the residual media was likely still present in the suspension and may have contributed to the observed growth in the clean spores and was likely the reason for the observed growth in the crude preparation. However, the growth observed was not considered statistically significant and therefore additional studies need to be conducted to determine if this may have been a factor. The size of Bt Al Hakam spore aerosols alone, with no media present, was not measured by

microscopy in this study, however, previously reported sizes would indicate that Mode 1 may have been too small to have contained Bt Al Hakam spores (EPA 2012) or at least contained very few spores verses Mode 2 and was primarily made up of residual media in the clean preparation. The lack of growth in Mode 2 for the clean Bt Al Hakam preparation, which likely contained most of the Bt Al Hakam spores, showed little affinity for uptake of water, as would be expected based on the previous observation that *Bacillus thuringiensis* spores are hydrophobic. It is possible that some uptake of water by the spores was not captured by the AHGA measurements. The initial d^a of the spores in Mode 2 was 1.12 μm, which if assuming a dry density of *Bacillus* spores of 1.42 g/mL (Carrera et al., 2008) and a dynamic shape factor of 1.2 (Sturm 2003) the corresponding d^{ve} would have been approximately 1.03 μm. If these spore containing particles did uptake any water, and assuming the shape did approach that of a sphere and the density approached that of water, then under these conditions, the dve would have had to have increased to 1.12 μm, resulting in a volumetric change in growth of a factor of 1.09 which would not have been captured by measurement with the APS® .

Growth of *Pseudomonas fluorescens*

Pseudomonas fluorescens was selected for this study to represent gram-negative vegetative bacteria and because if its indication as a CCN and IN bacteria. Both the dirty and clean preparations of *P. pseudomonas* showed little growth when exposed to increasing relative humidity. These results agree with previous studies

performed by Johnson (1998) in which *P. fluorescens* showed no significant growth when aerosolized in the absence of phosphate buffered saline. However, similar to this study, the authors also concluded that changes in the geometric equivalent diameter might have been hard to discerns with the use of an aerodynamic measurement. Park et al., (2011) observed the growth of *P. fluorescens* due to condensation under supersaturated conditions performed at higher temperature and water vapor content than those used in this study

Growth of MS2

The MS2 in *E. coli* lysate grew significantly with increasing relative humidity. MS2 phage itself has been demonstrated to by hydrophobic (Thomson and Yates, 1999). Most probably, the uptake of water observed for the MS2 aerosols was due to the presence of the EM271 media used for cultivation of the *E. coli* and co-aerosolized with the viruses. In the dirty preparation of MS2 phage, the *E. coli* lysate was present, and potentially may have contributed to growth observed. In the previous study performed by Lee and Kim (2002), *E. coli* was observed to have a growth factor of ~ 1.1 between 80 and 90% RH. However, it is hard to determine whether these measurements can be directly compared to those in this study, as the authors did not specify whether the *E. coli* was aerosolized in water or media. However, the observation that the growth factors in this study between the *E. coli* lysate containing. filtered, and EM271 MS2 phage were all the same, at 1.2 at the highest RH tested, implies that EM271 media itself was the component contributing to uptake of water.

This is also supported by the observed DRH and ERH for these suspensions being very similar to those of NaCl and the fact that EM271 media itself contains 8 g/ L NaCl.

Growth of Media

The key result of this study is the observed growth of the aerosols containing no biological components, just growth media and buffers. Both MEM and PBS demonstrated growth factors ranging from 16 to 26% of the original aerodynamic size. In both of these media, the DRH and ERH matched that of NaCl aerosols, which is to be expected, given the NaCl concentration in MEM is 6.8 g/L and in PBS 8 g/L. In the case of the one culture media tested, NB, which contains no NaCl, very little growth, was observed. Based on the results of the media experiments, it is very clear that the media dominates the hygroscopic uptake of water when present in a mixture of bioaerosols, especially in cases where NaCl was present. Cab-o-sil aerosol showed no growth, which given that it is insoluble in water, was not unexpected. Cab-o-sil was not coaerosolized with media or the biologicals in this study, but given the hydrophobic properties of this silica material, it may decrease the amount of uptake of water if present in a mixture and should be considered for future experiments to be coaerosolized with more hydrophilic components.

Growth of Biological Aerosols-Implications for Respiratory Deposition

The deposition of aerosols in the human respiratory track is dependent on the size of the particle which may increase if it hydrophilic given that the relative humidity of air in the lungs approaches 100%. Reponen et al. (1996) calculated the theoretical

changes in deposition of particles from 1-10 microns in the respiratory track with growth factors ranging from 1.1 to 2. Particles in the size ranges of 0.5 to 2 microns were determined to have the most significant increase in deposition in the respiratory track when growth factors of 1.1 to 2 microns were used for aerodynamic size with changes in regional deposition being observed as particle size increased. Studies that intend to investigate the health effects or virulence of different biological aerosols need to consider effect of the growth media or stabilization buffers used for aerosolization. If, for example, PBS is used to increase the survival of osmotically sensitive organisms in suspension during the aerosolization process, then there is the potential for these particles to either grow or to not dry to a complete solid state, depending on RH, and therefore provide a misinterpretation of results. Smaller biological aerosols (submicron), being characterized and quantified ex vivo during inhalation and lethal dose testing may in fact grow to larger particles and rather than deposit in the alveolar region, may deposit in the head airways region. The researcher unaware of the hygroscopic growth may assume the particles deposited in the alveolar. The site of the deposition in the respiratory system is known to be determinant of the disease severity and progression for many respirable diseases caused by microorganisms. Previous studies have shown the lethal dose of pathogenic bacteria such as, *Fransicella tularenis* and *Bacillus anthracis* and toxins such as Ricin increase with aerosol particle size (Bartrand, et al., 2008; Roy et al., 2003). Consistently in scientific studies in which the lethality or virulence of a biological pathogen as an aerosol is measured, the pathogen is aerosolized in a medium that contains large amounts of salts, specifically, NaCl.

Rarely, do the authors investigate the effects of the aerosolization medium on the results of the study. For example, the study performed by Roy et al., (2003) utilized Ricin diluted into phosphate buffered saline prior to exposure of mice to measure the size dependent change in lethal dose of the toxin. No reference to the effect of the use of the saline on the potential growth of the particles upon inhalation is made in the paper, despite having results that differ from a previous study performed with the same toxin and size of particles. In an early study performed by Lester (1948) comparing the survival of influenza A virus at different relative humidities, the percent of infected mice at RH=50% increased from 22.5 to 100% when the virus preparation was dialyzed against distilled water to remove the NaCl (originally present in the aerosolization suspension at 5 g/L). The study concluded that removal of the NaCl contributed to higher survival of influenza at 50% as an aerosol, however, it may have also been possible that without the NaCl present, the influenza aerosol did not grow in the respiratory system due to uptake of water, and thus were able to be deposited farther down into the alveolar region requiring a much lower dose to cause infection. A study performed by Reed et al., (2011), to determine the median lethal dose (LD_{50}) of Ebola virus via inhalation, utilized virus spiked into Hanks buffered saline solution (HBSS), which contain 8 g/L of NaCl, for aerosolization. The authors were not able to measure the lethal dose of the virus to noise in the microtitration assay used for enumeration of the virus during experiments; however, they were able to report the LD_{50} was below 10 virions. However, this study also takes no account of the size of the aerosol generated

or the effect of the media used for aerosolization on the inhaled size of the aerosols and thus potential shift in deposition locale and immune response.

RH Effects on Viability

Relative humidity has a direct effect on the survival of biological aerosols (Songer, 1976; Zhao et al., 2011; Peccia 2001; Donaldson 1973). Many studies attempt to understand how seasonality, and thus variations in RH affects the emergence and spread of diseases such as the common cold and influenza (Lowen et al., 2014; Schaffer et al., 1976, Shaman and Kohn 2009). As in the case of inhalation studies, caution should be used when considering the aerosolization medium containing the biological to be studies. The uptake of water by salts or other components present in the aerosol after generation may either attract water to the surface or conversely, deter water from the particle. In either case, the true effect of RH on the actual bioaerosol will be masked by the interaction of the other constituents present, making laboratory studies difficult to correlate to the natural phenomena attempting to be studied. While not directly able to be compared to this study, one interesting result of the study performed by Park et al., (2011) on the growth of *P. fluorescens* showed that the latent heat of vaporization due to the condensation process was implicated in the loss in viability of the organisms tested. If a component other than the microorganism were driving this condensation process, such as salt, then that may be a mechanism of deactivation that otherwise would not occur on the organism being studied. Studies performed by Thomas and Yates showed that for MS2 Phage, inactivation of the virus was due to the presence of

a dynamic air-water-solid interface the ionic strength of the solution containing the virus. A study by Trouwborst and Jong (1973) showed that a maximum in the inactivation of MS2 aerosolized with NaCl was at maximum at 75% RH decreasing on either side of this RH, very close the DRH of NaCl at 75% when the air-water-solid interface was expected to be highest, therefore also indicating deactivation by this mechanism. Zhao et al., (2011) measured the effects of temperature, RH, absolute humidity, and evaporation potential (the difference between the saturated vapor pressure of water in air at a given temperature and the actual vapor pressure) on the aerosol stability of Gumboro Vaccine virus. Piercy et al. (2011) reported the aerosol stability of Marburg and Ebola filovirus when aerosolized using Dulbecco's modified Eagle's medium (DMEM) tissue culture media which contains 8 g/L of NaCl at 50-55% RH (which is above the ERH of NaCl) and reported decay rates ranging from 4.81 to 2.72% per min. It is possible that had the studies using this medium been performed a lower RH, below the ERH of NaCl, or even above the DRH of NaCl, the decay rates measured may be have been different due to the loss or gain of water content in the aerosol changing the local microenvironment in which the virus is present.

Limitations of the AHGA System and Future Experiments

A system was developed for measurement of the aerodynamic growth of biological aerosols. The AHGA system was able to accurately measure and demonstrate the DRH and ERH of aerosols that have been previously reported. The growth factors measured using this system were based on aerodynamic growth, and as

discussed previously, may not capture any geometric or physical size growth or changes of the aerosol due to uptake of water. Ideally, the system should be able to provide both the change in aerodynamic size and some indication of the change in physical size and shape. If water was adsorbed by the aerosol and not able to be resolved by the AHGA, then it makes interpretation of the effect of RH on the viability of biological aerosols using this system impossible. The system was not designed to be able to measure the viability of the test bioaerosols downstream of the RH changes. However, ultimately, the goal of such studies is to understand the stability of any given organisms when exposed to varying RH and to be able to predict the actual size of the aerosol and the effect of the water uptake pathway (wet to dry, dry to dryer, dry to wet) on the viability of such organisms.

The resolution at which these studies was performed (10% increments of RH) was also too broad to capture the true DRH and ERH of the test aerosols. Future studies should focus on identifying the critical DRH and ERH for each bioaerosols down to ±1%. High fidelity models for predicting the deposition of the bioaerosols in the respiratory track will require some degree of the kinetics of the water uptake and loss to be known. In its current configuration, the AHGA system cannot provide such information, but systems such as optical imaging coupled with particle suspension, such as an electrodynamic particle balance could be used to collect such information. However, the AHGA can be used to identify the DRH and ERH of the aerosol and thus drastically reduce the number of experiments needing to be performed on single aerosols for determining kinetics. The size dependent transmission of the AHGA was

also a limitation of this system. DRH and ERH are known to be particle size and temperature dependent and so future studies should look to determine the relationship between the size of the initial particle, growth factors, and hygroscopic properties, along with the effects of temperature. Upgrades to the system need to provide the ability to control the temperature of the system and to allow for transmission and measurements of particle ranging from submicron to micron.

CONCLUSION

The aerodynamic properties of a bioaerosol are important for understanding deposition in the respiratory track and transport in the environment. The uptake or loss of water from a bioaerosol is dependent on the chemical composition of the aerosol and the relative humidity. A test system was developed that allowed for the hygroscopicity (deliquescence and efflorescence) properties of different bioaerosols and media to be measured. The Aerodynamic Hygroscopic Growth Analyzer system utilizes aerodynamic particle size measurements in series before and after humidification of an aerosol to determine the growth factors of bioaerosols. *Bacillus thuringiensis* Al Hakam spores, *Pseudomonas fluorescens* bacteria did not show significant growth (greater than 10%) when aerosolized in water or in spent growth media. MS2 phage in *E. coli* lysate grew a factor 20%, which was attributed to the presence of NaCl in the growth media used for aerosolization. Media and buffers were studied to attempt to isolate the observed hygroscopic properties of bioaerosols alone. MEM and PBS grew ~20%, which also was attributed to the high concentration of NaCl in the media. Whereas, nutrient broth media and Cab-o-sil, showed little to no growth. In the current

study, NaCl dominated the hygroscopic properties of the bioaerosols or media in which it was present. The results of this study demonstrate the importance of understanding the effect of media and buffers during laboratory studies in which the size distribution, viability, stability, transport, of a bioaerosols are being measured.

Chapter 5: Summary and Implications

The motive of much of the research presented in this dissertation was in protecting the homeland and military assets from the potential threat of biological weapons. This requires a priori understanding of the risks associated with a given biological pathogen if released as a biological weapon and an understanding of the ability to detect, protect, and mitigate against such an attack. One of the key components in determining the risks associated with an attack utilizing a biological agent is the environmental fate and transport of a given pathogen. There are many plume trajectory models used by the biodefense community to predict the long-range concentrations and resulting affected populations of an infectious aerosol release. Two key inputs to these models for aerosolized pathogens are the environmental stability and the infectivity due to inhalation. Based on these risks models, prioritization can be made for investments in medical countermeasures (such as vaccinations and prophylaxis) for those biological pathogens that pose the greatest risks to human populations and sensor development can be tailored to focus on the high priority pathogens and their associated signatures.

Much of the empirical data generated by the bioaerosol research community is leveraged in both these risk models and in sensor development for biodefense. The field of bioaerosol research itself is multi-faceted with topics ranging from the role biological aerosols play in atmospheric chemistry and physics to the effects on human health. Researchers across multiple disciplines require knowledge of the chemical and physical properties of biological aerosols, which vary depending on the type of bioaerosol, location or application for which they are being measured. Measurement of these properties continues to be a challenge with new methods being developed, characterized, and applied. Given the various environments in which the measurement of biological aerosols are desired (i.e. outdoor and indoors, high altitudes, controlled laboratory settings, battlefields, hospitals etc.) the applicability and limitations of these measurements need to be understood by researchers.

The goal of this dissertation was to identify some of the environmental factors that affect the physical and chemical properties and measurement of aerosolized biological aerosols.

Many sensor technologies have been developed that are utilized for measurement of bioaerosols in real-time. These sensors are generally designed and characterized in a laboratory. However, the environments in which these sensors are required to operate typically contain background and interferant aerosols, which are chemically complex and temporally dynamic in nature. Sensors need to be evaluated for effectiveness at discriminating between background aerosols and biological aerosols of interest. Testing in the actual settings in which the sensors are intended to

operate can be economically and logistically difficult. A novel test system was described in this dissertation that simulates the natural fluctuations in biological and non-biological aerosol concentrations in a controlled laboratory setting for testing sensors. The DyCAG system (or concept) is a tool that can be used by researchers who are testing and evaluating new biological aerosol sensor technologies to provide initial assessments of how the sensor will operate in a truly operationally relevant environment and how such an environment may affect the performance or measurements made by novel technologies. Future testing and evaluation strategies for sensor developers can utilize the complexity of the aerosol creatable using the DyCAG for determining limits of detections for biological aerosols of interest, such as infectious pathogens or even atmospherically relevant bioaerosols such as CNN or IN, in complex environmental backgrounds. The DyCAG also allows for early determination of the sensitivity of a sensor to potential interferant aerosol materials that can reduce the overall cost and expended effort in maturing technologies that ultimately are not capable of performing as required in operationally relevant settings.

Any potential changes that may have occurred to a bioaerosols due to exposure in the ambient environment may not be present in those being used for testing in a laboratory. A study was presented here that demonstrated the effects of atmospheric processing, in this case, exposure to ozone and water vapor, on the spectral properties of biological aerosols used for sensing. This study highlighted the need to recreate these potential changes, by performing aerosol-aging studies, to further understand the expected range of spectral signatures for a given biological material of interest. While

this study focused specifically on the spectral shifts that were measured by an optical sensor, this concept can be applied broadly to other technologies used for the enumeration of biological aerosols, including methods such as lateral flow immunoassays or PCR. The spectral shifts noted in this study, are indications that chemical changes are occurring and since the surfaces of biological aerosols are likely to be the most susceptible to chemical modifications, assays that rely on surface chemistries could potentially be affected by atmospheric aging. An example this was demonstrated, where the degradation of extracellular DNA and loss of genomic signature by PCR assay was suspected due to exposure to ozone. These results present a new challenge to accurately measuring bioaerosol concentrations and highlight the need to fully characterize technologies being implemented for these types of studies. The coupling of aging chambers with a system like the DyCAG could be used to study this very problem by bringing together the background aerosol component and aging properties of the ambient environment to simultaneously test the range of potential signatures of bioaerosols that a sensor can accurately measure. In order to do this, the key atmospheric constituents responsible for changing a bioaerosols need to be understood so they can be recreated in a laboratory. The aging of bioaerosols and subsequent shifts in spectral properties observed in this study is a key process that is not currently being considered by sensor developers for biological aerosols. If the spectral properties measured in a laboratory setting are different from those than may occur in an outdoor setting, then sensors are being developed that may not be capable of measuring the presence of the many potential permutations in the signatures of any

given biological aerosol of interest. It is important for future researchers to understand these limitations and to set detection requirements for technology development that include these many variations of the signature of any given biological component.

Water vapor plays a critical role in the spectral properties, size distribution, and activity of biological aerosols. The affinity for water of a biological aerosol and the key thermodynamic conditions in which the highest likelihood of any water interactions may occur should be measured. In two of the studies presented in this dissertation, the effects of water vapor on the physical properties of bioaerosols were demonstrated. Water played a significant role in the oxidation of two types of bioaerosols, spores and phages, and subsequent spectral shifts and loss of biological activity. Critical relative humidities for uptake and loss of water were also measured and showed to be very dependent on the chemical composition of the media present in the bioaerosols. By determining these key relative humidity values and the effects of media used for the studies, the range of RH values to be used for aging experiments can be narrowed, focusing on those most likely to result in the most significant chemical and physical changes. Aging experiments can then be performed at critical RH values that will affect the environmental stability, ultimately providing the empirical data that is needed in risk models to determine the effects of infectious aerosol releases.

The studies presented here improve our understanding of how biological aerosols and their measurement are impacted by external factors when in their native state. Very few studies have attempted to understand these factors or have even addressed the potential impacts they have on the measurement and stability of

biological aerosols. These studies were not intended to cover the full range of potential factors that can affect bioaerosol measurement but rather to identify factors that can affect their measurement due to changes in the chemical and physical properties. There are broad implications associated with empirical data that misrepresents the stability of pathogenic bioaerosols in the environment or the development of sensors that cannot accurately detect the presence of these pathogens. This dissertation highlights the need for more cautious research in any of the fields in which the measurement of biological aerosols is currently being pursued.

Bibliography

Ariya, Parisa A., and Marc Amyot. "New Directions: The Role of Bioaerosols in Atmospheric Chemistry and Physics." *Atmospheric Environment* 38 (2004): 1231-232. Web.

Asgharian, B., and O. R. Moss. "Particle Suspension in a Rotating Drum Chamber When the Influence of Gravity and Rotation Are Both Significant." *Aerosol Science and Technology* 17.4 (1992): 263-77. Web.

Bartrand, Timothy A., Mark H. Weir, and Charles N. Haas. "Dose-Response Models for Inhalation of Bacillus Anthracis Spores: Interspecies Comparisons." *Risk Analysis* 28.4 (2008): 1115-124. Web.

Bauer, Heidi, Heinrich Giebl, Regina Hitzenberger, Anne Kasper-Giebl, Georg Reischl, Franziska Zibuschka, and Hans Puxbaum. "Airborne Bacteria as Cloud Condensation Nuclei." *Journal of Geophysical Research* 4658th ser. 108.D21 (2003): AAC 2-1-AC 2-5. Print.

Benbough, J. E., and A. M. Hood. "Virucidal Activity of Open Air." *Journal of Hygiene* 69.04 (1971): 619. Print.

Canada. DEFENCE RESEARCH ESTABLISHMENT SUFFIELD RALSTON (ALBERTA). *Design of a Chamber for CBW Aerosol Studies with Relative Humidity and Particle Concentration Control*. By J. Ho. N.p.: Defense Technical Information Center, 1989. Print.

Canada. DEFENCE SCIENCE AND TECHNOLOGY ORGANISATION VICTORIA (AUSTRALIA) AERONAUTICAL AND MARITIME RESEARCH LAB. *Background Bioaerosols and Aerosols at Two Sites in Northern Australia: Preliminary Measurements*. By R. I. Tilley, J. Ho, and D. Eamus. N.p.: Defense Technical Information Center, 2001. Print. ADB272376.

Carrano, J., T. Jeys, D. Cousins, J. Eversole, J. Gillespie, D. Heally, N. Licata, W. Loerop, M. O'Keefe, A. Samuels, J. Schultz, J. Walter, N. Wong, B. Billote, M. Munly, E. Reich, and J. Roots. "Chemical and Biological Sensor Standards Study." *United States of America, Defense Advanced Research Projects Agency, Department of Defense* (n.d.): n. pag. *DTIC, Fort Belvoir, VA*. Web.

Carrera, M., R.o. Zandomeni, and J.-L. Sagripanti. "Wet and Dry Density of Bacillus Anthracis and Other Bacillus Species." *Journal of Applied Microbiology* 105.1 (2008): 68-77. Web.

Carrera, M., R.o. Zandomeni, J. Fitzgibbon, and J.-L. Sagripanti. "Difference between the Spore Sizes of Bacillus Anthracis and Other Bacillus Species." *J Appl Microbiol Journal of Applied Microbiology* 102.2 (2007): n. pag. Web.

Cataldo, Franco. "DNA Degradation with Ozone." *International Journal of Biological Macromolecules* 38.3-5 (2006): 248-54. Print.

Cliff, J. B., K. H. Jarman, N. B. Valentine, S. L. Golledge, D. J. Gaspar, D. S. Wunschel, and K. L. Wahl. "Differentiation of Spores of Bacillus Subtilis Grown in Different Media by Elemental Characterization Using Time-of-

Flight Secondary Ion Mass Spectrometry." *Applied and Environmental Microbiology* 71.11 (2005): 6524-530. Print.

Cox, C. S., A. Balows, and M. Sussman. "The Microbiology of Air." *Topley and Wilson's Microbiology and Microbial Infections*. Ed. L. Collier. 9th ed. London: Oxford UP, 1998. 339-50. Print.

Cox, C. S., A. M. Hood, and Jean Baxter. "Method for Comparing Concentrations of the Open-Air Factor." *Applied Microbiology* 26.4 (1973): 640-42. Print.

Cox, C. S. "Airborne Bacteria and Viruses." *Science Progress* Part 4 73 (1989): 469-99. Web.

Currier, R. P., D. J. Torraco, J. B. Cross, G. L. Wagner, P. D. Gladden, and L. A. Vanderberg. "Deactivation of Clumped and Dirty Spores of Bacillus Globigii." *Ozone-Science and Engineering* 23.4 (2001): 285-94. Print.

Deguillaume, L., M. Leriche, P. Amato, P. A. Ariya, A. M. Delort, U. Poschl, N. Chaumerliac, H. Bauer, A. I. Flossmann, and C. E. Morris. "Microbiology and Atmospheric Processes: Chemical Interaction of Primary Biological Aerosols." *Biogeosciences* 5 (2008): 1073-084. Print.

Donaldson, A. I., and N. P. Ferris. "The Survival of Foot-and-mouth Disease Virus in Open Air Conditions." *Journal of Hygiene* 74.03 (1975): 409. Print.

Donaldson, A. I. "The Influence of Relative Humidity on the Aerosol Stability of Different Strains of Foot-and-Mouth Disease Virus Suspended in Saliva." *Journal of General Virology* 15.1 (1972): 25-33. Web.

Doyle, R. J., F. Nedjat-Haiem, and Jyoti S. Singh. "Hydrophobic Characteristics of Bacillus Spores." *Current Microbiology* 10 (1984): 329-32. Web.

Dua, S. K., and P. K. Hopke. "Hygroscopic Growth of Assorted Indoor Aerosols." *Aerosol Science and Technology* 24.3 (1996): 151-60. Print.

Eversole, J., W. K. Cary, C. S. Scotto, R. Pierson, M. Spence, and A. J. Campillo. "Continuous Bioaerosols Monitoring Using UV Excitation Fluorescence: Outdoor Test Results." *Field Analytical Chemistry and Technology* 15.4 (2001): 205-12. Web.

Franc, Gary D., and Paul J. DeMott. "Cloud Activation Characteristics of Airborne Erwinia Caratovora Cells." *Journal of Applied Meteorology* 37 (1998): 1294-300. Print.

Fuzzi, Sandro, Paolo Mandriolo, and Antonio Perfetto. "Fog-Droplets-An Atmospheric Source of Secondary Biological Aerosol Particles." *Atmospheric Environment* 31.2 (1997): 287-90. Print.

Goldberg, L. J., H. M.S. Watkins, E. E. Boerke, and M. A. Chatigny. "The Use of a Rotating Drum for the Study of Aerosols Over Extended Periods of Time." *American Journal of Hygiene* 68 (1958): 85-93. Web.

Haagen-Smit, A. J. "Chemistry and Physiology of Los Angeles Smog." *Industrial & Engineering Chemistry* 44.6 (1952): 1342-346. Print.

Hill, S. C., R. G. Pinnick, S. Niles, F. F. Fell, Y. L. Pan, J. Bottiger, B. V. Bronk, S. Holler, and R. K. Chang. "Fluorescence from Airborne Microparticles: Dependence on Size, Concentration of Fluorophores, and Illumination Intensity." *Applied Optics* 40.18 (2001): 3005-013. Web.

Hill, S. C., R. G. Pinnick, Y. L. Pan, S. Holler, R. C. Change, J. Bottiger, B. T. Chen, C. S. Orr, and G. Feather. "Real-Time Measurement of Fluorescent Spectra from Single-Airborne Biological Particles." *Field Analytical Chemistry and Technology* 4-5 SI.3 (1999): 221-39. Web.

Hill, Steven C., Ronald G. Pinnick, Paul Nachman, Gang Chen, Richard K. Chang, Michael W. Mayo, and Gilbert L. Fernandez. "Aerosol-fluorescence Spectrum Analyzer: Real-time Measurement of Emission Spectra of Airborne Biological Particles." *Applied Optics* 34.30 (1995): 7149. Print.

Hill, Steven C., Yong-Le Pan, Chatt Williamson, Joshua L. Santarpia, and Hanna H. Hill. "Fluorescence of Bioaerosols: Mathematic Model Including Primary Fluorescing and Absorbing Molecules in Bacteria." *Optics Express* 21.19 (2013): 22285-22313. Web.

Hinds, William C. *Aerosol Technology: Properties, Behavior, and Measurement of Airborne Particles*. New York: Wiley, 1999. Print.

Hu, Dawei, L. Qiao, J. Chen, X. Ye, X. Yang, T. Cheng, and W. Feng. "Hygroscopicity of Inorganic Aerosols: Size and Relative Humidity Effects on the Growth Factor." *Aerosol and Air Quality Research Aerosol Air Qual. Res.* 10 (2010): 255-64. Web.

Huffman, J. A., B. Treutlein, and U. Pöschl. "Fluorescent Biological Aerosol Particle Concentrations and Size Distributions Measured with an Ultraviolet Aerodynamic Particle Sizer (UV-APS) in Central Europe." *Atmos. Chem. Phys. Atmospheric Chemistry and Physics* 10.7 (2010): 3215-233. Web.

Ignatenko, A. V., B. A. Tatarinov, N. N. Khovratovich, V. P. Khrapovitskii, and S. N. Cherenkevich. "Spectral Fluorescent Investigation of the Action of Ozone on Aromatic Amino Acids." *Zhurnal Prikladnol Spektroskopii* 37.1 (1982): 64-68. Web.

Ignatenko, A. V. "Use of the Method of Tryptophan Fluorescence to Characterize Disruptions of the Structure of Ozonized Proteins." *Journal of Applied Spectroscopy* 49.1 (1988): 691-95. Web.

Ishizaki, K. "Inactivation of Bacillus Spores by Gaseous Ozone." *Inactivation of Bacillus Spores by Gaseous Ozone* 60.1 (1986): 67-72. Print.

Ivnitski, D., D. Morrison, and D. J. O'Neil. "Critical Elements of Biological Sensor Technology for Deployment in an Environmental Network System." *NATO Security through Science Series Defense against Bioterror* (2005): 207-20. Web.

Johns, M., L. Harrington, R.w. Titball, and D. L. Leslie. "Improved Methods for the Detection of Bacillus Anthracis Spores by the Polymerase Chain Reaction." *Letters in Applied Microbiology* 18.4 (1994): 236-38. Print.

Johnson, D. L. "The Effect of Phosphate Buffer on Aerosol Size Distribution of Nebulized Bacillus Subtilis and Pseudomonas Fluorescens Bacteria." *Aerosol Science and Technology* 30.2 (1999): 202-10. Web.

Jones, R. M., M. Nicas, A. Hubbard, M. Sylvester, and A. Reingold. "The Infectious Dose of Francisella Tularensis (Tularemia)." *Applied Biosafety* 10.4 (2005): 227-39. Web.

Julian W Tang. "The Effect of Environmental Parameters on the Survival of Airborne Infectious Agents." *Journal of the Royal Society Interface* 6 (2009): S737-746. Print.

Kaku, K. C., D. A. Hegg, D. S. Covert, J. L. Santarpia, H. Johnson, G. Buzurious, and D. R. Collins. "Organics in the Northeastern Pacific and Their Impacts on Aerosol Hygroscopicity in the Subsaturated and Supersaturated Regimes." *Atmospheric Chemistry and Physics* 4115th ser. 6.4101 (2006): 4101-115. Print.

Kesavan, Jana, Deborah Schepers, and Andrew R. Mcfarland. "Sampling and Retention Efficiencies of Batch-Type Liquid-Based Bioaerosol Samplers." *Aerosol Science and Technology* 44.10 (2010): 817-29. Web.

Kim, Seung W., M. A. Ramakrishnan, Peter C. Raynor, and Sagar M. Goyal. "Effects of Humidity and Other Factors on the Generation and Sampling of a Coronavirus Aerosol." *Aerobiologia* 2007.23 (2007): 239-48. Print.

Koshikawa, T., M. Yamazaki, M. Yoshimi, S. Ogawa, A. Yamada, K. Watabe, and M. Torrii. "Surface Hydrophobicity of Spores of Bacillus Spp." *Journal of General Microbiology* 135 (1989): 2717-722. Web.

Lee, Byung Uk, Seong H. Kim, and Sang Soo Kim. "Hygroscopic Growth of E. Coli and B. Subtilis Bioaerosols." *Journal of Aerosol Science* 33 (2002): 1721-723. Web.

Lester, W. "The Influence Of Relative Humidity On The Infectivity Of Air-Borne Influenza A Virus (Pr8 Strain)." *Journal of Experimental Medicine* 88.3 (1948): 361-68. Web.

Lighthart, B., and B. T. Shaffer. "Airborne Bacteria in the Atmospheric Surface Layer: Temporal Distribution Above a Grass Seed Field." *Applied Environmental Biology* 61.4 (1995): 1492-496. Web.

Lin, Xuejun, Klaus Willeke, Vidmantas Ulevicius, and Sergey A. Grinshpun. "Effect of Sampling Time on the Collection Efficiency of All-Glass Impingers." *American Industrial Hygiene Association Journal* 58.7 (1997): 480-88. Web.

Lowen, A. C., and J. Steel. "Roles of Humidity and Temperature in Shaping Influenza Seasonality." *Journal of Virology* 88.14 (2014): 7692-695. Web.

Lowen, Anice C. "Influenza Virus Transmission Is Dependent on Relative Humidity and Temperature." *PLos Pathogens* E151 3.10 (2007): 1470-476. Print.

May, K. R., H. A. Druett, and L. P. Packman. "Toxicity of Open Air to a Variety of Microorganisms." *Nature* 221 (1969): 1146-147. Web.

Mik, G. De, and Ida De Groot. "Mechanisms of Inactivation of Bacteriophage φX174 and Its DNA in Aerosols by Ozone and Ozonized Cyclohexene." *Journal of Hygiene* 78.02 (1977): 199. Print.

Mortazavi, Roya, Christopher T Hayes, and Parisa A. Ariya. "Ice Nucleation Activity of Bacteria Isolated from Snow Compared with Organic and Inorganic Substrates." *Environmental Chemistry* 5 (2008): 373-81. Print.

Mudd, J. B., R. Leavitt, Alpaslan Ongun, and T. T. McManus. "Reaction of Ozone with Amino Acids and Proteins." *Atmospheric Environment* 3.6 (1969): 669-81. Web.

O'connell, K. P., J. R. Bucher, P. E. Anderson, C. J. Cao, A. S. Khan, M. V. Gostomski, and J. J. Valdes. "Real-Time Fluorogenic Reverse Transcription-PCR Assays for Detection of Bacteriophage MS2." *Applied and Environmental Microbiology* 72.1 (2006): 478-83. Print.

Pan, Yong Le, Justin Hartings, Ronald G. Pinnick, Steven C. Hill, Justin Halverson, and Richard K. Chang. "Single-Particle Fluorescence Spectrometer for Ambient Aerosols." *Aerosol Science and Technology* 37.8 (2003): 628-39. Web.

Pan, Yong-Le, Steven C. Hill, Ronald G. Pinnick, Hermes Huang, Jerold R. Bottiger, and Richard K. Chang. "Fluorescence Spectra of Atmospheric Aerosol Particles Measured Using One or Two Excitation Wavelengths: Comparison of Classification Schemes Employing Different Emission and Scattering Results." *Opt. Express Optics Express* 18.12 (2010): 12436. Web.

Pan, Yong-Le, Joshua L. Santarpia, Shanna Ratnesar-Shumate, Elizabeth Corson, Jonathan Eshbaugh, Steven C. Hill, Chatt C. Williamson, Mark Coleman, Christopher Bare, and Sean Kinahan. "Effects of Ozone and Relative Humidity on Fluorescence Spectra of Octapeptide Bioaerosol Particles." *Journal of Quantative Spectroscopy and Radiative Transfer* 133 (2014): 538-50. Web.

Park, Chul Woo, Ki Young Yoon, Young Do Kim, Jae Hong Park, and Jungho Hwang. "Effects of Condensational Growth on Culturability of Airborne Bacteria: Implications for Sampling and Control of Bioaerosols." *Journal of Aerosol Science* 42.4 (2011): 213-23. Web.

Peccia, Jordan, Holly M. Werth, Shelly Miller, and Mark Hernandez. "Effects of Relative Humidity on the Ultraviolet Induced Inactivation of Airborne Bacteria." *Aerosol Science and Technology* 35.3 (2001): 728-40. Web.

Piercy, T.j., S.j. Smither, J.a. Steward, L. Eastaugh, and M.s. Lever. "The Survival of Filoviruses in Liquids, on Solid Substrates and in a Dynamic Aerosol." *Journal of Applied Microbiology* (2010): n. pag. Web.

Pinnick, R., S. C. Hill, Y. L. Pan, and R. C. Chang. "Fluorescence Spectra of Atmospheric Aerosol at Adelphi, Maryland, USA: Measurement and Classification of Single Particles Containing Organic Carbon." *Atmospheric Environment* 38.11 (2004): 1657-672. Web.

Pöhlker, C., J. A. Huffman, and U. Pöschl. "Autofluorescence of Atmospheric Bioaerosols – Fluorescent Biomolecules and Potential Interferences." *Atmos. Meas. Tech. Atmospheric Measurement Techniques* 5.1 (2012): 37-71. Web.

Pryor, W. A., and R. M. Uppu. "A Kinetic Model for the Competitive Reactions of Ozone with Amino Acid Residues in Protein in Reverse Micelles." *Journal of Biological Chemistry* 268.5 (1993): 3120-126. Web.

Radar, D. J., and P. H. McMurry. "Application of the Tandem Differential Mobility Analyzer to Studies of Droplet Growth or Evaporation." *Journal of Aerosol Science* 17.5 (1986): 771-87. Web.

Ratnesar-Shumate, Shanna A., Michael L. Wagner, Charles Kerechanin, Gerard House, Kelly Brinkley, Christopher Bare, Neal Baker, Rachel Quizon, Jason Quizon, Alex Proescher, Eric VanGieson, and Joshua L. Santarpia. "Improved Method for the Evaluation of Real-Time Biological Aerosol Detection Technologies." *Aerosol Science and Technology* 45.5 (2011): 635-44. Print.

Ratnesar-Shumate, Shanna, Joshua L. Santarpia, Yong-Le Pan, Steven Hill, and Don Collins. *Effects of Atmospheric Processing on the Properties and Transport*

of Bioaerosols Final Report. Rep. no. AOD-13-0414. Laurel, MD: Johns Hopkins U Applied Physics Laboratory, 2013. Print.

Ratnesar-Shumate, Shanna, Yong-Le Pan, Steven C. Hill, Sean Kinahan, Elizabeth Corson, Jonathan Eshbaugh, and Joshua L. Santarpia. "Fluorescence Spectra and Biological Activity of Aerosolized Bacillus Spores and MS2 Bacteriophage Exposed to Ozone at Different Relative Humidities in a Rotating Drum." *Journal of Quantitative Spectroscopy and Radiative Transfer* 153 (2015): 13-28. Web.

Reed, Douglas S., Matthew G. Lackemeyer, Nicole L. Garza, Lawrence J. Sullivan, and Donald K. Nichols. "Aerosol Exposure to Zaire Ebolavirus in Three Nonhuman Primate Species: Differences in Disease Course and Clinical Pathology." *Microbes and Infection* 13.11 (2011): 930-36. Web.

Reponen, Tiina, Klaus Willeke, Vidmantas Ulevicius, Auvo Reponen, and Sergey Grinshpun. "Effect of Relative Humidity on the Aerodynamic Diameter and Respiratory Deposition of Fungal Spores." *Atmospheric Environment* 30.23 (1996): 3967-974. Print.

Roy, Chad, Martha Hale, Justin Hartings, Louise Pitt, and Steven Duniho. "Impact of Inhalation Exposure Modality and Particle Size on the Respiratory Deposition of Ricin in BALB/c Mice." *UIHT Inhalation Toxicology* 15.6 (2003): 619-38. Web.

Rubel, G. O., and K. H. Fung. "Influence of Saline Media on the Fluorescence Emission of Bacillus Spores." *Applied Optics* 38.31 (1999): 6673-676. Print.

Samuels, A. C., J. L. Santarpia, J. R. Bottiger, S. Hunter, and E. W. Stuebing. "Test Methodology Development for Biological Agent Detection Systems." *Proceedings of SPIE* 6378 (2006): n. pag. Web.

Santarpia, J. L., D. Cunningham, J. Gilberry, S. Kim, and J. Quizon. "Transport and Characterization of Ambient Biological Aerosol Near Laurel, MD." *Biogenetics Discussion* 7 (2010): 6725-747. Web.

Santarpia, Joshua L., Runjun Li, and Don R. Collins. "Direct Measurement of the Hydration State of Ambient Aerosol Populations." *Journal of Geophysical Research* 109.D18209 (2004): 1-16. Print.

Santarpia, Joshua L., Yong-Le Pan, Steven C. Hill, Neal Baker, Brian Cottrell, Laura McKee, Shanna A. Ratnesar-Shumate, and Ronald G. Pinnick. "Changes in Fluorescence Spectra of Bioaerosols Exposed to Ozone in a Laboratory Reaction Chamber to Simulate Atmospheric Aging." *Optics Express* 20.28 (2012): 29867-9881. Print.

Schaffer, B. T., and B. Lighthart. "Survey of Culturable Airborne Bacteria at Four Diverse Locations in Oregon: Urban, Rural, Forest, and Coastal." *Microbial Ecology* 34.3 (1997): 167-77. Web.

Schaffer, F. L., M. E. Soergel, and D. C. Straube. "Survival of Airborne Influenza Virus: Effects of Propagating Host, Relative Humidity and Composition of Spray Fluids." *Archives of Virology* 51 (1976): 263-73. Web.

Schroder, K. L., P. J. Hargin, D. J. Schmitt, D. J. Rader, and I. R. Shokair. "Development of an Unattended Ground Sensor for Ultraviolet Laser-Induced Fluorescence Detection of Biological Agent Aerosols." *Proceedings of SPIE* 3855 (1999): 82-91. Web.

Seinfeld, John H., and Spyros N. Pandis. *Atmospheric Chemistry and Physics: From Air Pollution to Climate Change*. New York: Wiley, 1998. Print.

Semler, D. D., and A. P. Roth. *Simulated Field Trials Using an Indoor Aerosol Test Chamber*. Tech. no. Working Paper # A096944. Edmonton: DyCOR Technologies, 2004. Print.

Shaman, J., and M. Kohn. "Absolute Humidity Modulates Influenza Survival, Transmission, and Seasonality." *Proceedings of the National Academy of Sciences* 106.9 (2009): 3243-248. Web.

Sivaprakasam, Vasanthi, Alan L. Huston, Cathy Scotto, and Jay D. Eversole. "Multiple UV Wavelength Excitation and Fluorescence of Bioaerosols." *Optics Express* 12.19 (2004): 4457. Print.

Songer, J. R. "Influence of Relative Humidity on the Survival of Some Airborne Viruses." *Applied and Environmental Microbiology* 15.1 (1967): 35-42. Web.

Spotts Whitney, Ellen A., Mark E. Beatty, Thomas H. Taylor, Robbin Weyant, Jeremy Sobel, Matthew J. Arduino, and David A. Ashford. "Inactivation of Bacillus Antracis Spores." *Emerging Infectious Diseases* 9.6 (2003): 623-27. Print.

Sturm, R. "Modeling the Deposition of Bioaerosols With a Variable Size and Shape in the Human Respiratory Tract-A Review." *Journal of Advanced Research* 3 (2012): 295-304. Web.

Sun, Jiming, and Parisa A. Ariya. "Atmospheric Organic and Bio-Aerosols as Cloud Condensation Nuclei (CCN): A Review." *Atmospheric Environment* 40 (2006): 795-820. Print.

Tang, I. N., and H. R. Munkelwitz. "Composition and Temperature Dependence of the Deliquescence Properties of Hygroscopic Aerosols." *Atmospheric Environment* 27.4 (1993): 467-73. Web.

Tang, I. N. "Chemical and Size Effects of Hygroscopic Aerosols on Light Scattering Coefficients." *Journal of Geophysical Research* 101.D14 (1996): 19245-9250. Web.

Tang, J. W. "The Effect of Environmental Parameters on the Survival of Airborne Infectious Agents." *Journal of The Royal Society Interface* 6.Suppl_6 (2009): n. pag. Web.

Theruvathu, Jacob A., Roman Flyunt, Charuvila T. Aravindakumar, and Clemens Von Sonntag. "Improved Methods for the Detection of Bacillus Anthracis."

Journal of the Royal Society of Chemistry Perkin Transmission 2 (2001): 269-74. Web.

Thompson, S., and M. Yates. "Bacteriophage Inactivation at the Air-Water-Solid Interface in Dynamic Batch Systems." *Applied and Environmental Microbiology* 65.3 (1999): 1186-190. Web.

Tilley, R. I., J. Ho, and D. Eamus. *Background Bioaerosols and Aerosols at Two Sites in Northern Australia: Preliminary Measurements*. Rep. no. DTSO-TR-1203. N.p.: National Technical Information Service-Defense Technical Information Center, 2001. Print.

Toprak, E., and M. Schnaiter. "Fluorescent Biological Aerosol Particles (FBAPs) Measured with the Waveband Integrated Bioaerosol Sensor WIBS-4: Laboratory Tests Combined with a One Year Field Study." *Atmospheric Chemistry and Physics Discussions Atmos. Chem. Phys. Discuss.* 12.7 (2012): 17607-7656. Web.

Treutlein, B., and U. Poschl. "Measurement of Primary Biogenic Aerosol Particles With An Ultraviolet Aerodynamic Particle Sizer (UVAPS)." *Geophysical Research Abstracts* 9.09832 (2007): n. pag. Web.

Trouwborst, T., and J. C. De Joung. "Interaction of Some Factors in the Mechanism of Inactivation of Bacteriophage MS2 in Aerosols." *Applied and Environmental Microbiology* 26.3 (1973): 252-57. Web.

TSI Incorporated. *Model 3321 Aerodynamic Particle Sizer Spectrometer*. Shoreview: TSI Incorporated, 2004. Print.

TSI Incorporated. *Ultraviolet Aerodynamic Particle Sizer Spectrometer Model 3314*. Shoreview: TSI Incorporated, 2014. Print.

United States of America. United Stated Army Environmental Hygiene Agency. Department of Defense-Office of Technology Assessment. *Title Kuwait Oil Fire Health Risk Assessment*. Vol. 39-26-L192-91. N.p.: n.p., 1994. Print.

Van De Hulst, H. C. *Light Scattering by Small Particles*. Reprint ed. N.p.: Dover Publications, 1981. Print.

Vanderberg, L. A. "Detection of Biological Agents: Looking for Bugs in All the Wrong Places." *Applied Spectroscopy* 54.11 (2000): 376A-85A. Web.

Wang, Z., S. M. King, E. Freney, T. Rosenoern, M. L. Smith, Q. Chen, M. Kuwata, E. R. Lewis, U. Pöschl, W. Wang, P. R. Buseck, and S. T. Martin. "The Dynamic Shape Factor of Sodium Chloride Nanoparticles as Regulated by Drying Rate." *Aerosol Science and Technology* 44.11 (2010): 939-53. Web.

Westphal, Andrew J., P. B. Price, Terrance J. Leighton, and Katherine E. Wheeler. "Kinetics of Size Changes of Individual Bacillus Thuringiensis Spores in Response to Changes in Relative Humidity." *Proceedings of the National Academy of Science* 100.6 (2003): 3461-466. *Proceedings of the National Academy of Science*. Web. <www.pnas.org/cgi/doe/10.1073/pnas.232710999>.

Whitney, E. A.S., M. E. Beatty, T. H. Taylor, R. Weyant, J. Sobel, M. J. Arduino, and D. A. Ashford. "Inactivation of Bacillus Anthracis Spores." *Emerging Infectious Diseases* 9.6 (2003): 623-27. Web.

Willeke, Klaus, and Paul A. Baron. *Aerosol Measurement: Principles, Techniques, and Applications*. New York: Van Nostrand Reinhold, 2001. Print.

Wilson, G. A., and J. Brady. "Design Consideration and Signal Processing Algorithms for Laser-Induced Fluorescence Airborne Pathogen Sensors." *Proceedings of SPIE* 5617 (2004): 1-13. Web.

Wilson, G. A., and R. K. Defreeze. "Autofluorescence Detection Using UV Diode Laser Simultaneous Excitation of Multiple Wavelengths." *Proceedings of SPIE* 5071 (2003): 253-63. Web.

Yezza, A., R. D. Tyagi, J. R. Valero, and R. Y. Surampalli. "Production of Bacillus Thuringiensis-based Biopesticides in Batch and Fed Batch Cultures Using Wastewater Sludge as a Raw Material." *Journal of Chemical Technology and Biotechnology* 80.5 (2005): 502-10. Web.

Young, S. B., and P. Setlow. "Mechanisms of Bacillus Subtilis Spore Resistance to and Killing by Aqueous Ozone." *Journal of Applied Microbiology* 96 (2004): 1133-142. Web.

Zhao, Y., A. J. A. Aarnink, R. Dijkman, T. Fabri, M. C. M. De Jong, and P. W. G. Groot Koerkamp. "Effects of Temperature, Relative Humidity, Absolute Humidity, and Evaporation Potential on Survival of Airborne Gumboro

Vaccine Virus." *Applied and Environmental Microbiology* 78.4 (2011): 1048-054. Web.